TRACE ELEMENT VARIATION IN *DOSIDICUS GIGAS* STATOLITHS USING LA-ICP-MS

A Dissertation

by

NANCY SCARLETT M. ARBUCKLE

Submitted to the Office of Graduate Studies of
Texas A&M University
in partial fulfillment of the requirements for the degree of

DOCTOR OF PHILOSOPHY

Approved by:

Chair of Committee,	John H. Wormuth
Committee Members,	Shari Yvon-Lewis
	Niall Slowey
	Franco Marcantonio
Head of Department,	Piers Chapman

December 2012

Major Subject: Oceanography

ABSTRACT

Range expansion events of the Humboldt squid reveal our inadequate understanding of populations of this species. Despite recent hatching, reproductive, tagging, genetic and dietary studies of *Dosidicus gigas*, much speculation remains concerning geographic migration, stock assessment and habitat preferences. This study provides evidence that statolith trace elemental variations can be useful in distinguishing among geographic populations. Specimens were collected from the Galapagos Islands, southern California, and Washington State. A dissection method was recorded and published. By using laser ablation methods, discrete measurements of 10 elements were collected at 6 to 7 ablation sites covering embryonic, paralarval, juvenile and adult stages. Analysis of Variance revealed important ontogenic elemental variations among ablation locations. Multivariate Analysis of Variance, ordination techniques and discriminant function analysis with permutation testing were all utilized to compare and characterize the variations found in elemental concentrations. Significant ontogenic variations were found for 8 out of the 10 focus elements; this is the first report for 5 of these elements for this species. The geographic populations were effectively classified as distinct group for the first time using these methods. Elemental fingerprint signatures were found to be significantly different at multiple ontogenic growth regions of the statolith. Seattle and California paralarvae exhibited similar elemental signatures despite significant differences in those found in the embryonic core and juvenile regions of the

statolith. These methods are a useful tool in providing stock assessment and can be improved for use in future population dynamics models.

DEDICATION

This dissertation is dedicated to Dr. John H. Wormuth, an exemplary graduate advisor. He has served the Oceanography Department at Texas A&M University for 40 years, acting as a champion to the graduate students and often giving selflessly despite his expertise being sometimes overlooked. His advice is not measured by traditional standards, but will be valuable for the rest of my life. Without the opportunities, resources and direction he provided, this research would not have been possible. It has been an honor to work with him and it will be an honor to call John my friend and colleague.

It is also dedicated to my family who provides unconditional support, especially my mother, Ann Kelly. She has given me the life-long encouragement to endlessly explore, forever wonder and desire to learn. She made me a scientist.

ACKNOWLEDGEMENTS

I would like to thank my committee. Dr. Yvon-Lewis, Dr. Slowey and Dr. Marcantonio guided and supported this research in many essential facets. I would like to especially thank Dr. John H. Wormuth, my committee chair, advisor and major professor. His influence, assistance, and expertise helped bring this research to fruition.

Additionally, two free software programs were used in this dissertation. Thanks go to Dr. Cin-Ty Lee of Rice University and Markus Wälle of the Swiss Institute of Technology, Zurich for making these applications available online.

Thanks also go to my friends and colleagues and the department faculty and staff for making my time at Texas A&M University a great experience. Special thanks go to Stuart Pearce for his vast patience and extensive aid. I also want to extend my gratitude to the Ecuadorian Navy science program, INOCAR, and the sport-fishing vessel, Coroloma, which aided in sampling efforts. Acknowledgement and thanks go to Dr. Kirt Onthank for testing the dissection guide and providing samples as well.

TABLE OF CONTENTS

Page

LIST OF FIGURES

LIST OF TABLES

1. INTRODUCTION

Due to unsustainable fishing practices and chronic weak stock management, an estimated 50% of ocean commercial taxonomic stocks have collapsed (Worm et al., 2006). Estimates indicate that at the current rate, nearly all fishing industries will have collapsed by 2050 (Pauly et al., 2003). The epidemic loss of species richness witnessed in the last century may have cascading effects through biological connectivity (Worm et al., 2006, Hastings and Harrison, 1994, Cowen et al., 2007). In order to prevent this continued loss of biodiversity, there must be a better understanding of the life cycles and behaviors of targeted species. Focusing on species with great potential for sustainable fisheries should increase successful management practices. Methods involving trace elemental chemistry in the calcified structures of cephalopods provide opportunities to accomplish these goals for key species of interest.

Cephalopod fisheries have been growing for decades despite incomplete identification of stock populations. In 2006, 4.3 million metric tons of cephalopods were caught globally (Food and Agriculture Organization of the United Nations, 2008). China, Japan, and Korea produce the largest annual landings of squid with Japan being the largest importer of squid (Sonu, 2004). The value of squid and cuttlefish imports to Japan in 2003 was over 526 million US Dollars (Sonu, 2004). Although there is a vested interest in the survival of cephalopod species, management practices lag behind those in place for fish (teleost) species .

Squid are pelagic and neritic invertebrates with some species inhabiting every zone of the ocean from polar to tropics, coastal to deep water (Roper et al., 1984). As r-selected species, cephalopods demonstrate high fecundity with reproduction generally occurring only once near the termination of a short lifespan with few species living longer than two years (Roper et al., 1984, MacArthur and Wilson, 1967, Nigmatullin et al., 2001). Teuthiod, or squid, species display highly intelligent behavior, show generalist feeding strategies and have exhibited problem solving skills, which are characteristics common among most cephalopods (Nesis, 1983, Hanlon and Messenger, 1996, Markaida, 2006).

Some commercially important teuthiod species include near-shore schooling species such as the California Market Squid, *Doryteuthis opalescens* (Anderson, 2000), as well as large muscular members of the Ommastrephidae family (Sonu, 2004). Annually, ommastrephid squid comprise between 70-80% of total global squid landings (Sonu, 2004). They are strong swimmers with thick walled mantle muscles and large rhomboidal fins (Roper et al., 1984). Many species of this family grow quickly, increasing in size 1000% in only a year by hatching at 0.001 kg and reaching up to 1 kg or more (Roper et al., 1984, Wormuth et al., 1992, Nigmatullin et al., 2001). The largest ommastrephid, *Dosidicus gigas*, can grow to a maximum mantle length of 1.5 m, a total maximum length of 4 m, and maximum weight of 120 kg (Roper et al., 1984, Wormuth, 1998, Nigmatullin et al., 2001).

Although the life cycle of *D. gigas*, or the Humboldt squid, is poorly understood, international fisheries have been targeting this species for over 20 years (Food and

Agriculture Organization of the United Nations, 2007). During the five year period from 2002 to 2006, world catches of Humboldt squid more than doubled from 400,171 metric tonnes to 848,858 metric tonnes (Food and Agriculture Organization of the United Nations, 2008). These squid have attracted international attention in recent years not only for fishery potential but also for their predatory role in the ecosystem (Field et al., 2007, Roper et al., 1984). Current interest involving Humboldt squid has developed due to recent changes to the historical distributional patterns of *D. gigas* and mainly concerns population dynamics and connectivity (Field, 2007). Previously, 35 degrees north has been held as the northern range extent in the Pacific Ocean for this species with rare sightings farther north (Roper et al., 1984, Wormuth, 1998). However, in the last 15 years scientists have witnessed an increase in the resident population off the coast of California with sightings as far north as the Bering Sea in Alaska (Zeidberg and Robison, 2007, Wing, 2006). The presence of local government fishing limits for Humboldt squid in Washington State indicates that these squid are now more common in the Northeastern Pacific (Pearcy, 2002).

Scientists suspect that this habitat expansion was caused by a combination of factors including ENSO (El Nino Southern Oscillation) events and the removal of competitors and predators by human fishing (Keyl et al., 2008). Ommastrephid squid have been suspected as a critical link between tertiary trophic levels and large predators such as marine mammals, swordfish and sharks *(Field et al., 2007, Watanabe et al., 2004)*. Many of these predators have been heavily fished in the Pacific Ocean (Worm et al., 2006). In addition to reducing mortality, this also reduces competition for some prey

items. The range expansion of Humboldt squid and evidence of permanent residences in northern locations generate further questions of ecological impacts, connectivity, and population structure. Fishing industries have already witnessed effects of the migration of this adept opportunistic predator (Field et al., 2007). Again, as ommastrephid squid, *D. gigas* grow fast and consume large quantities of prey (Nigmatullin et al., 2001, Roper et al., 1984, Wormuth, 1998). By demonstrating flexibility in feeding strategies and intelligence, Humboldt squid adapt when provided the opportunity, whether or not the animals that they prey upon are accustomed to rapid, intense predation pressures (Field et al., 2007). Relationships have been shown between a new presence of Humboldt squids and the decline of local fisheries species (Caddy and Rodhouse, 1998, Ehrhardt, 1991). Although tagging studies have been useful tools for regional and behavioral studies, some called for a complete comprehensive examination of the Humboldt stock to assess the effect on connected prey species (Gilly et al., 2006, Field, 2007).

Despite the effects that recent variations on *D. gigas* stocks have on fish populations, the life cycle, migration patterns and population dynamics of this squid are poorly understood. Previous studies of squid population dynamics utilized length-frequency data or genetics (e.g. Nesis, 1983, Markaida et al., 2004, Semmens et al., 2007, Palumbi, 2003). In 2008, Sinfer and colleagues determined that length frequency data was insufficient for teuthiod studies due to atypical and non-linear growth patterns (Sifner, 2008). Humboldt squid exhibit multiple size-at-maturity strategies depending on environmental conditions and it has been suggested that this permits dynamic range expansions (Nesis, 1983, Nigmatullin et al., 2001, Keyl et al., 2008, O'Dor, 1992).

Morphological evidence suggests that northern and southern sub-populations exist (Wormuth, 1976), and in 2007 these stocks were successfully distinguished using randomly amplified polymorphic DNA (RAPD) genetic analysis (Sandoval-Castellanos et al., 2007). However, others have attempted to establish migration patterns of Humboldt squid populations across the equator (Ikeda et al., 2002b). Additionally, the 2007 DNA study provides only a north-south division of populations for one year and offers no information about the life cycle of the Humboldt squid (Sandoval-Castellanos et al., 2007). Examination of statolith elemental signatures stands out as an ideal method to expand research in these areas (Arkhipkin, 2005).

Statoliths are composed of aragonitic calcium carbonate similar to calcium carbonate found in foraminifera, corals, gastropod and bivalve shells, and fish otoliths (Figure 1) (e.g. Smith et al., 1979, Zacherl et al., 2003, Eggins et al., 2003, Levin, 2006, Campana and Neilson, 1985, Clarke, 1978, Radtke, 1983, Rosenthal et al., 1997). In cephalopods, statoliths begin forming in the statocysts, cavities in the cranial cartilage, before hatching and continue growing after hatching by the deposition of an organic rich layer followed by an organic poor layer every day (Clarke, 1978, Zumholz et al., 2007a, Bettencourt and Guerra, 2001). This deposition process provides an accurate daily increment which can be used to estimate the age of an individual. Although this has not been verified for *D. gigas*, it has been confirmed for other ommastrephid squid and is generally assumed as a fair estimation (Rodhouse et al., 1994, Dawe et al., 1985, Nakamura and Sakurai, 1991, Lipinski, 1986). Additionally, trace elements are incorporated into the calcium carbonate matrix of statoliths (Arkhipkin, 2005, Radtke,

1983). Studies have shown that the patterns and levels of trace elements found in statoliths and otoliths can be correlated to environmental conditions experienced by an individual or to their feeding behaviors (e.g. Zacherl et al., 2003, Campana and Neilson, 1985, Arkhipkin, 2005, Zumholz et al., 2006).

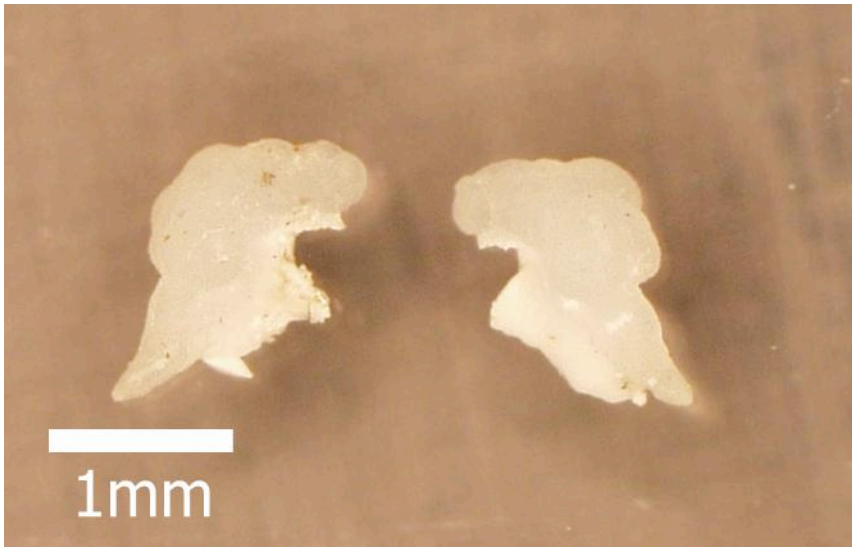

Figure 1. Paired *Dosidicus gigas* statoliths.

One of the original studies of this biochemical phenomenon established a proxy for past ocean temperatures by inversely correlating ambient seawater temperature to strontium-calcium ratios in coral skeletons (Smith et al., 1979). Three species of reef building corals were all shown to have strontium concentrations higher than ambient seawater. While seawater Sr:Ca remains constant with temperature, the three species of corals each demonstrated different rates of strontium incorporation that varied inversely with temperature. Additionally, these rates were shown to be different from inorganic carbonate strontium levels, which also vary inversely with temperature, indicating

biological fractionation (Smith et al., 1979). It is important to note that the relationship found between Sr:Ca and temperature varied among genera of reef-building corals, that growth rate is also dependent on temperature in these corals, and these are stationary symbiotic organisms (Smith et al., 1979). Studies have shown that this type of inverse relationship with temperature is also found for magnesium concentrations in planktonic foraminifera tests (e.g. Rosenthal et al., 1997, Lear et al., 2002, Eggins et al., 2003). The elemental compositions of fish otoliths have been measured for decades and studies have been successful in natal habitat reconstruction and distinction between coastal oceanic species (Thorrold, 1998, Swearer et al., 1999). Significant linear relationships between otolith strontium concentration and temperature were found in laboratory reared fish. However, this relationship was complicated for anadromous fish as salinity also demonstrated an influence on otolith strontium concentrations (Martin et al., 2004). Using a combination of trace elemental measurements has proved a successful tool in determining stock assessment or origin in mixed stocks in oceanic fish, such as tuna (Rooker et al., 2001). Similar work with gastropods and crustaceans has been promising and demonstrate some of the possibilities for statolith research (Thorrold et al., 2002, Zacherl et al., 2003, Arkhipkin, 2005, Campana and Neilson, 1985). Ultimately, the relationship between trace elements in biologically secreted calcified structures and environmental conditions enables the reconstruction of an individual's life history or can be used to distinguish between populations that experience different environments, but must be interpreted with caution when attempting to discern environmental variables (e.g. Warner et al., 2009, Arkhipkin et al., 2004, Zumholz et al., 2007c, Campana and

Neilson, 1985, Zacherl et al., 2003, Thorrold et al., 2002, Ikeda et al., 2002b, Zumholz et al., 2006).

Several studies have been conducted using cephalopod statolith microchemistry demonstrating the power, as well as the limitations, of this type of research. Early research efforts involved dissolving the entire statolith in acid for liquid mass spectrometry and distinguishing between seasonal spawning cohorts (Arkhipkin et al., 2004). Using a small Atlantic schooling species, *Loligo gahi*, one study resolved spring and autumn cohorts and three geographic sub-regions north and south of the Falkland Islands and the Patagonian shelf by measuring element to calcium ratios of magnesium, manganese, cadmium, strontium, barium and lead. This species is known to reside in shallower (<100 m) waters as small juveniles and migrate to deeper (up to 500 m) waters as they grow. Barium and cadmium were found to correlate with depth of individuals, while magnesium and manganese were believed to relate to dietary effect on the organic layers. The same study also investigated the relationship of elemental concentration to temperature and found significant negative linear variations for strontium and barium, but significant positive linear variations for magnesium and manganese (Arkhipkin et al., 2004). Other studies were unable to discern a significant relationship between temperature and strontium concentrations when studying ommastrephid squid in the Pacific Ocean (e.g. Yatsu et al., 1998, Ikeda et al., 2002b, Ikeda et al., 2002a). Here it is important to remember that even stationary coral genera exhibit differing relationships between strontium concentration and ambient temperature (Smith et al., 1979). The differences between results of strontium relationships to temperature found in studies

using ommastrephid and loligonid studies may be due to the extreme daily vertical migrations that ommastrephid squid undergo as suggested by (Arkhipkin et al., 2004).

Laser ablation inductively coupled plasma mass spectrometry (LA-ICP-MS) was used to study statolith microchemical variation in the Atlantic squid species, *Gonatus fabricii* (Zumholz et al., 2007c). Significant variations were found for magnesium, manganese, zinc, strontium, yttrium, zirconium, barium and uranium, demonstrating the possibilities for LA-ICP-MS in future statolith studies. Elemental concentration variations were explained using expected or known behaviors of *G. fabricii*. For example, Ba:Ca variations correlated to depth of habitat, while Sr:Ca and U:Ca variations inversely mirrored ontogenic migrations from warmer to colder waters (Zumholz et al., 2007c).

Another comparable study was conducted with the goal of reconstructing natal hatching grounds of adult specimens (Warner et al., 2009). By measuring calcium, magnesium, manganese, strontium and barium, some significant differences were found among populations of paralarval squid by geographic location. Additionally, by measuring elemental concentrations in the cores of adult market squid (*Doryteuthis opalescens*) and the cores of paralarval market squid from several locations, this study was able to use LA-ICP-MS to assign natal grounds to adult specimens. Although this is a powerful method of analysis, natal reconstruction requires multiple year sampling of larval squid from all likely nursery locations (See Warner et al., 2009). The elemental ranges are valuable for comparison in a manner similar to the *G. fabricii* study as well as

the methodology for distinguishing between populations by geographic location (Warner et al., 2009, Zumholz et al., 2007c).

Some attempts have been made to evaluate the variations in elemental chemistry across ommastrephid squid statoliths. A few studies using particle induced x-ray emission (PIXE) focused strongly on strontium incorporation as a proxy for ambient water temperature and all found no such relationship (Ikeda et al., 1997, Ikeda et al., 1998, Ikeda et al., 2003). One of these PIXE analyses did measure calcium, chromium, copper, iron, manganese, strontium, titanium, and zinc, but only reported that copper and zinc showed signs of ontogenic influences in *Todarodes pacificus*, an ommastrephid squid (Ikeda et al., 1998). In a 2002 PIXE study, a relationship in Humboldt squid statoliths between Cu:Ca and the El Nino Southern Oscillation was found with concentrations being higher in El Nino years; however, no pattern for strontium incorporation with temperature was revealed (Ikeda et al., 2002b).

In 2011, the first study of Humboldt squid statolith microchemistry using LA-ICP-MS was published (Liu et al., 2011). Two important aspects of this study are the elements sampled and the geographic sample range. Specimens were all sampled from the southern hemisphere, off Peru and northern Chile. Only magnesium, calcium, sodium, strontium and barium were measured (Liu et al., 2011). As found previously, no significant relationship between temperature and Sr:Ca could be determined for this species (Liu et al., 2011, Ikeda et al., 2002b). Elemental variations were significant for sodium, strontium, and barium (Liu et al., 2011). The authors proposed that Ba:Ca and Sr:Ca shifts indicate depth of habitat and found that Mg:Ca and Sr:Ca variations may

distinguish between seasonal cohorts. No elemental variations were able to significantly distinguish between regional populations in this study (Liu et al., 2011).

Ten elements were chosen for the study presented here and selection was based upon the successful measurement and utilization in previous carbonate microchemical research endeavors. Most were chosen due to previously resolved relationships between concentration in carbonates and environmental variables, behavioral influences or dietary effects. Although not every element chosen has been linked properly through laboratory-rearing exercises, the overall elemental signature, or fingerprint, should differentiate between geographic locations (Arkhipkin et al., 2004, Arkhipkin, 2005, Warner et al., 2009). A brief review of studies will now be given by element.

Magnesium has been a standard element of interest in cephalopod carbonate studies (e.g. Arkhipkin et al., 2004, Warner et al., 2009, Zumholz et al., 2007c, Liu et al., 2011). Statolith magnesium concentrations are third highest after calcium and strontium (Arkhipkin et al., 2004, Warner et al., 2009, Zumholz et al., 2007c, Liu et al., 2011). Although magnesium maintains a generally uniform distribution in ocean water, it has been found to be physiologically regulated by cephalopods (Zumholz et al., 2007c, Bettencourt and Guerra, 2000). It has been suggested that Mg:Ca values decline with size of squid statolith based growth rates (Arkhipkin et al., 2004, Zumholz et al., 2007c). A pattern of magnesium enrichment in the core of statoliths has been documented, and studies have shown that high magnesium levels are necessary for statolith formation (Warner et al., 2009, Zumholz et al., 2007c, Bettencourt and Guerra, 2000). However, one study did not find significant Mg:Ca variations across statoliths of *D. gigas* and also

measured a large variance in outer regions of the statolith (Liu et al., 2011). The very low values for magnesium found in this study suggest that some of the ablations may not have actually struck the core or that the peak of magnesium was not used as an interval of sampling (See Warner et al., 2009, Liu et al., 2011). Another possibility is that mixed cohorts muddled the Mg:Ca variations since Liu et al. (2011) did report that Mg:Ca differences aided in distinguishing between cohorts. Magnesium has also been linked to temperature of the ambient environment in field studies, but it is important to note that growth rate is also correlated to water temperature (Arkhipkin et al., 2004).

Manganese has also been frequently used in cephalopod carbonate studies as the fifth highest compositional element of squid statoliths (e.g. Arkhipkin et al., 2004, Warner et al., 2009, Zumholz et al., 2007c). It also demonstrates variability in ocean waters, with higher concentrations found near surfaces, with increasing variability due to dust influx, and lower concentrations at depth with variability in low oxygen environments (Johnson et al., 1996, Donat and Bruland, 1994, Bruland, 1983). Some authors suggest that relative to levels found in statoliths, manganese concentration is nearly uniform in the ocean indicating the variations seen in statoliths are due to taxon-specific uptake methods (Arkhipkin et al., 2004, Zumholz et al., 2007c). It has also been demonstrated that diet can influence the manganese incorporated into the statolith in some cephalopods (Zumholz et al., 2007c).

Copper exhibits a nutrient like profile with reduced concentrations in surface waters (Bruland, 1983, Donat and Bruland, 1994). It has not been measured in many statolith studies but was successfully used to distinguish between ENSO environments

for *D. gigas* using PIXE, with copper being significantly higher in El Niño years (Ikeda et al., 2002b). No studies found reported relationships to temperature or diet, but one study suggests a relationship to ontogenic stages in a pacific ommastrephid squid, *T. pacificus* (Ikeda et al., 1998).

Zinc has also been reported to have a nutrient like profile (Bruland, 1983, Donat and Bruland, 1994). It is less frequently investigated in carbonate studies, but a few statolith studies have measured Zn:Ca values. One using LA-ICP-MS and an Atlantic squid species found that statolith cores were enriched compared to outer regions (Zumholz et al., 2007c). This was also found for cuttlefish, although no dietary influences could be determined (Zumholz et al., 2006). One PIXE study using *T. pacificus* found a positive correlation between zinc concentration and integrated water temperature (Ikeda et al., 1996). In 2002, zinc concentrations were higher in *D. gigas* statoliths collected in El Niño years than those collected in non-El Niño years. It was suggested that these differences could be related to ontogeny as was found in a mackerel study (Ikeda et al., 2002b, Papadopoulou et al., 1978). If this variation is similar in Humboldt squid, it could be an artifact of dietary bioaccumulation as the individual grows and consumes larger prey. The same *D. gigas* study found significant differences between ENSO years, with concentrations being higher in El Nino years (non-upwelling) (Ikeda et al., 2002b).

Yttrium concentration has been measured in a few squid statolith studies and has a nutrient-like profile in the ocean. In a LA-ICP-MS study of laboratory reared cuttlefish, diet has been shown to effect yttrium concentration (Zumholz et al., 2006). In

wild *G. fabricii*, Y:Ca was measured as higher in cores than mid-statolith regions (Zumholz et al., 2007c). These findings suggest potential for this element to aid in discriminating between populations based on diet.

Zirconium has been reported has having a nutrient like distribution (Bruland, 1983, Donat and Bruland, 1994) and is less frequently measured for statolith studies. However, two studies revealed zirconium enrichment in statolith cores despite a lack of dietary influence (Zumholz et al., 2007c, Zumholz et al., 2006). Zirconium may also have potential for discriminating between populations.

Barium follows magnesium in rank of cephalopod statolith compositional elements and is frequently measured in carbonate microchemical studies (e.g. Arkhipkin et al., 2004, Warner et al., 2009, Zumholz et al., 2007c, Liu et al., 2011). Barium distribution in the oceans exhibits a nutrient-like profile with sources being river water, runoff and upwelling from deep water (Chan et al., 1977). Ba:Ca variations have been successfully linked to both freshwater runoff and depth for squid species (e.g. Arkhipkin et al., 2004, Zumholz et al., 2007c). A negative relationship between Ba:Ca and water temperature was found for laboratory reared cuttlefish, confirming field studies of squid statoliths (Arkhipkin et al., 2004, Zumholz et al., 2007c). One study also found that diet can significantly influence statolith composition of barium in cuttlefish. It was determined that a change in feeding behaviors could result in a 2^{o}C error in barium calculated temperature (Zumholz et al., 2006). Ba:Ca variations should be beneficial distinguishing between coastal and offshore groups where no upwelling occurs depending on dietary influence and temperature.

Lead is not frequently measured in squid statolith research. Dissolved lead has a scavenged element vertical profile due to atmospheric inputs with occasional minimums at the surface when and where inputs are low (Donat and Bruland, 1994). Two studies did record lead present in squid statoliths, but no significant pattern could be found (Warner et al., 2009, Zumholz et al., 2007c). Although not verified in cephalopod studies, gastropod larvae have been successfully reassigned to natal groups using Pb:Ca, which was found to be more distinct among populations than barium and strontium (Zacherl et al., 2003). One source of lead to the statolith could be diet or directly from the environment and could distinguish between pristine and polluted environments (Zacherl et al., 2003).

Uranium has rarely been measured in squid statolith studies, but a U-shaped pattern in U:Ca across the statolith was reported for an Atlantic squid species using LA-ICP-MS. In that study, it was suggested that variations were related to both temperature and salinity through deep offshore migrations (Zumholz et al., 2007c). Generally, uranium has a conservative distribution in the ocean varying only with salinity, which indicates that any variations should be physiologically controlled and may vary with taxonomy (Bruland, 1983, Donat and Bruland, 1994).

Temperature and other environmental parameters have been thought to influence strontium concentrations in carbonate materials for decades, so strontium is perhaps the most highly investigated element in carbonate microchemistry studies. Many cephalopod statolith investigations focus on relationships between strontium and ambient temperature reconstructions (e.g. Ikeda et al., 1997, Ikeda et al., 2002a,

Zumholz et al., 2007a). Although Sr:Ca was found to be significantly related to temperature in a small loligonid squid, this was not established for two ommastrephid squid in other studies (Ikeda et al., 1997, Ikeda et al., 2002b). Arkhipkin and his colleagues postulated that the diurnal migration behavior of the oceanic ommastrephids, which involves vertical movements of hundreds of meters every day, confounded a direct Sr:Ca relationship with water temperature (Arkhipkin et al., 2004). Later studies using nano-scale technology found a daily fluctuation in Sr:Ca in another vertically migrating squid, *Gonatus fabricii*, however, the authors remained unconvinced that the relationship was strictly temperature related citing activity levels and consumption of prey as possible sources of the variation (Zumholz et al., 2007a). This skepticism was likely due to previous work demonstrating dietary influence. In 2006, an experiment involving cuttlefish raised at a constant temperature and varying diet did show Sr:Ca correlation to diet, which confounds any strontium correlation with temperature in the wild (Zumholz et al., 2006). In later work, the experiment with cuttlefish was repeated and furthered to identify the strontium-temperature relationship for specimen with no variation in diet, however none was discernible (Zumholz et al., 2007b). These laboratory rearing experiments with controlled conditions provide arguably the best evidence for a lack of temperature effects on cephalopod statolith strontium concentration. One such study showed definitively that there is no effect of temperature on Sr:Ca (Zumholz et al., 2007a). Another investigation revealed periodic variations in *T. pacificus* statolith Sr:Ca despite being raised at a constant temperature (Ikeda et al.,

2002a). This brief review emphasizes the controversy associated with using strontium as a simple temperature proxy in highly motile animals in volatile environments.

Ultimately, the use of microchemical signatures provides a useful tool in discriminating between populations, life history reconstruction and behavioral evidence. Since cephalopods exhibit complex trace elemental uptake mechanisms, multiple studies have cautioned against applying equations calculated for the trace elemental relationships in one species for another (e.g. Arkhipkin et al., 2004, Ikeda et al., 1997, Zumholz et al., 2007b). At the present time it is not possible to verify direct correlations between the environment and squid statolith concentrations without live-rearing experiments, which are not yet possible for the species of focus, *D. gigas*.

Statistical analysis for ecological population dynamic studies has grown widely diverse and complex in application. A common basic application is the student's t-test. When examining two groups or treatments, it is standard to apply a t-test to compare the means of a single variable for a significant difference at the $\alpha = 0.05$ level. This means that the null hypothesis is that the means are the same, but if the p-value resulting from the calculations is less than that level, the null hypothesis is rejected. However, when it is necessary to compare the means of a single variable or factor for more than two groups or samples at one time Analysis of Variance (ANOVA) must be used. Since ANOVA can compare two sample means while controlling for others, it is more powerful than a series of t-tests. If the resulting p-value is less than 0.05, it indicates that all sample means evaluated are the not the same. In order to determine specifically which sample means are statistically different, a multiple comparisons test, such as

Tukey's HSD test, is examined post-hoc, or after the fact. This is necessary to account for the fact that there are more than two sample means being compared to prevent an overestimation of significance, or a Type I error, from occurring. Assumptions for this test include normality and homogenous variances. If two factors were to be investigated simultaneously, a two-way ANOVA can be used. This would test for significant effects of both factors as well as if any interactions were occurring between the factors. If interactions did occur, the interpretation of the p-values for each of the factors would be more complicated. Therefore it is beneficial to perform a two-way ANOVA to check for interaction effects (Gotelli and Ellison, 2004).

ANOVA can be applied to a series of measurements of the same factor, such as measurements of a single element taken at different spots on a statolith. However, when multiple factors are used, such as many elements measured at various spots on a statolith, Multivariate Analysis of Variance (MANOVA) must be employed to evaluate similarities or differences of groups. Multivariate normality is required for MANOVA, and one way of assuring this is to check for univariate normality of all associated factors. In MANOVA, rather than comparing the means among groups, the multivariate means are compared as centroids and a single p-value can still represent the confidence level for declaring each group as different based upon centroids (Gotelli and Ellison, 2004).

In order to visualize the differences described by statistical p-values multivariate ordination can be performed. Two measurements or variables, (j=1,2) , can be plotted for the same observation or individual, i. Then the Euclidian distance can be determined in two dimensions (Equation 1). In the same manner, multivariate ordination involves

plotting three or more measurements or factors in multidimensional space (Equation 2). The vector resulting from the best fit line of multiple observations of variables can be used to reduce the number of dimensions being investigated. This new vector is considered a new variable called a principle axis. Each sample or observation has a score along this new axes based upon the original measurements for each variable and the corresponding loading for that axis (Gotelli and Ellison, 2004).

$$d_{i,j} = \sqrt{\left(y_{i,1} - y_{j,1}\right)^2 + \left(y_{i,2} - y_{j,2}\right)^2} \quad \text{Eq. 1}$$

$$d_{i,j} = \sqrt{\left(y_{i,1} - y_{j,1}\right)^2 + \left(y_{i,2} - y_{j,2}\right)^2 + \left(y_{i,3} - y_{j,3}\right)^2 \ldots} \quad \text{Eq. 2}$$

Two descriptive multivariate ordination methods of interest are Correspondence Analysis (CA) and Principle Component Analysis (PCA). Often used as a method of relating species to sampling site characteristics, CA allows for both the observations and the variables to be plotted in the same space. Distances between observations and variables cannot be directly interpreted in these plots. However, they can still be useful in explaining which variables may be causing variation among observations or groups (Gotelli and Ellison, 2004).

It is essential to normalize data before performing PCA so that a variable with a greater magnitude does not dominate calculations of distance. To emphasize this, imagine three variables where two are on the scale of nanometers, while the third is on

the scale of meters. Although a great change in the first two variables would not result in any change of the Euclidean distance between two observation points, a small difference in the third variable would seem to create a significant change. This prevents much useful information being obtained from the resulting principle components. Normalization was achieved by subtracting the mean of each element for each ablation location for each geographic group from each measurement and then dividing by the standard deviation of that mean. The principle component ranks are calculated as eigenvalues of the variance-covariance matrix, which is equivalent to the correlation matrix when using normalized data. Thus an eigenvalue is computed for each principle component assigning the maximum amount of variance possible. The sum of the eigenvalues provides the total variance or a percent of the total variance is explained by each of the principle components. A simple bar graph of the percent variability explained by each of the principle components, or a scree plot, can aid in determining how many principle component dimensions are contributing significantly to the total variance (Gotelli and Ellison, 2004). These selected dimensions are used to plot the observation scores and bootstrapped confidence intervals allow for quantitative interpretation (White and Ruttenberg, 2007). Generally, only the first few principle components are plotted, which achieves the goal of reducing high dimension multivariate data to a few comprehensible dimensions (Gotelli and Ellison, 2004).

Although the previous methods provide a successful visualization of the multivariate data, Discriminant Function Analysis (DFA) provides a quantitative method of distinguishing among populations. DFA provides a means of classifying observations

into groups based upon similarities or differences in multivariate means and multivariate variances. One common example of this type of classification is taxonomy. While CA and PCA ordination methods involve examining the patterns of variances along a gradient of measurements, DFA defines the limits of the gradients (Gotelli and Ellison, 2004). It is essential to use randomization tests, such as jackknifing, which provides a p-value to confirm with a confidence at the $\alpha = 0.05$ level that resulting classifications are better than what would be achieved by chance (White and Ruttenberg, 2007).

Using the statistical tests described and insight from previously published research, the research presented here intends to provide information that will aid in the understanding of the Humboldt squid life history and population structure by measuring statolith elemental composition with LA-ICP-MS. Examining the ontogenic changes in the levels of trace elements incorporated into Humboldt statoliths may provide insight into the changes in behaviors, habitats and diet an individual might undergo during its lifetime. This will be investigated using ANOVA to determine patterns found in elemental variation across the statolith. Findings will provide for the creation of a life-history standard for this species of squid which will aid in stock assessment. By sampling at three distinct geographic locations, similarities in behavior, habitat or diet despite differences in region, may help reveal stock details of this opportunistic species. The similarities of natal hatching areas for geographically separated adult populations will be tested using MANOVA. Similarities in trace elemental signatures measured in the core of specimen from different regions may indicate similar behavior, or similar hatching grounds and subsequent migrations. Both possibilities may provide insight into

the locations of ideal spawning areas allowing for proper management of fisheries. Finally, using multivariate ordination and classification of the trace elemental ratios of statoliths removed from squid collected at three geographic locations will test the null hypothesis that there is no difference among the elemental signatures found in the statoliths of Humboldt squid from different geographic regions. This will provide the basic stock assessment of squid fished in different regions by showing if they experience the same environmental conditions which indicates a similar stock or natal origin. Otherwise it will declare these groups significantly different stocks. These findings can be used to support or refute previous studies (Warner et al., 2009, Liu et al., 2011, Sandoval-Castellanos et al., 2007). Ultimately this research will collectively test the null hypothesis that the analysis of trace elemental chemistry in statoliths is not an effective method for studying populations of *Dosidicus gigas*. These findings may help with the stock assessment required for adequate fisheries management practices.

2. METHODS

2.1 Sampling

Samples were collected from three distinct geographic regions: the Galapagos Islands, Ecuador, in September 2008; Oceanside, California, in June of 2007; and Seattle, Washington, in October 2008. Sample sizes varied due to availability of specimens with 48 squid collected from Ecuador, 9 from California, and 17 from Seattle. Statoliths were dissected from the cranial cartilage immediately after capture or the entire head was frozen and the statoliths were removed later after thawing. The dissection method available, (Lipinski, 1980), proved to be difficult in application. The entire dissection was documented and photographed. Pictures were edited in a free graphic image manipulation program, GIMP, and the updated methods were developed into a guide. The effectiveness of the guide was tested by providing it to a colleague with no previous statolith dissection experience. Using the guide, 17 pairs of statoliths were successfully removed with no complications or coaching. The updated method was published in Arbuckle and Wormuth (2011), which can be found in the appendix (© IEEE 2011).

Once dissected, all statolith pairs were rinsed with de-ionized water and stored dry in labeled flat-bottom screw-top vials. One statolith per specimen was mounted in thermoplastic epoxy resin pucks. Double-sided non-reactive tape was used to position the statolith concave up on a glass plate before pouring the epoxy. After curing for 12-24 hours, the pucks were removed from the glass plate, tape and mold. Specimen

identification numbers were carved into the epoxy and excess material was removed by lathe. The statoliths were then ground and polished to reveal growth increments. Grinding was performed manually using ultra-fine grain sandpaper for 30-90 seconds. Polishing required a spinning lapping table, 6 micron diamond grit polishing solution and cloth polishing disks. Depth of grinding and growth increments were checked regularly using light microscopy and, if needed, statoliths were reprocessed until the core was visible at or just below the surface of the puck (Jackson, 1994).

The growth increments were photographed using a light microscope at 40x. Age was estimated by counting the growth increments by light microscope at 40x or by compiling microscope images using the align tool in Adobe Photoshop. Each growth ring was assumed to equal one day (Lipinski, 1986, Dawe et al., 1985, Jackson, 1994, Nakamura and Sakurai, 1991, Rodhouse et al., 1994). Average age of specimen was approximately 133 days, ranging from 100 to 175 days. Age estimations were used to check for cohorts by hatching season and all were found to be from the same late spring to early summer hatching season.

2.2 Laser Ablation

Elemental measurements were conducted in the R. Ken Williams Radiogenic Isotope Geosciences Lab using a Thermo Element XR-ICP-MS (high-resolution inductively coupled plasma mass spectrometer) and an Analyte 193 nm ultra-short pulse excimer laser ablation sampler. Laser ablation procedures were developed and adjusted through several trials on statoliths from the largest sample set (Ecuador) and using calcite crystals provided by Dr. Brent Miller. The final LA-ICP-MS method and settings

are reported in Table 1. Calcium was chosen as an internal standard and the value of calcium concentration was taken from the literature (Zumholz et al., 2007c). National Institute of Standards and Technology (NIST) glasses were used for tuning the mass spectrometer, external precision and calibrations. NIST 610, 612 and 614 were analyzed between every three statoliths and at the end of the day. The settings and method were the same for the NIST glass standards and the samples.

Table 1. LA-ICP-MS settings and method.

Elements Sampled: ^{24}Mg ^{43}Ca $^{87}Sr^{++}$ ^{55}Mn ^{63}Cu ^{64}Zn ^{85}Rb ^{86}Sr ^{87}Sr ^{89}Y ^{90}Zr ^{138}Ba ^{207}Pb ^{238}U		
Resolution Setting:		Low
Carrier Gas:		Helium/Argon mix
Spot Size:		39 micron circle
Gas Flow:		
	Ar	~1L/min
	He	~0.8L/min
Energy:		50%
Cone Type:		Nickel T-1001-X
Sample time:		0.002
Samples per peak:		10
Mass window:		10%
Integration type:		Peak top
Detection Mode:		Triple

The location of the first ablation spot was centered on the core for each statolith. The diameter of the laser was set to the minimum size that would ablate the entire core. Each consecutive ablation site was 0.2 μm from the center of the previous ablation center on a transect along the growth lines from the core to the outer edge of the statolith

along the longest distance (Figure 2). At least 5 ablations were made on each statolith, with the maximum being 8 ablations on some of the statoliths collected from California. The maximum number of ablations made on statoliths from Seattle was 7 and the maximum for the Galapagos was 6.

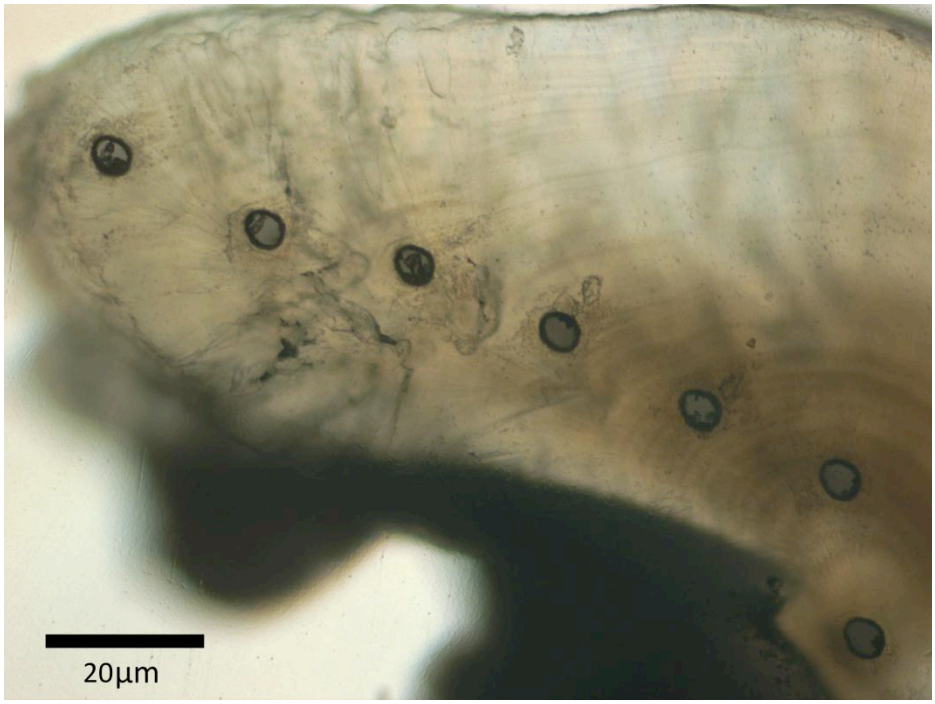

Figure 2. Post-ablation view of a polished statolith with growth rings and 7 ablation craters visible.

Raw output from the LA-ICP-MS exports as counts per second of each element for each run. A run is defined here as one measurement cycle through all elemental isotopes sampled. Each ablation crater consisted of 100 runs, of which approximately 30 runs were collected with the laser off in order to establish a background blank. The remaining 70 runs were collected while the laser was firing on the statolith. Using a Matlab script, the raw output were reformatted and adjusted for mass interferences to be

compatible for the data processing software. The calculations for these corrections are summarized in Equation 3.

$$^{43}Ca_{corrected} = {}^{43}Ca_{measured} - \left({}^{87++}Sr \left(\frac{[^{86}Sr]}{\left({}^{87}Sr - \left(\frac{^{85}Rb}{2.59324} \right) \right)} \right) \right) \qquad \text{Eq. 3}$$

Two data processing software platforms were tested. The first program is a visual basic script written and made available by Dr. Cin-Ty Lee of Rice University. The second is a Matlab script and stand-alone Matlab complier, SILLS, available through, Markus Wälle of the Swiss Institute of Technology, Zurich. Based on simplicity and user familiarity, the visual basic program was chosen for final data processing, although both programs returned similar output results. Within the visual basic program, settings were chosen for limits of detection and the internal standard (43Ca). The expected values for the NIST standards were imported from the most recent comprehensive analysis of the concentrations chosen (Jochum et al., 2011). To quantify the reproducibility of the method, the external analytical precision was verified. Three concentrations of standard reference materials from the National Institute of Standards and Technology (NIST) were ablated ten times using the same method and settings as were used for all samples. The percent relative standard deviation (%RSD) was calculated to compare the results across elements using Equation 4, where Me refers to one of the elements measured.

$$\%RSD = \left(\frac{s_{Me}}{\bar{x}_{Me}}\right) * 100 \qquad \text{Eq. 4}$$

Actual sample signal for each statolith core was determined by a peak in the magnesium signal, because cores have been shown to be magnesium enriched (e.g. Zumholz et al., 2007c, Ruttenberg et al., 2005). For each statolith, the depth of all subsequent ablations was set to the core depth by using the same interval of runs unless tilting of the statolith was evident. When this was the case, the run interval was shifted accordingly.

Calibration curves were made for every three statoliths, using three consecutive replicate ablations for each of the three standard reference NIST glasses. For each element of interest, the element to calcium ratio for the measured intensities was plotted against the expected concentrations of the same. Concentration of the internal standard was taken from the literature to be 400,000 ppm (Zumholz et al., 2007c). The best fit line using the three standards and the origin returned a slope as an R^2 value for each element which can be used as a correction factor for estimating the measured concentrations in samples, m. Although only the background-corrected element to calcium ratios (Me/Ca) were needed for statistical analysis, the program also provides estimated concentrations using Equation 5, with m being the calibration coefficient, Me being an element, Ca being the internal standard, calcium.

$$C_{Me}^{Sample} = C_{Ca}^{Sample} * \frac{I_{Me}^{Sample}}{I_{Ca}^{Sample}} * m \qquad \text{Eq. 5}$$

A new calibration line was plotted for every three statoliths to correct for instrument drift. The values for limit of detection (LOD) were also calculated by the program as 3 standard deviations of the background signal as shown in Equation 6.

$$LOD_{Me}^{Sample} = C_{Ca}^{Sample} * \frac{3* \sigma_{Me}^{bkgrd}}{I_{Ca}^{Sample}} * \frac{C_{Me}^{SRM}}{C_{Ca}^{SRM}} * \frac{I_{Ca}^{SRM}}{I_{Me}^{SRM}} \quad \text{Eq. 6}$$

2.3 Statistical Analysis

In order to determine the effectiveness of these methods for population studies of Humboldt squid, several statistical methods were employed using Matlab to resolve specific information about the elemental composition of the statoliths collected. Elemental ratios resulting from the processing described above were initially checked for outliers. If $|x_i - \bar{x}| > 2s$, then x_i was considered an outlier and removed for all subsequent analysis. After selecting only statoliths measured under the same conditions and removing outliers, the subset of data remaining will be called the subdata. The subdata include 13 statoliths from the Galapagos, 8 from California and 14 from Seattle. Normality and homoscedasticity were verified for the remaining data using histograms of the data fit to a normal distribution, quantile-quantile (QQ) plots against a standard normal, and Bartlett's test of homogeneous variances.

Analysis of Variance (ANOVA) was applied to the subdata to determine if the differences in mean values between ablation craters were significant within each of the three separate populations for each element. The purpose of this analysis was to reveal variations in elemental composition of the statoliths during the lifetime of Humboldt

squid if any were present. Although there were slight deviations from normality for these small sample groups, simulation studies have shown the false positive rate is not highly effected the violation of the normality assumption (Lindman, 1974, Glass et al., 1972, Harwell et al., 1992). In order to determine which ablation spots contributed to a significant ANOVA result, post-hoc Tukey multiple comparisons of the means were examined ($\alpha \leq 0.05$). The multiple comparisons test, or Tukey's HSD, was chosen over a series of t-tests as it takes into account the fact that more than two samples were taken even though only two means are compared, reducing the chance of type II errors. Additionally, Two-Way Analysis of Variance was performed to be sure no interactions occurred between specimen and elements by spot in each geographic region.

Significant differences between the elemental ratios measured at the core and the outer most ablation spot might suggest differences in natal waters and waters where animals were captured or died. ANOVA was again used to compare the means of all elements measured at the core and at the final ablation spot available to examine this idea. This was repeated for the second ablation spot versus the last ablation in order to remove maternal effects present in the yolk and to compare the water inhabited by hatchlings rather than water where eggs incubate. The final spot is defined as the last ablation spot with a value for every statolith observation. Since the specimens collected from the Galapagos Island were younger than those collected from the other locations, the final spot for statoliths from California and Seattle is the 6th and for the Galapagos is the 5th.

The data was further condensed to remove all missing values. Zirconium was removed entirely since it was the element with the highest number of values below the detection limits. Only ablation spots 1 through 5 were used since all of the Galapagos would have missing values for all elements for the sixth ablation spot. After this filtering, the data set is called the final data. The final data was again checked for normalcy and homoscedasticity, which improved.

To investigate differences in the overall elemental signatures among the three geographic regions, MANOVA was performed on the final dataset to compare the means of all elements measured at the core, the second ablation site and at the 5th ablation site. The final ablation site for MANOVA is defined as the 5th ablation spot, since it was the last spot taken for all three groups. Significant differences between the elemental signatures could indicate that there are distinguishable differences in the populations. If elemental signatures are similar, it is reasonable to deduce that the populations are experiencing similarities in ontogenic behavior or environment. Due to small sample size and deviation from homogeneous variances, Pillai's Trace statistic was used in place of the F statistic when applicable.

Correspondence analysis (CA) was performed on the final dataset to visualize the relationships among elements and relationships among individual squid. CA was repeated combining the individuals for each region to visualize the relationships among the elements and among the geographic regions.

To determine which elements were candidates for distinguishing variables between the three geographic populations, the means and 95% confidence intervals were

plotted and the multiple comparisons were reviewed. Element-spots were selected when at least one of the three groups were significantly different than at least one of the other two groups. These included some or all of the spots from Mg, Mn, Cu, Sr, Y, Ba and U. The Me/Ca ratios for those elements at chosen spots were normalized according to Equation 7, as required for the operation of Principle component analysis (PCA). This data will be called the normalized dataset. PCA was performed on the normalized dataset and 95% confidence ellipses were calculated and drawn on plots of the principle component scores for the relevant dimensions.

$$x_{i,std} = \frac{\left(\mu_{(Me/Ca),spot} - x_{i,0}\right)}{s_{(Me/Ca),spot}} \qquad \text{Eq. 7}$$

Finally, discriminant function analysis (DFA) with permutation testing was performed on the principle components to resolve significant variations in collective Me/Ca signatures among populations by testing the ability of these methods to distinguish among geographic groups. DFA was conducted using the normalized data, which was the input for PCA, and again using the scores that resulted from the PCA. A jackknife method was chosen for the permutation test and consisted of 1000 iterations of randomly selected datasets with one individual held out to determine if successful reclassification of the final individual into the correct a priori group was significantly different from reclassification by chance.

3. RESULTS

3.1 Calibrations

The results of the external precision test can be seen in Table 2. As the percent relative standard deviation is on average less than 3%, the LA-ICP-MS is assumed to be in excellent working order. This was consistent throughout the duration of the sampling period.

Calibration curves were made for every set of three statoliths. An example calibration curve plot is shown in Figure 3. The measured values and expected concentrations for the three NIST glass standard reference materials were plotted versus the measure and expected intensities of the NIST standard reference materials. The best fit line for the three resulting points was forced through the origin, returning an R^2 value representing the severity of the calibration. All calibration curves were very near $R^2=1$, with most being $R^2>0.99$. This indicates that very little corrections were necessary when calculating the estimated concentration of each element.

Table 2. Summary of 10 consecutive ablations of the three standard reference materials. Average, sample standard deviation, percent relative standard deviation and expected values as determined by Jochum et al., 2011, are given.

	NIST 610				NIST 612				NIST 614			
	Average	*s*	%RSD	Expected	Average	*s*	%RSD	Expected	Average	*s*	%RSD	Expected
^{24}Mg	358.642	4.085	1.139	432	56.666	0.452	0.798	68	33.797	0.342	1.013	33.8
^{55}Mn	478.913	4.614	0.963	444	39.884	0.658	1.649	38.7	1.405	0.155	11.027	1.42
^{63}Cu	409.430	8.653	2.113	441	33.601	0.854	2.542	37.8	1.364	0.092	6.719	1.37
^{64}Zn	535.021	12.383	2.315	460	41.406	0.540	1.304	39.1	2.771	0.240	8.659	2.79
^{87}Sr	542.050	31.946	5.894	515.5	78.532	2.691	3.427	78.4	45.790	0.716	1.564	45.8
^{89}Y	500.247	10.162	2.031	462	39.486	0.411	1.040	38.3	0.789	0.023	2.960	0.79
^{90}Zr	469.302	10.711	2.282	448	38.163	0.646	1.693	37.9	0.845	0.054	6.415	0.848
^{138}Ba	470.416	5.802	1.233	452	39.622	0.389	0.981	34.3	3.198	0.090	2.811	3.2
^{207}Pb	465.079	20.802	4.473	426	38.326	0.638	1.665	38.57	2.318	0.072	3.126	2.32
^{238}U	506.596	8.478	1.673	461.5	38.117	0.357	0.937	37.38	0.822	0.022	2.621	0.823

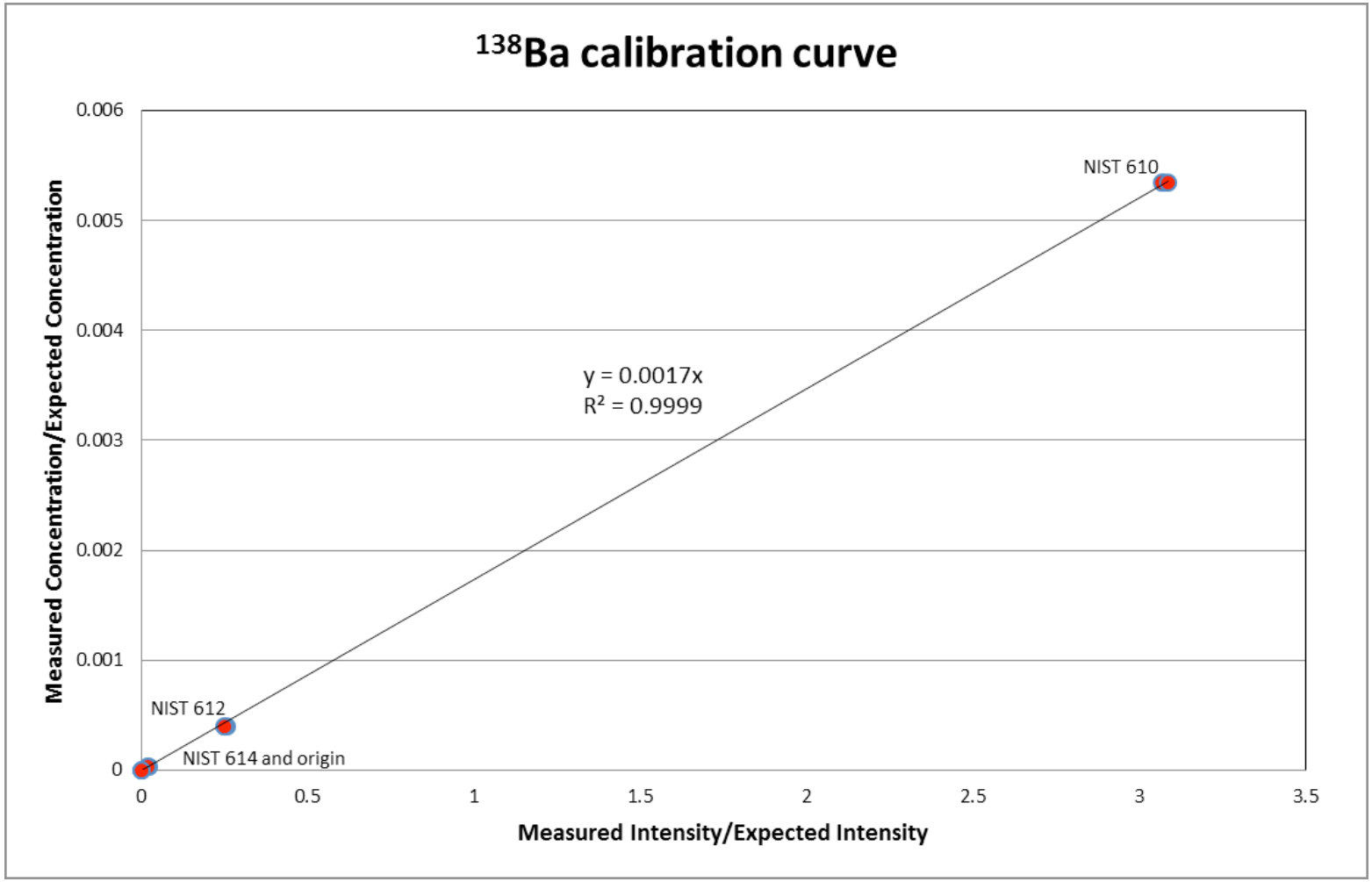

Figure 3. Example calibration curve plot of the three NIST glass standard reference materials, 610, 612, and 614. The regression line has been forced through the origin.

3.2 Descriptive Statistics

A summary of all estimated concentrations was compiled into Table 3.

Table 3. Summary of estimated elemental concentrations in parts per million. Ranges, averages and sample standard deviations are given.

	Minimum	Maximum	Average	s
^{24}Mg	27.739	568.174	128.299	73.232
^{55}Mn	0.195	5.092	1.267	0.848
^{63}Cu	0.042	9.816	0.378	0.689
^{64}Zn	0.154	5.463	0.748	0.682
^{87}Sr	1.553	7965.301	6322.841	727.456
^{89}Y	3.93E-03	0.380	4.22E-02	3.18E-02
^{90}Zr	5.14E-05	0.473	4.20E-02	5.20E-02
^{138}Ba	3.415	27.224	7.874	4.066
^{207}Pb	0.025	5.589	0.174	0.482
^{238}U	1.77E-05	1.098	2.37E-02	6.41E-02

As a reminder, the subdata is a subset of the total dataset as described in the methods. A summary of the element to calcium (Me/Ca) measurements for the subdata was compiled into Table 4 and a summary of the estimated concentrations for the subdata was compiled into Table 5.

Table 4. Summary of element/calcium ratio values in millimol per mol. Ranges, averages, and sample standard deviation are given.

	Minimum	Maximum	Average	s
^{24}Mg	0.105	0.524	0.198	0.077
^{55}Mn	3.43E-04	9.73E-03	2.41E-03	1.72E-03
^{63}Cu	5.44E-05	4.51E-03	1.61E-04	3.20E-04
^{64}Zn	1.22E-04	3.44E-03	3.63E-04	2.84E-04
^{87}Sr	1.031	1.426	1.208	0.077
^{89}Y	2.36E-05	1.11E-04	4.69E-05	1.09E-05
^{90}Zr	3.40E-06	1.03E-04	1.63E-05	1.38E-05
^{138}Ba	5.04E-03	3.25E-02	1.28E-02	5.58E-03
^{207}Pb	1.41E-05	2.72E-04	5.73E-05	2.97E-05
^{238}U	5.19E-06	1.49E-04	3.17E-05	2.80E-05

Table 5. Summary of estimated elemental concentrations in parts per million of the subdata. Ranges, averages, and sample standard deviations are given.

	Minimum	Maximum	Average	s
^{24}Mg	86.575	568.174	158.422	73.860
^{55}Mn	0.195	5.092	1.186	0.915
^{63}Cu	0.042	3.623	0.195	0.507
^{64}Zn	0.154	4.545	0.487	0.557
^{87}Sr	5632.021	7743.052	6642.988	437.763
^{89}Y	2.00E-02	0.132	4.31E-02	1.53E-02
^{90}Zr	6.44E-03	0.473	3.45E-02	5.41E-02
^{138}Ba	3.415	27.224	9.081	4.659
^{207}Pb	0.026	5.589	0.177	0.694
^{238}U	1.77E-05	1.098	2.25E-02	1.11E-01

3.3 Assumptions

Normalcy and homoscedasticity were examined for the subdata. Figure 4 shows a histogram where the red line is an overlay of a true normal distribution for comparison. The data, although slightly skewed, is approaching normality and it is assumed that the overall population meets the normalcy requirement, despite the sample size being small.

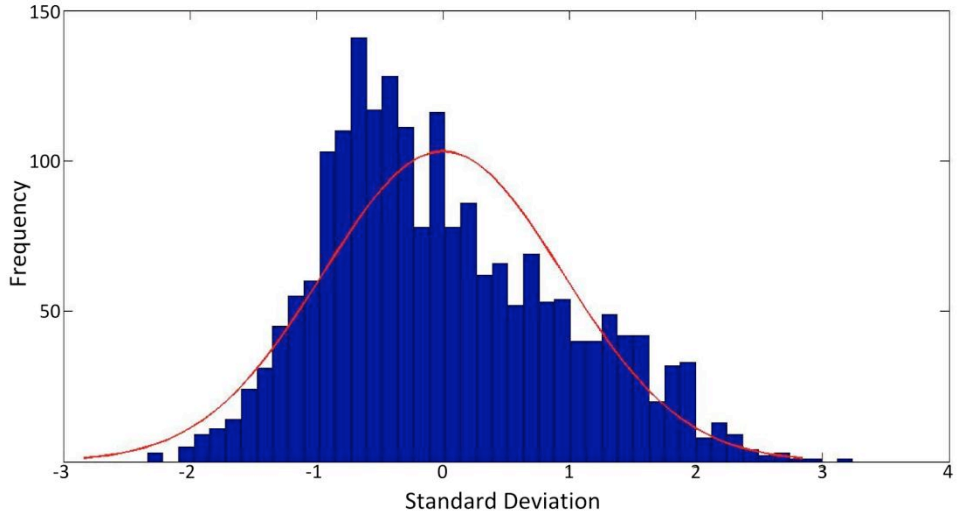

Figure 4. Histogram of subdata with a normal distribution overlay.

Additionally, a quantile-quantile plot of the subdata is shown in Figure 5. Again, the subdata perform reasonably well versus a standard normal distributions with some deviations at the tails.

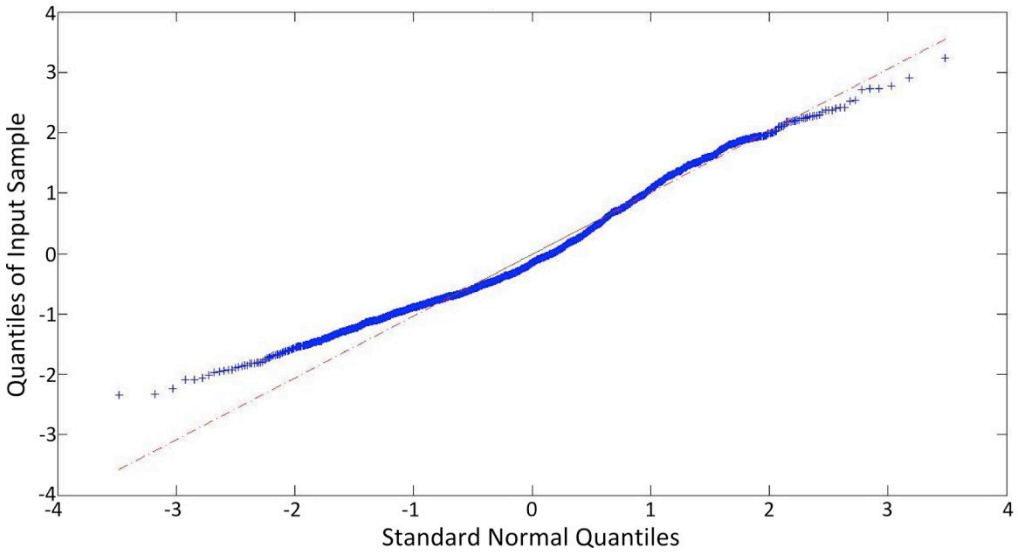

Figure 5. QQ plot of subdata against a standard normal distribution.

Homoscedasticity, or homogeneous variances, was verified using Barlett's test and the results are presented in Table 6. The null hypothesis for this test is similar to a t-test: H_o= variances are the same. With $p \geq 0.05$, the null hypothesis cannot be rejected and the assumption of homogeneous variances is met.

Table 6. Bartlett's test for homogeneous variances results for the subdata.

Group	Count	Mean	Std Dev
1	535	-1.87E-11	0.9240
2	612	1.63E-12	0.9505
3	874	4.58E-12	0.9597
Pooled	2021	-2.47E-12	0.9473

Barlett's statistic	1.014
Degrees of freedom	2
p-value	0.602

3.4 Spatial Variation of Elements

The following figures (Figures 6-15) plot the means of each Me/Ca ratio for each ablation spot for the three geographic locations as calculated using the subdata. Error bars represent the 95% confidence interval for each mean. Means and confidence intervals for the 8th spot were not plotted for two reasons: there were only four statoliths large enough to support an 8th ablation; and they were all from the California samples, which prevents comparison to the other populations.

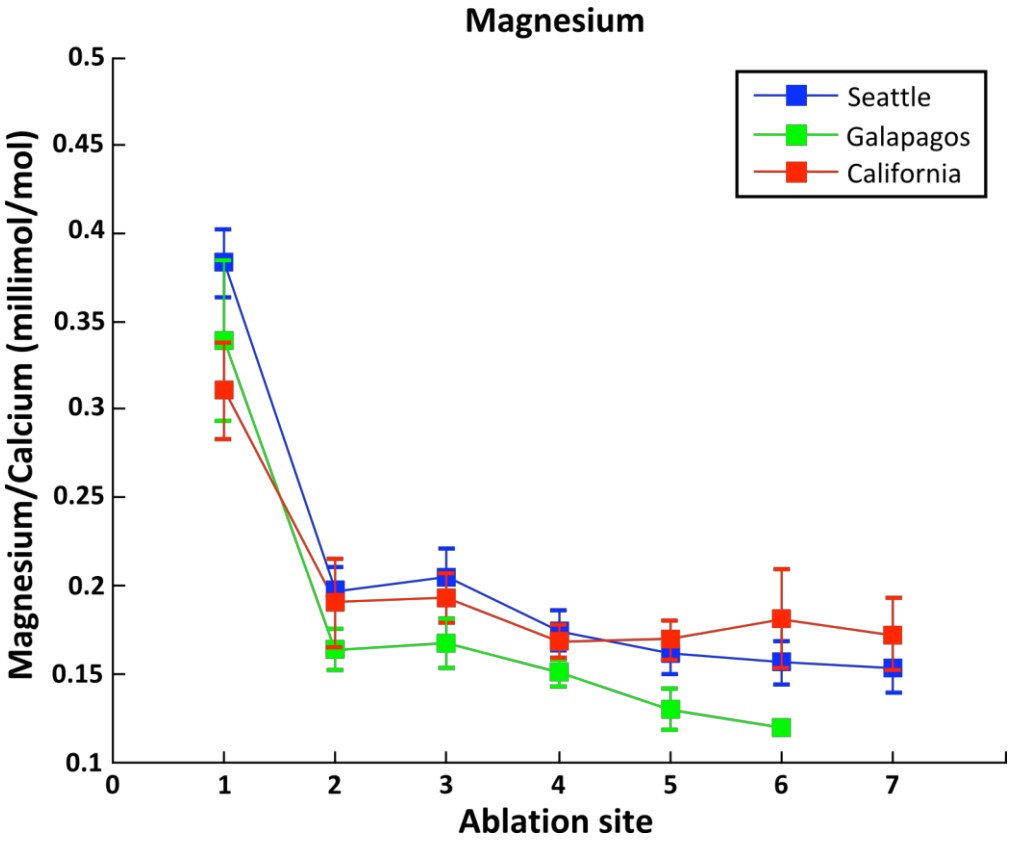

Figure 6. Average magnesium/calcium ratios with 95% confidence intervals for three geographic regions.

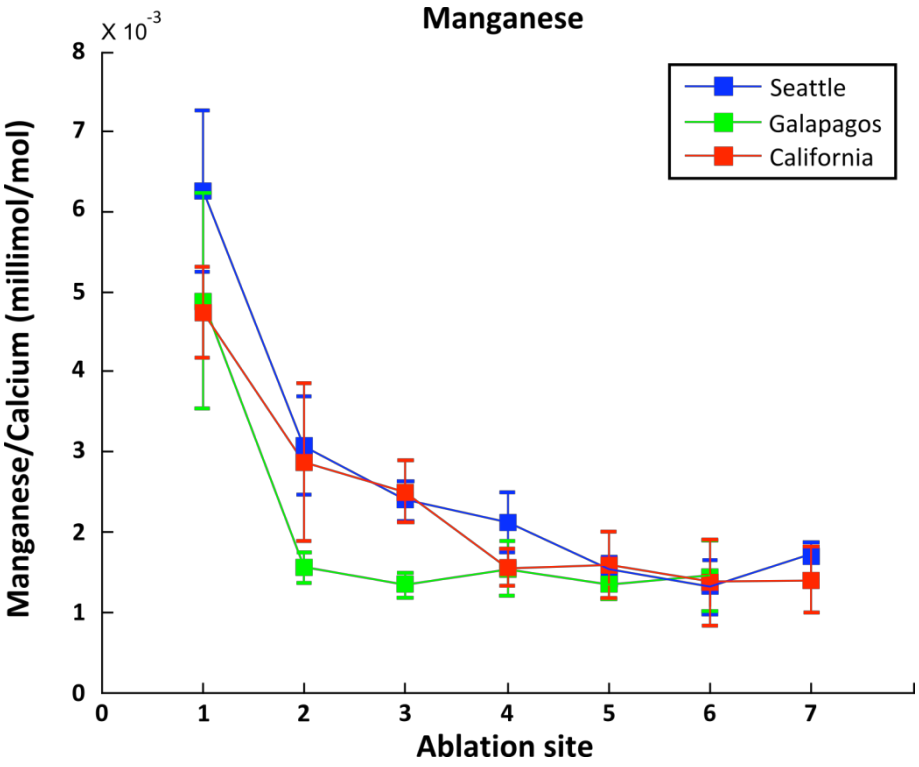

Figure 7. Average maganese/calcium ratios with 95% confidence intervals for three geographic regions.

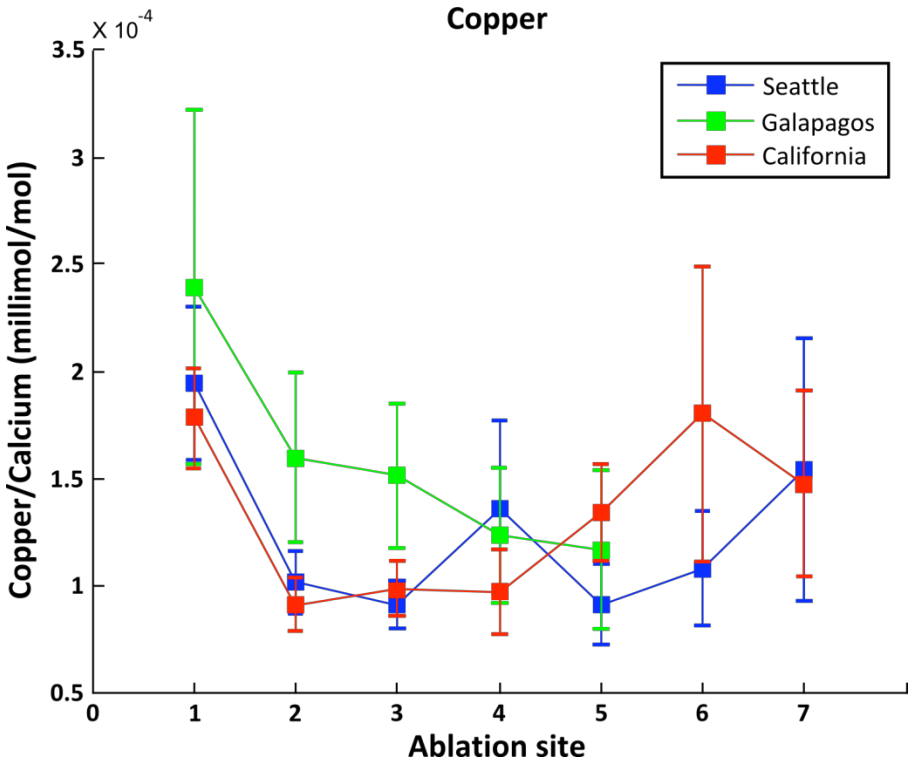

Figure 8. Average copper/calcium ratios with 95% confidence intervals for three geographic regions.

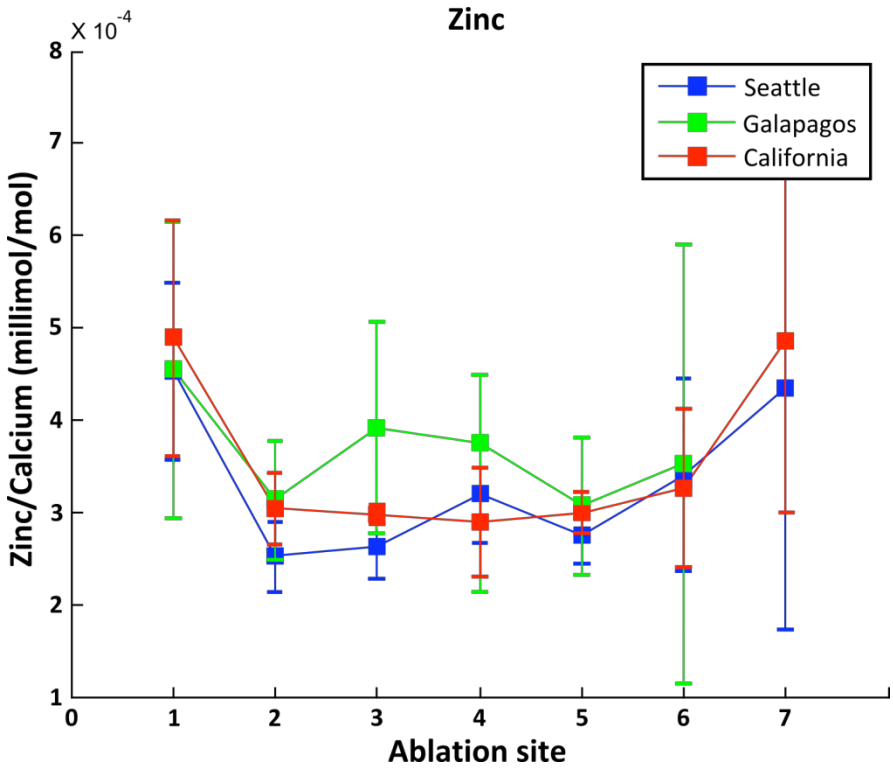

Figure 9. Average zinc/calcium ratios with 95% confidence intervals for three geographic regions.

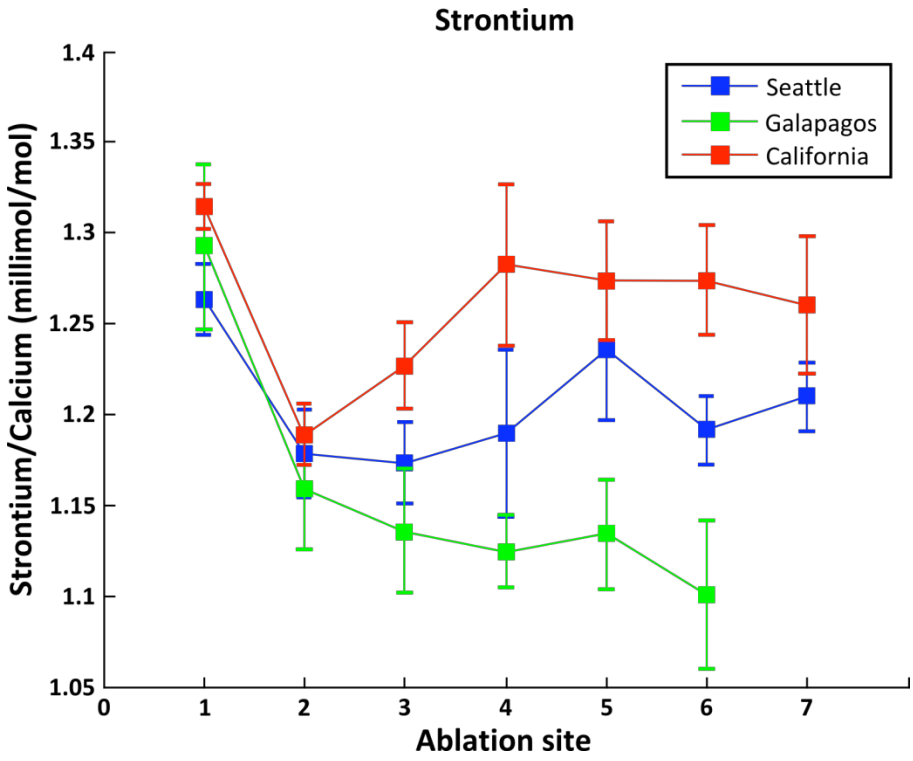

Figure 10. Average strontium/calcium ratios with 95% confidence intervals for three geographic regions.

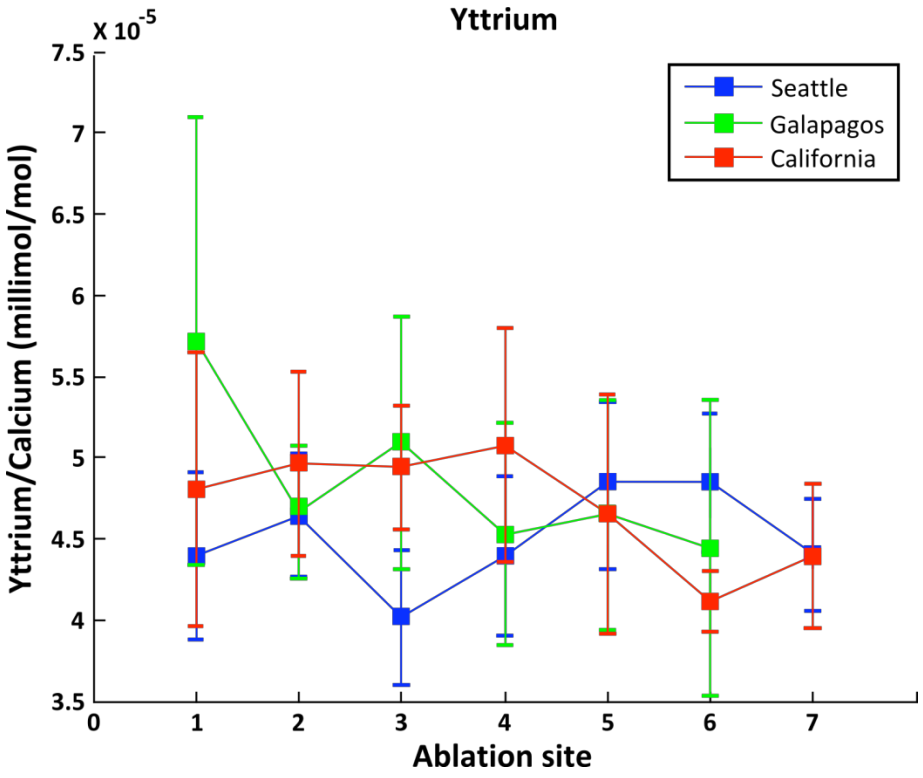

Figure 11. Average yttrium/calcium ratios with 95% confidence intervals for three geographic regions.

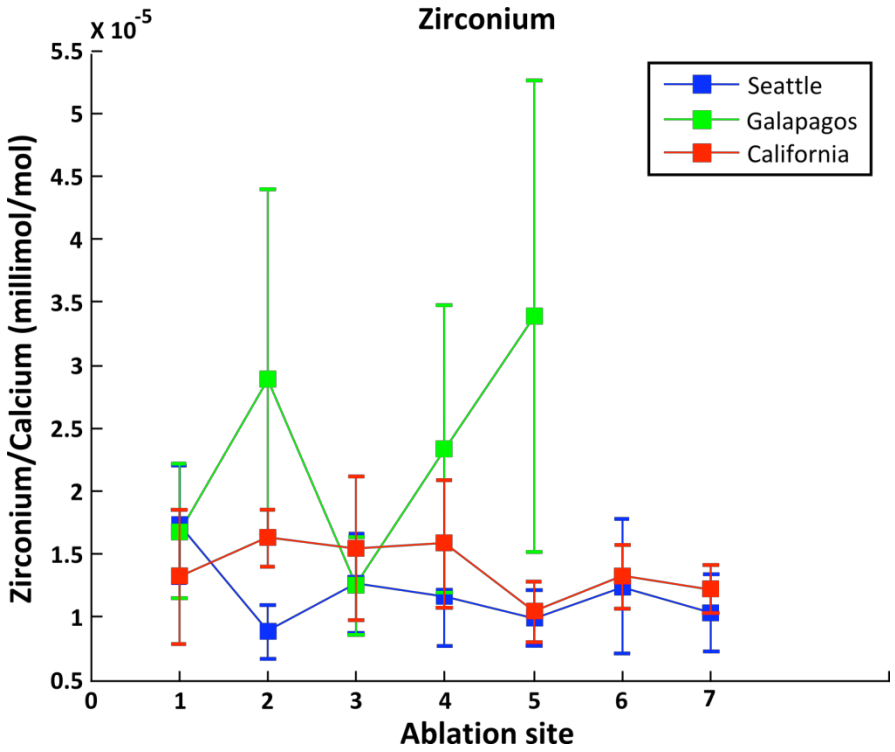

Figure 12. Average zirconium/calcium ratios with 95% confidence intervals for three geographic regions.

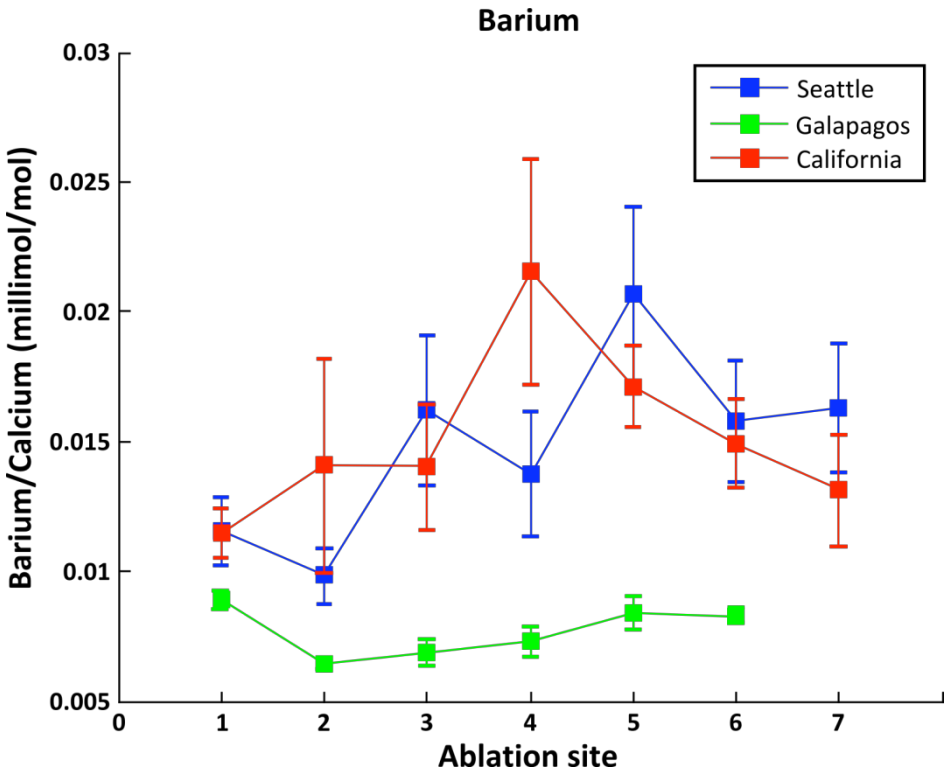

Figure 13. Average barium/calcium ratios with 95% confidence intervals for three geographic regions.

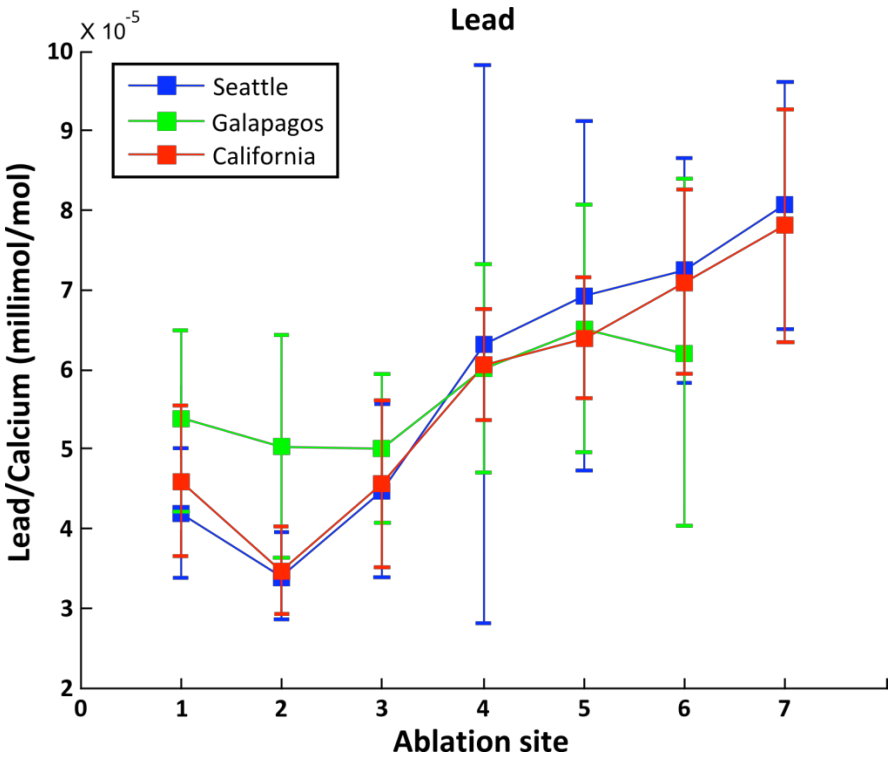

Figure 14. Average lead/calcium ratios with 95% confidence intervals for three geographic regions.

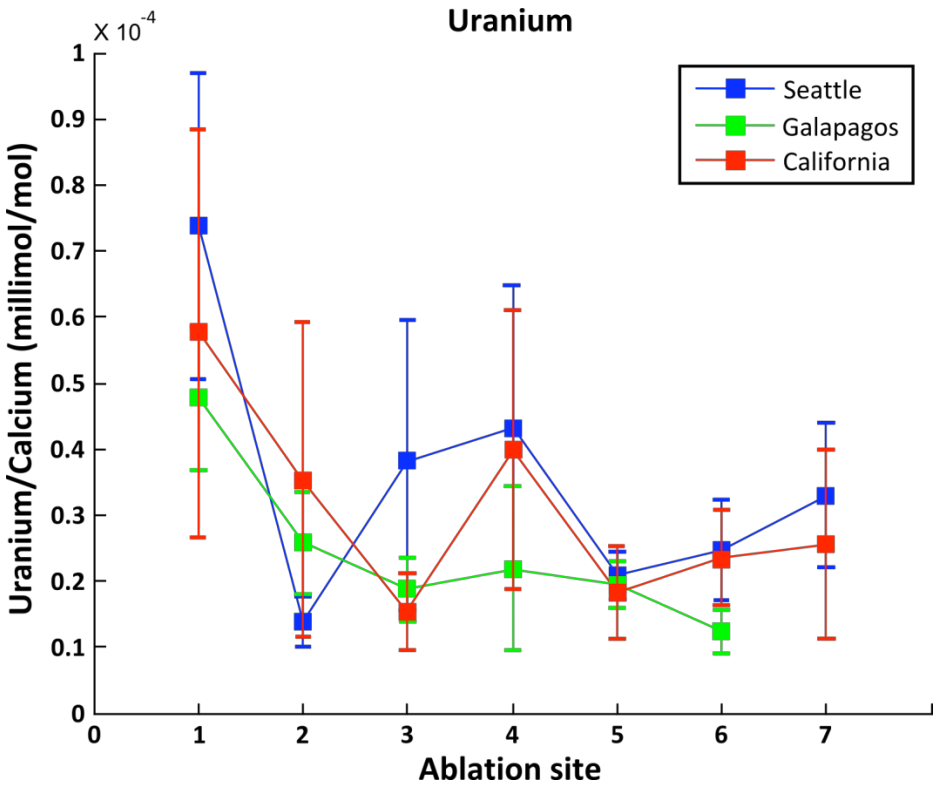

Figure 15. Average uranium/calcium ratios with 95% confidence intervals for three geographic regions.

3.5 Analysis of Variance

ANOVA results are compiled in Table 7. Each element was evaluated separately for each geographic location. The 8th ablation spots were again left out of this analysis. Significant p-values ($\alpha \leq 0.05$) are highlighted representing a variation is present in the Me/Ca across the statolith. Post-hoc Tukey HSD multiple comparisons were examined to isolate which ablation spots exhibited significant differences. The results will be discussed in the following section.

Two-way ANOVA revealed no interaction effects between specimen and elements by spot for any of the three geographic regions. Significant differences were confirmed among element spots with $p<0.0001$ for all three geographic regions. Interestingly the Galapagos specimens and Seattle specimens did show significant variations indicating mixed cohorts were present for these groups. This is supported by the back-calculated hatch date data from the growth ring age estimations.

To examine variation between two specific ablation spots, Analysis of Variance was performed again using only element to calcium ratios in the core and the final spot and once more on the second ablation spot and the final spot. Again, the final spot is defined as the last ablation spot with a value for every statolith observation making the final spot for statoliths from California and Seattle the 6th and for the Galapagos the 5th. These results are compiled in Tables 8 and 9.

Table 7. Summary of Analysis of Variance for each Me/Ca for ablation spots 1 through 6 or 7 for each of the three geographic locations. Significant p-values ($\alpha \leq 0.05$) are bold and highlighted. Any p-values smaller than $1x10^{-4}$ are listed as <0.0001.

	Seattle				California				Galapagos			
	df	MS	F value	p value	df	MS	F value	p value	df	MS	F value	p value
^{24}Mg	6	8.62E-02	126.384	**<0.0001**	6	1.79E-02	21.163	**<0.0001**	5	7.16E-02	44.567	**<0.0001**
^{55}Mn	6	4.00E-05	42.157	**<0.0001**	6	1.18E-05	18.575	**<0.0001**	5	2.31E-05	18.880	**<0.0001**
^{63}Cu	6	1.74E-08	5.071	**0.0002**	6	1.12E-08	5.588	**0.0002**	5	2.89E-08	2.868	**0.0225**
^{64}Zn	6	7.77E-08	2.270	**0.0451**	6	5.88E-08	3.934	**0.0031**	5	3.72E-08	0.924	0.472
^{87}Sr	6	1.44E-02	4.689	**0.0004**	6	1.20E-02	6.554	**<0.0001**	5	5.36E-02	14.295	**<0.0001**
^{89}Y	6	1.14E-10	1.674	0.138	6	9.25E-11	1.331	0.263	5	2.46E-10	1.118	0.361
^{90}Zr	6	5.07E-11	1.065	0.392	6	5.85E-11	2.082	0.075	5	8.59E-10	1.872	0.120
^{138}Ba	6	1.68E-04	8.420	**<0.0001**	6	8.23E-05	5.217	**0.0004**	5	1.05E-05	15.340	**<0.0001**
^{207}Pb	6	3.86E-09	3.453	**0.0044**	6	1.72E-09	10.014	**<0.0001**	5	4.30E-10	0.865	0.511
^{238}U	6	4.59E-09	5.406	**0.0001**	6	1.53E-09	2.481	**0.0382**	5	1.53E-09	7.198	**<0.0001**

Table 8. Summary of Analysis of Variance for each Me/Ca for ablations at the core versus the last spot for each of the three geographic locations. Significant p-values ($\alpha \leq 0.05$) are in bold and highlighted. Any p-values smaller than $1x10^{-4}$ are listed as <0.0001.

	Seattle				California				Galapagos			
	df	MS	F value	p value	df	MS	F value	p value	df	MS	F value	p value
^{24}Mg	1	3.16E-01	333.700	**<0.0001**	1	6.18E-02	59.375	**<0.0001**	1	2.52E-01	68.836	**<0.0001**
^{55}Mn	1	1.20E-04	54.485	**<0.0001**	1	3.83E-05	74.686	**<0.0001**	1	7.20E-05	23.780	**<0.0001**
^{63}Cu	1	8.84E-09	1.334	0.2616	1	3.34E-09	1.785	0.2064	1	8.65E-08	6.572	**0.0181**
^{64}Zn	1	2.09E-09	0.022	0.8829	1	2.87E-11	0.001	0.9797	1	1.24E-07	2.498	0.1289
^{87}Sr	1	1.70E-02	14.598	**0.0009**	1	9.52E-03	8.103	**0.0159**	1	1.50E-01	29.835	**<0.0001**
^{89}Y	1	9.39E-15	0.000	0.9904	1	5.42E-11	0.645	0.4388	1	6.53E-10	1.714	0.2047
^{90}Zr	1	4.90E-12	0.159	0.6952	1	1.68E-10	5.046	**0.0443**	1	1.23E-09	2.641	0.1250
^{138}Ba	1	1.39E-04	12.080	**0.0020**	1	8.94E-06	2.139	0.1716	1	1.58E-06	1.937	0.1786
^{207}Pb	1	8.58E-09	19.697	**0.0002**	1	3.34E-09	13.782	**0.0034**	1	7.33E-10	1.373	0.2544
^{238}U	1	9.05E-09	8.378	**0.0090**	1	3.01E-09	2.619	0.13664	1	4.35E-09	19.992	**0.0002**

Table 9. Summary of Analysis of Variance for each Me/Ca at the second ablation spot versus the last spot for each of the three geographic locations. Significant p-values ($\alpha \leq 0.05$) are in bold and highlighted. Any p-values smaller than $1x10^{-4}$ are listed as <0.0001.

	Seattle				California				Galapagos			
	df	MS	F value	p value	df	MS	F value	p value	df	MS	F value	p value
^{24}Mg	1	1.15E-02	22.810	**0.0001**	1	1.10E-03	1.083	0.3185	1	6.53E-03	16.046	**0.0006**
^{55}Mn	1	1.07E-05	13.273	**0.0014**	1	7.39E-06	5.789	**0.0332**	1	2.61E-07	2.252	0.1477
^{63}Cu	1	1.50E-08	3.128	0.0922	1	1.08E-08	7.521	**0.0178**	1	1.05E-08	2.341	0.1410
^{64}Zn	1	1.82E-07	2.200	0.1536	1	1.15E-07	4.709	0.050794	1	2.17E-10	0.015	0.9034
^{87}Sr	1	6.02E-03	3.674	0.0678	1	1.64E-02	12.504	**0.0047**	1	3.74E-03	1.122	0.3011
^{89}Y	1	3.31E-11	0.745	0.3973	1	1.11E-10	2.120	0.1710	1	1.77E-13	0.002	0.9660
^{90}Zr	1	9.04E-11	7.071	**0.0151**	1	7.23E-12	0.638	0.4414	1	1.08E-10	0.161	0.6938
^{138}Ba	1	2.40E-04	23.024	**<0.0001**	1	3.11E-06	0.131	0.7236	1	2.16E-05	30.301	**<0.0001**
^{207}Pb	1	1.29E-08	34.834	**<0.0001**	1	6.45E-09	36.934	**<0.0001**	1	1.26E-09	1.936	0.1787
^{238}U	1	1.94E-09	11.241	**0.0033**	1	2.75E-10	0.377	0.5530	1	2.19E-10	1.853	0.1886

3.6 Multivariate Analysis of Variance

Multivariate Analysis of Variance (MANOVA) was used to evaluate differences in the overall elemental signatures among the three geographic regions. MANOVA mathematics do not allow for empty values in the dataset. Empty values were present in the subdata for ablation spots 7 and 8 when statoliths were not large enough to allow for 8 ablation sites. Additional values were missing when elements measured returned values below the detection limit. These observations were condensed or removed. At this point, all zirconium measurements were removed as this element contained the greatest number of missing values due to readings below the detection limit. This final dataset includes 11 statoliths from the Galapagos, 8 from California and 11 from Seattle.

Results of MANOVA testing were compiled into Table 10. Again, the final ablation site for MANOVA is defined as the 5th ablation spot, since it was the last spot taken for all three groups.

3.7 Correspondence Analysis

Correspondence analysis (CA) was performed on the final dataset to visualize the relationships among elements and among individual squid. The results from this CA demonstrate that the first two dimensions reconstruct 98.09 % of the chi-square value (Table 11). Scores for each ablation for each individual squid are plotted on the first

Table 10. Summary of Multivariate Analysis of Variance using overall Me/Ca signatures for all three geographic locations and multiple comparisons between each pair of locations. Significant p-values ($\alpha \leq 0.05$) are in bold and highlighted. Any p-values smaller than $1x10^{-4}$ are listed as <0.0001.

	L	χ^2	df	p value
CORES	0.2043	36.5322	18	**0.0060**
2nd ablation	0.1735	40.2854	18	**0.0019**
5th ablation	0.1148	47.6146	18	**0.0002**

	California v Galapagos	California v Seattle	Galapagos v Seattle
CORES	0.0502	**0.0199**	**0.0033**
2nd ablation	**0.0185**	0.4081	**0.0042**
5th ablation	**<0.0001**	0.05721	**0.0424**
6th ablation	-	**0.0008**	-
7th ablation	-	**0.0110**	-

two dimensions in blue in Figure 16. Red spots represent the elements, ^{24}Mg ^{55}Mn ^{63}Cu ^{64}Zn ^{87}Sr ^{89}Y ^{138}Ba ^{207}Pb ^{238}U. Since there are five spots in this dataset for each squid, there are 145 observations for this figure. In order to clarify which observations are from each region, Figure 17 was created using the same data with geographic groups assigned the same color scheme used earlier. It is important to note that CA does not distinguish among the groups *a priori*, which is why the observations are traditionally monochromatic. The color scheme presented in Figure 17 is only for labeling purposes.

To simplify the relationships, CA was repeated combining the individuals in a mean for each region. This provides a visualization of the relationships among the elements and among the geographic regions by ablation location. The results show that 94.29% of the chi-square value can be reconstructed by the first two dimensions (Table 12). Again, the first two dimensions were used to plot the scores with red spots representing the elements in ascending value (Figure 18). Locations/spots are shown in blue. For clarity, a color scheme was added to the results in Figure 19.

Table 11. Correspondence analysis reconstruction of the final data.

Singular Value	Inertia	χ^2	Percent χ^2	Cumulative %
0.1180	0.0139	2.8624	87.14	87.64
0.0408	0.0017	0.3415	10.46	98.09
0.0148	0.0002	0.0450	1.38	99.47
0.0065	0.0000	0.0086	0.26	99.74
0.0043	0.0000	0.0039	0.12	99.85
0.0036	0.0000	0.0026	0.08	99.93
0.0030	0.0000	0.0019	0.06	99.99
0.0012	0.0000	0.0003	0.01	100
Total	0.0159	3.2662	100.00	

Table 12. Correspondence analysis reconstruction percent variance of the final data with individuals averaged by location.

Singular Value	Inertia	χ^2	Percent χ^2	Cumulative %
0.1011	0.0121	0.2608	92.26	92.26
0.0314	0.0010	0.0212	7.48	99.75
0.0052	0.0000	0.0006	0.21	99.96
0.0017	0.0000	0.0001	0.02	99.98
0.0011	0.0000	0.0000	0.01	99.99
0.0010	0.0000	0.0000	0.01	100
0.0006	0.0000	0.0000	0.00	100
0.0003	0.0000	0.0000	0.00	100
Total	0.0131	0.2827	100.00	

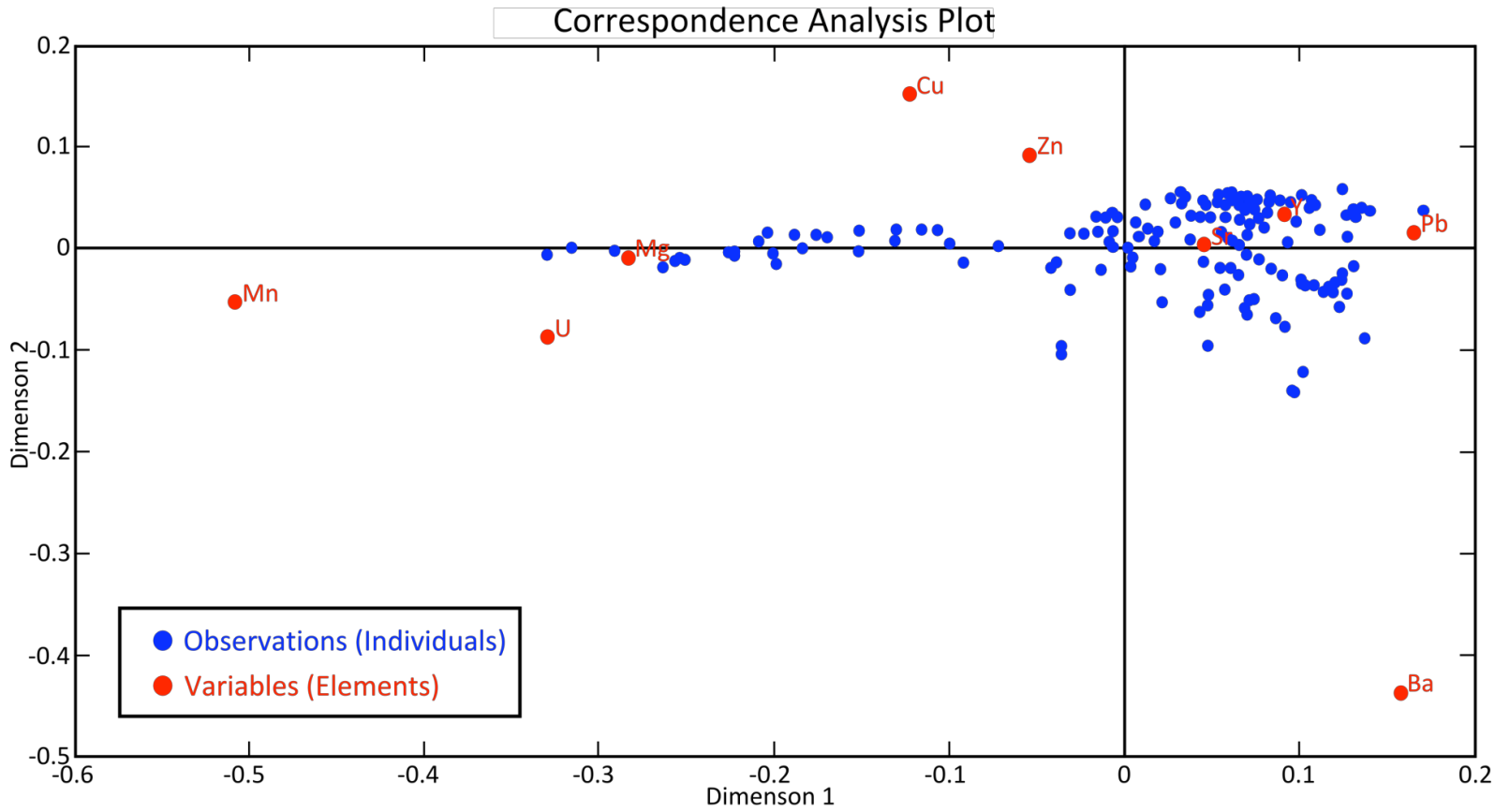

Figure 16. Plot of the first two dimensions for a correspondence analysis performed on the final data. Blue circles mark the score for each ablation spot for each of the individual squid. Red circles represent the 9 elements as labeled.

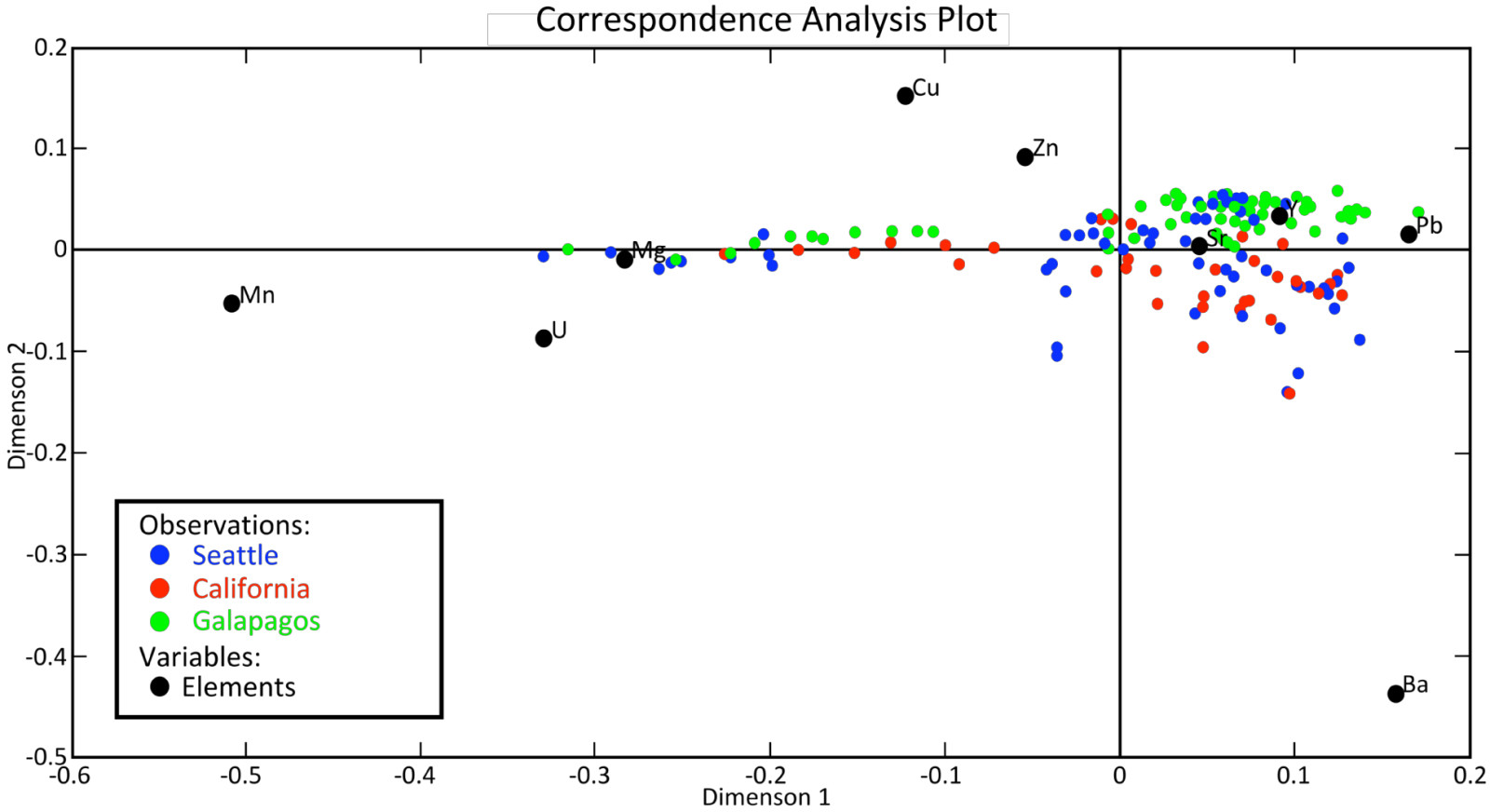

Figure 17. Plot of the first two dimensions for a correspondence analysis performed on the final data. Colored circles mark each ablation spot for each of the individual squid and each color represents one geographic region. Black circles represent the 9 elements as labeled.

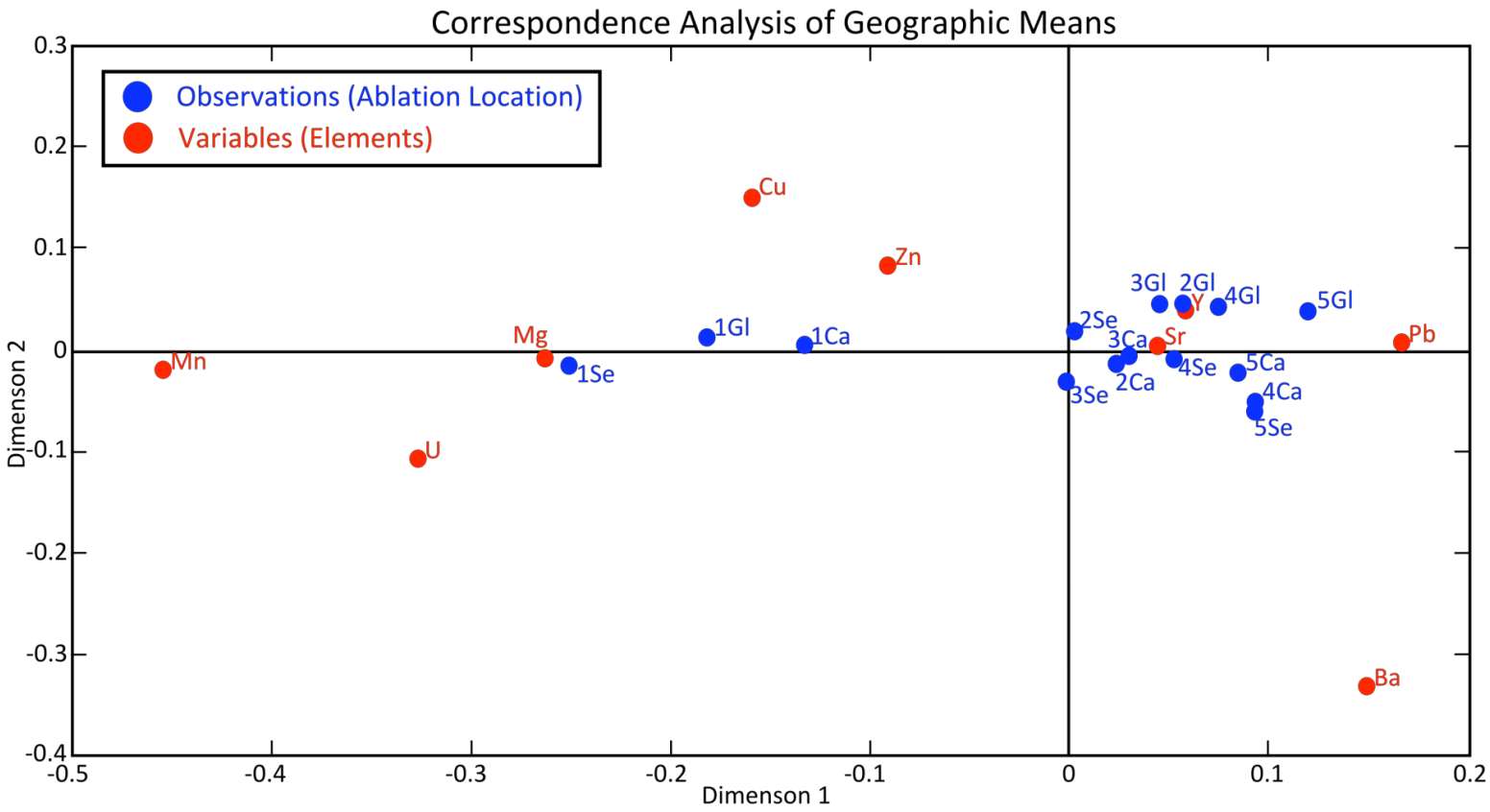

Figure 18. Plot of the first two dimensions for a correspondence analysis performed on the geographic means of the final dataset. Blue circles mark each ablation spot for each geographic region as labeled. Red circles represent the 9 elements as labeled.

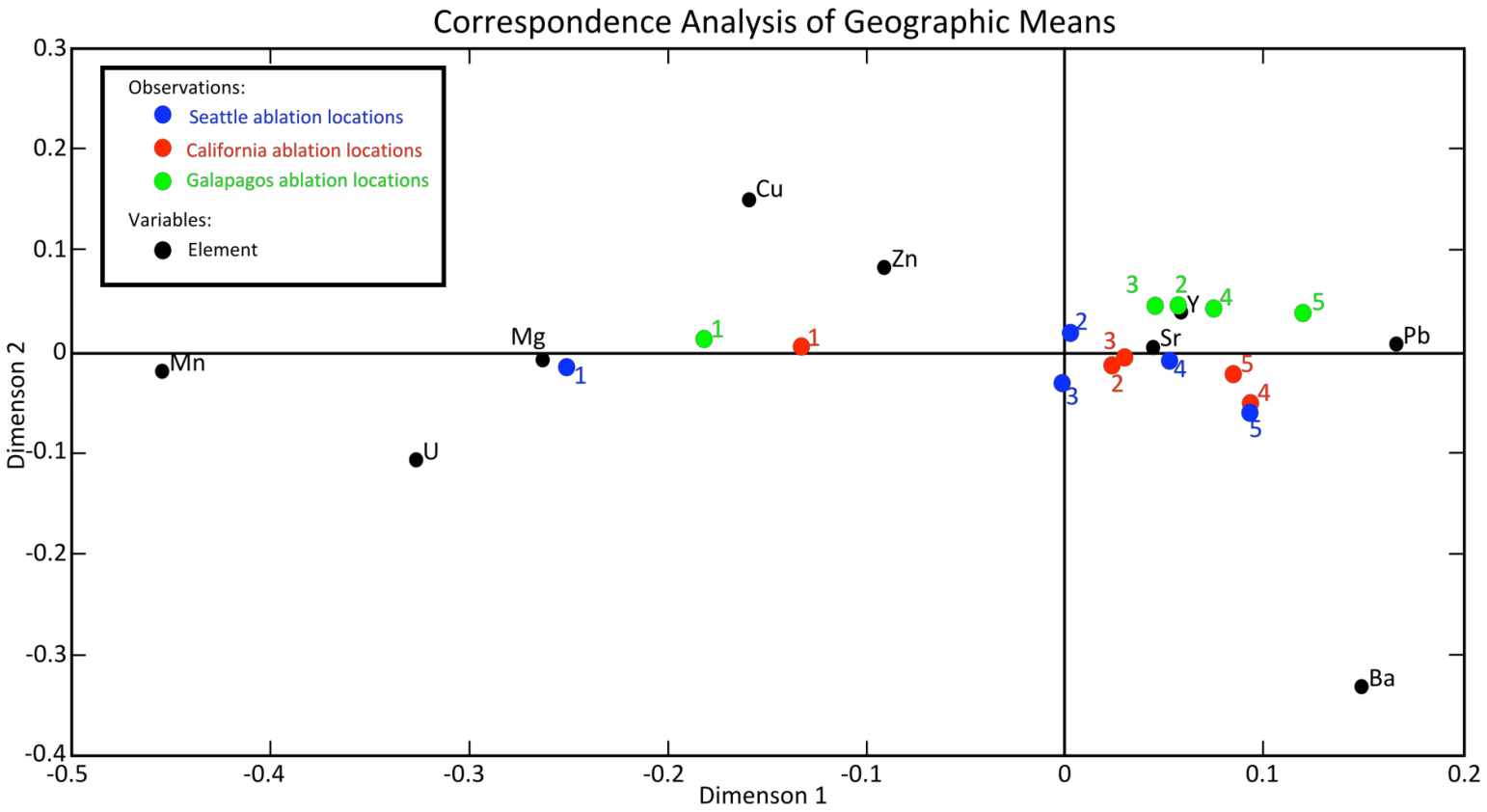

Figure 19. Plot of the first two dimensions for a correspondence analysis performed on the geographic means of the final dataset. Colored circles mark each ablation spot with one color representing each geographic region. Black circles represent the 9 elements as labeled.

3.8 Assumptions for Orientation

Normalcy and homoscedasticity were examined again after normalizing the data. Figure 20 shows a histogram where the red line is an overlay of a true normal distribution for comparison. The normalized data is a closer fit to the normal distribution than the subdata, and it is assumed that the overall population meets the normalcy requirement.

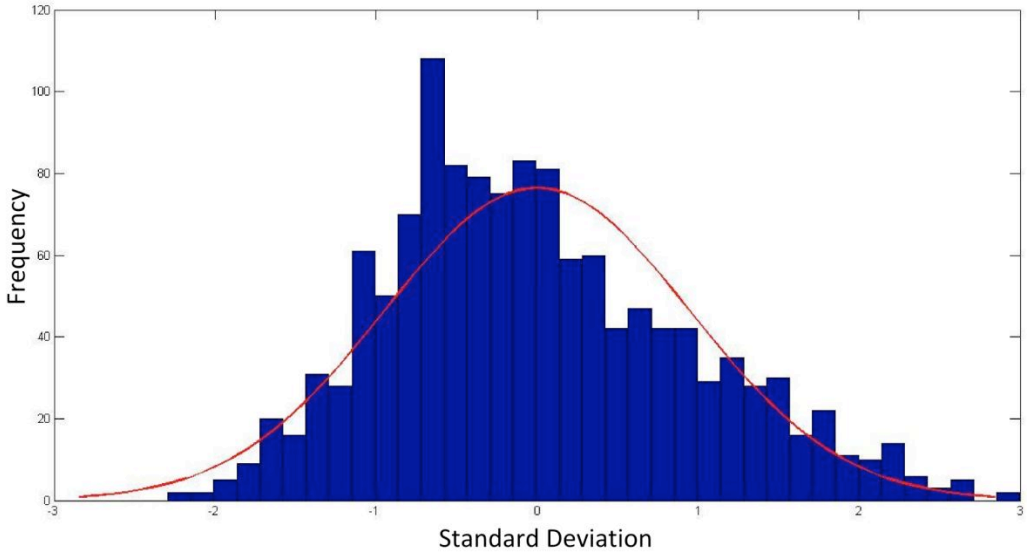

Figure 20. Histogram of the normalized data with a normal distribution overlay.

Again, a quantile-quantile plot of the normalized data was created (Figure 21). The normalized data again performs even better versus a standard normal distribution than the subdata did before normalization.

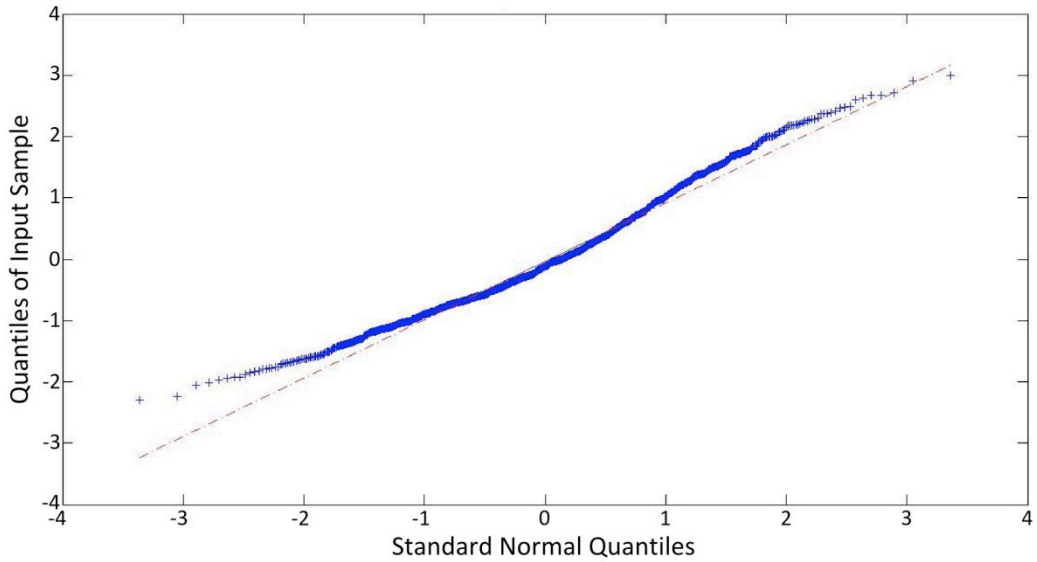

Figure 21. QQ plot of the normalized data against a standard normal distribution.

Homoscedasticity, or homogeneous variances, was again verified using Barlett's test and the results are presented in Table 13. The null hypothesis for this test is similar to a t-test where: H_0= variances are the same. With $p \geq 0.05$, the null hypothesis cannot be rejected and the assumption of homogeneous variances is met.

Table 13. Bartlett's test for homogeneous variances for the normalized data. The homoscedasticity assumption was met.

Group	Count	Mean	Std Dev
1	266	0.1545	0.37428
2	410	0.1522	0.36652
3	407	0.1693	0.38898
Pooled	1083	0.1592	0.37701

Barlett's statistic	1.473
Degrees of freedom	2
p-value	0.479

3.9 Principle Component Analysis

To maximize the results of the principle component analysis (PCA), the data was filtered and only select spots for each element were chosen from the normalized data. After examining the multiple comparisons and the XY plots with 95% confidence intervals, the following elements and the given ablation spots were selected: Magnesium, 1-5; Manganese, 2 and 3; Copper, 2,3, and 5; Strontium, 1,3,4,and 5; Yttrium, 3; Barium, 1-5; and Uranium, 2. All dimensions, percent variance explained and cumulative percent variance explained values are compiled in Table 14. A scree plot of the percent variance explained demonstrated a clear break between the first and second principle component (Figure 22). Since the first principle component only explains 40.68% of the variance, more components will be used to characterize the data. PCA showed that the first three dimensions explained 65.52% of the overall variance, which should provide a reasonable dimension reduction to represent any variations in the data.

To visualize the spatial distribution of the specimen and the variation in the elemental composition among the geographic regions, the scores for the specimen were plotted for the first three principle components in Figure 23. The principle component scores for each of the squid were plotted on the first two principle components in Figure 24, with 95% confidence ellipses for each of the three geographic locations: red for California, green for the Galapagos, and blue for Seattle. The id number for each squid relates it to the geographic region it was caught: 1-7 were collected off California; 8-18

off the Galapagos and 19-29 off Seattle. This was repeated for the first and third dimension and the second and third dimensions (Figures 25 and 26).

Table 14. Principle component analysis results showing the percent of the variance explained by each dimension and the cumulative percent explained.

Dimension	Percent Explained	Cumulative %
1	40.68	40.68
2	14.60	55.28
3	10.24	65.52
4	8.14	73.66
5	6.09	79.75
6	4.02	83.77
7	3.62	87.39
8	2.68	90.07
9	2.56	92.63
10	2.14	94.77
11	1.71	96.48
12	0.91	97.38
13	0.69	98.07
14	0.48	98.55
15	0.42	98.97
16	0.38	99.35
17	0.27	99.62
18	0.15	99.77
19	0.15	99.92
20	0.07	99.99
21	0.01	100.00

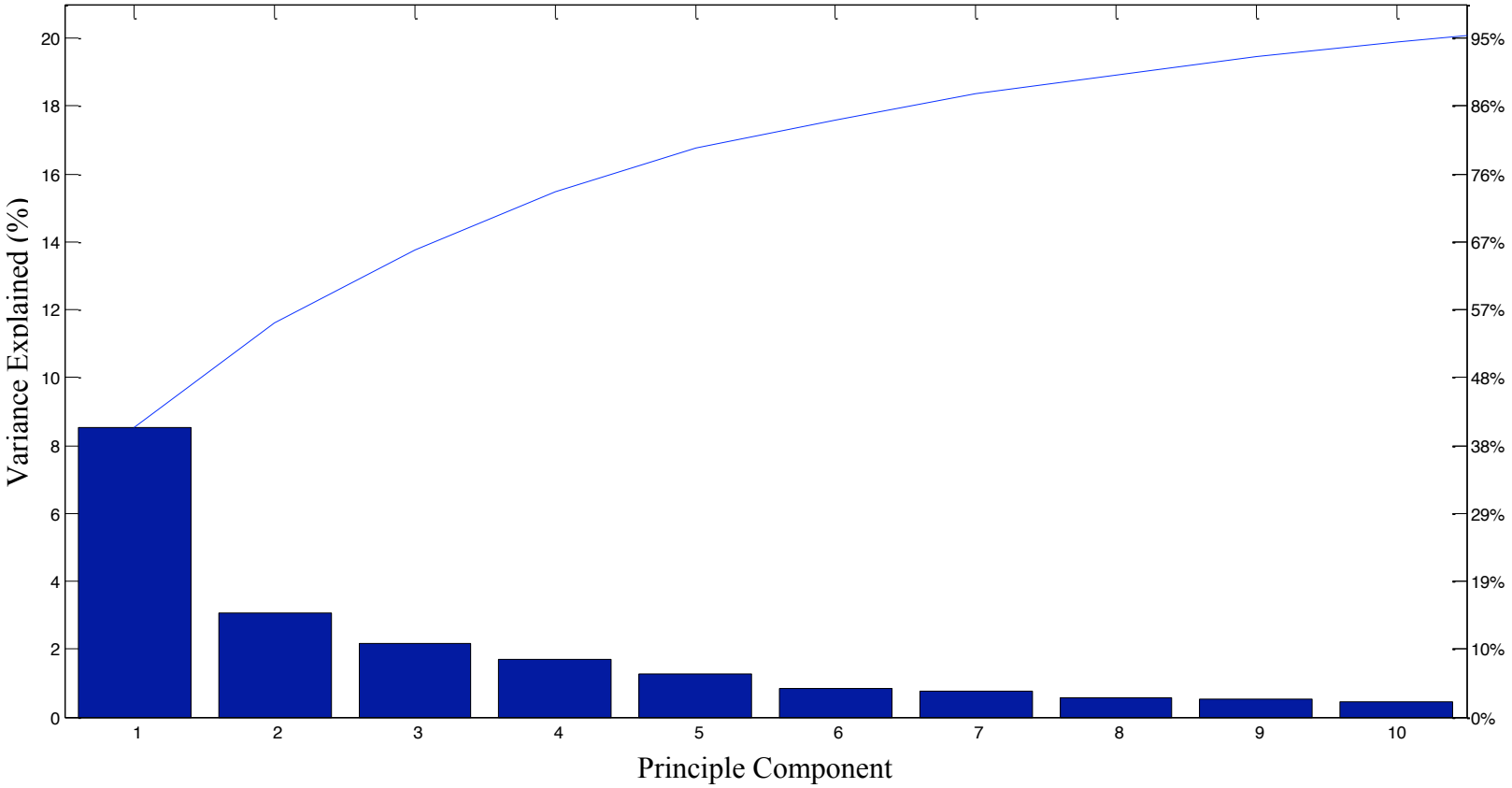

Figure 22. Scree plot of the percent variability explained by each of the first ten principal components.

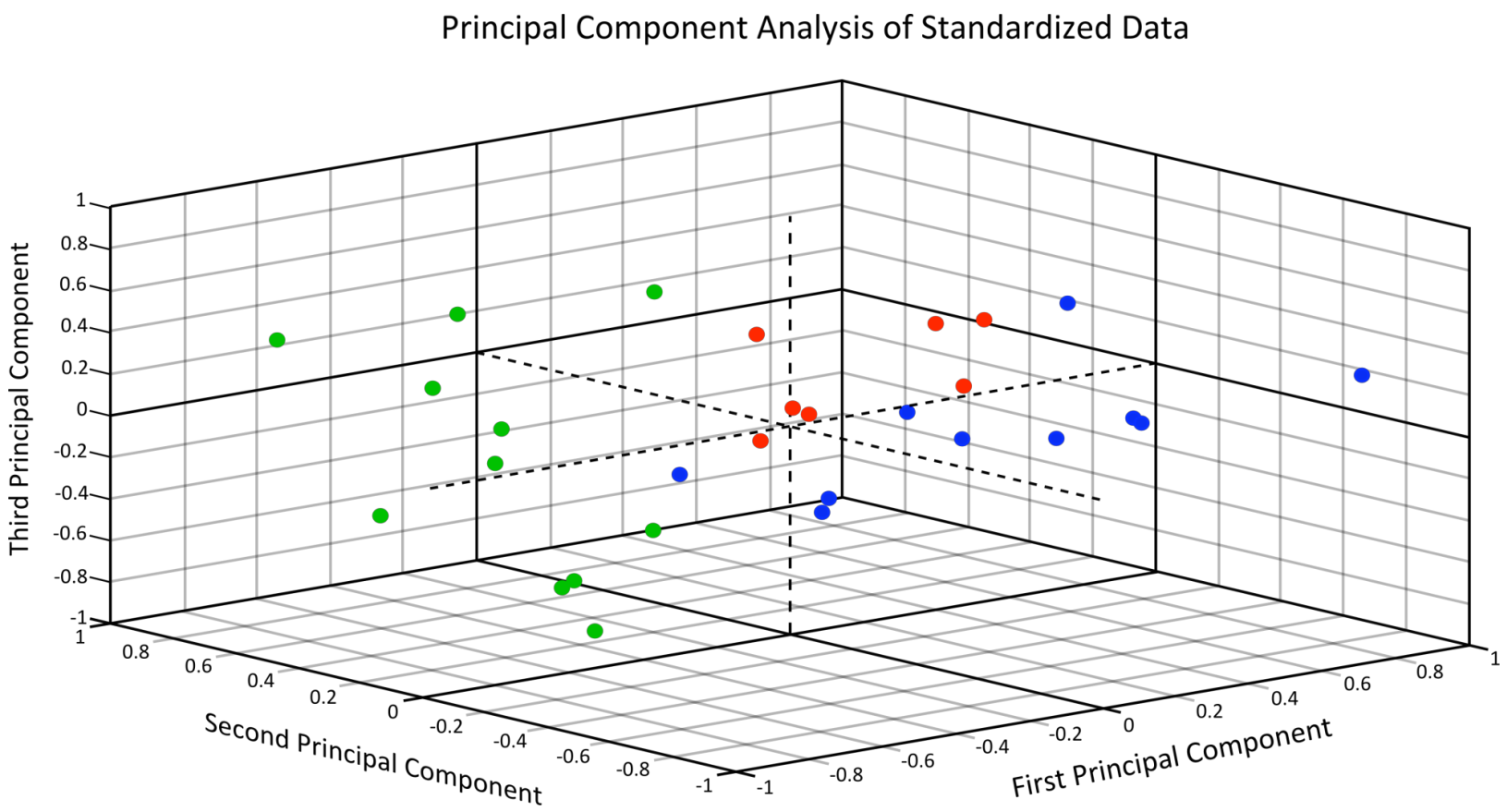

Figure 23. Three dimensional rendering of the first three principle components of the normalized final dataset. Blue lines represent the eigenvectors for each element spot used in the PCA. Green circles represent the specimen collected from the Galapagos, Red represents the specimen from California and blue are those from Seattle.

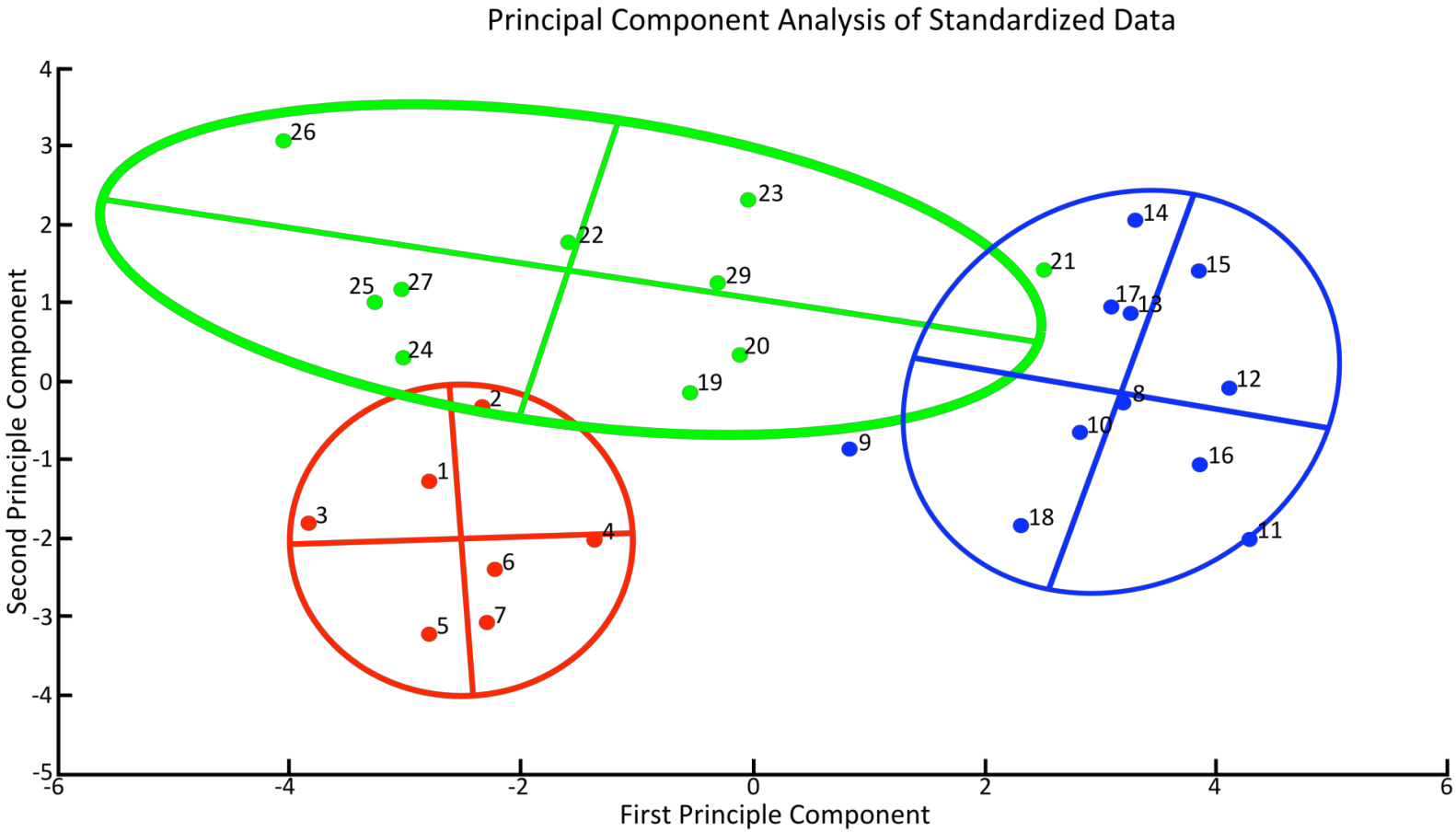

Figure 24. Plot of the first two principle components of the normalized final dataset. Markers 1-7 represent the scores of specimen collected in California and the 95% confidence ellipse is red. Markers 8-18 represent the scores of specimen collected in the Galapagos with a 95% confidence ellipse displayed in green. Markers 19-29 represent scores of specimen collected near Seattle with a blue 95% confidence ellipse.

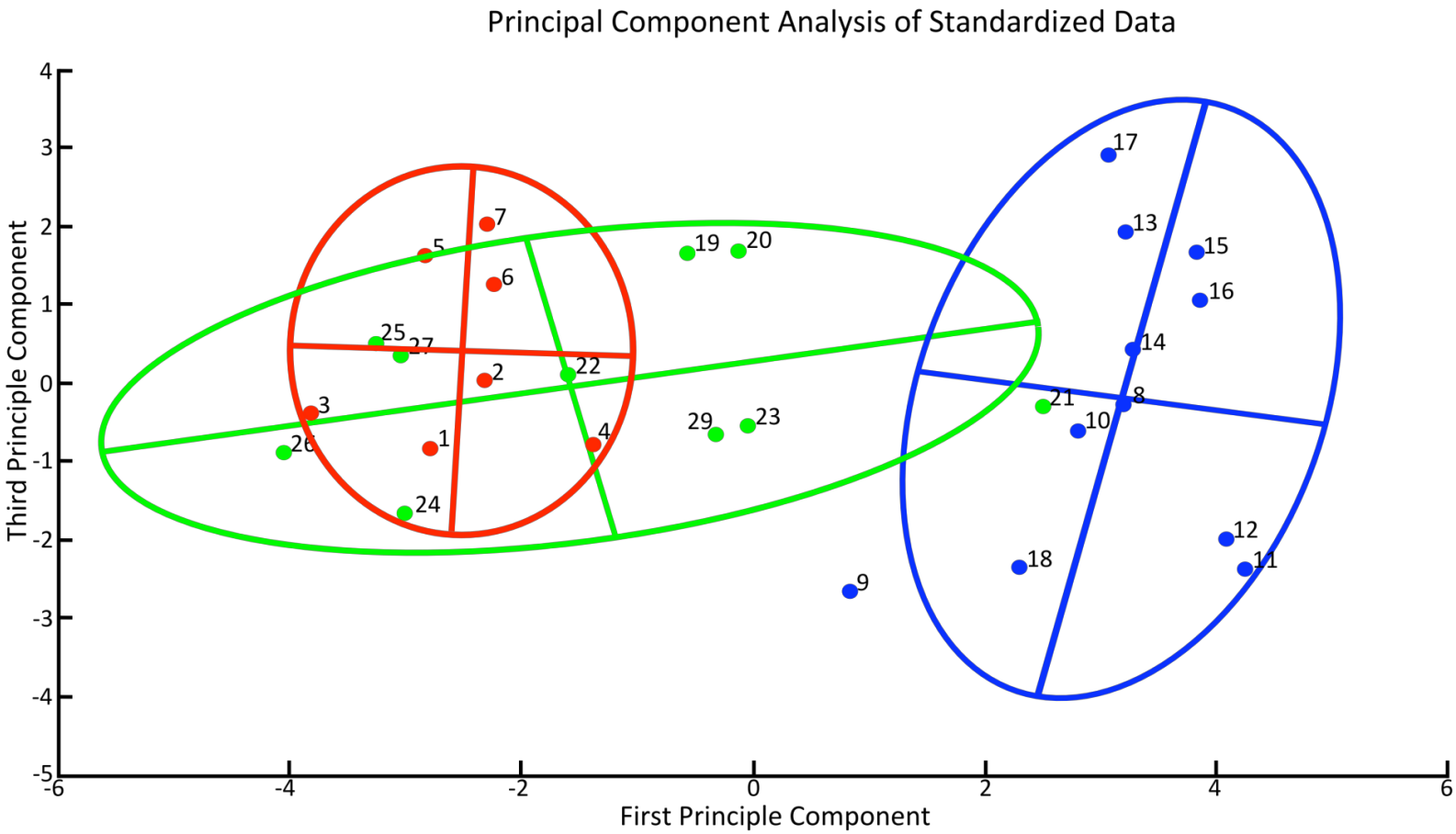

Figure 25. Plot of the first and third principle components of the normalized final dataset. Markers 1-7 represent the scores of specimen collected in California and the 95% confidence ellipse is red. Markers 8-18 represent the scores of specimen collected in the Galapagos with a 95% confidence ellipse displayed in green. Markers 19-29 represent scores of specimen collected near Seattle with a blue 95% confidence ellipse.

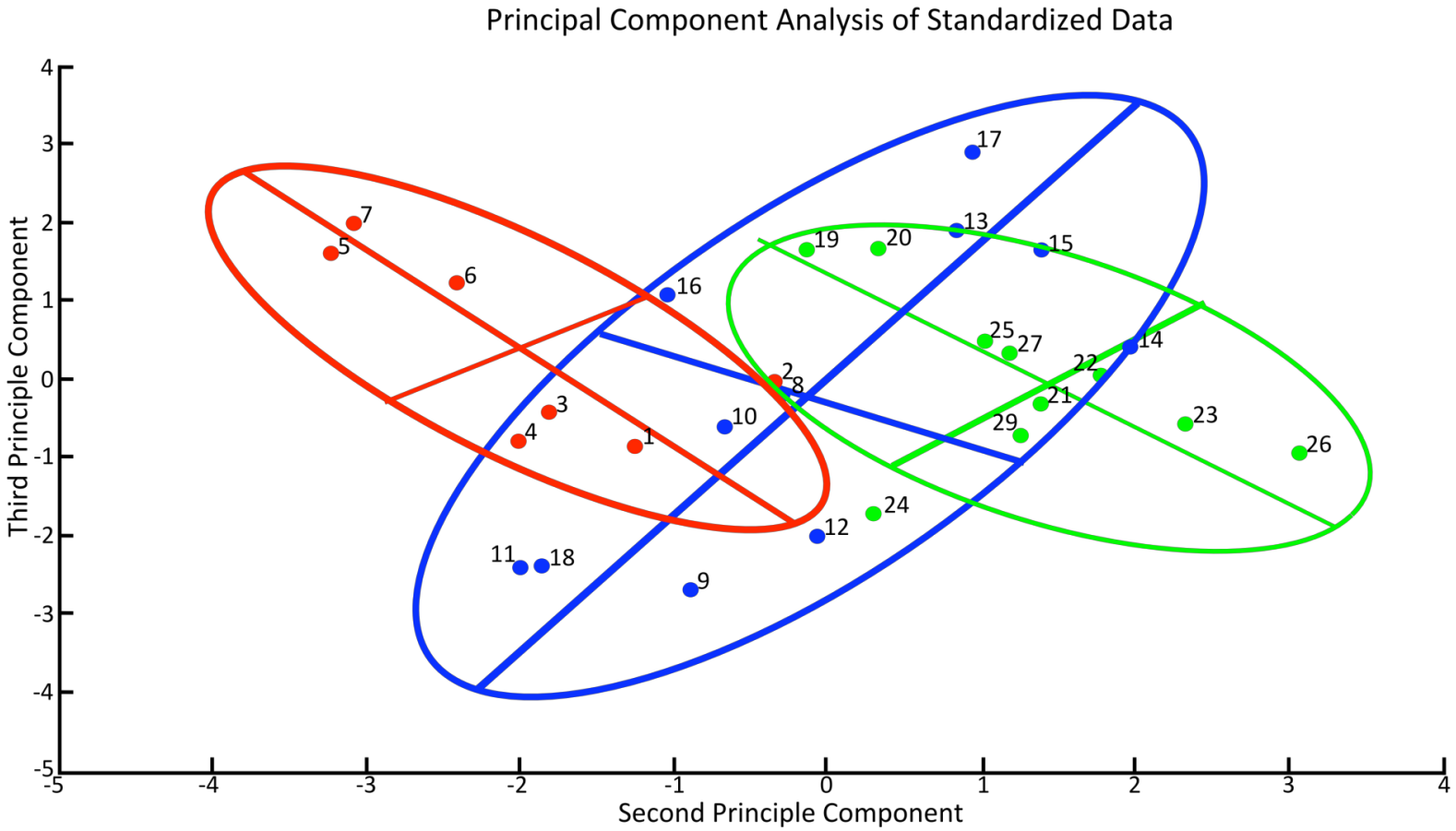

Figure 26. Plot of the second and third principle components of the normalized final dataset. Markers 1-7 represent the scores of specimen collected in California and the 95% confidence ellipse is red. Markers 8-18 represent the scores of specimen collected in the Galapagos with a 95% confidence ellipse displayed in green. Markers 19-29 represent scores of specimen collected near Seattle with a blue 95% confidence ellipse.

3.10 Discriminant Function Analysis

To quantify the success of using LA-ICP-MS for a population study of *D. gigas*, discriminant function analysis (DFA) was performed on the normalized data. The results show that the first two dimensions explain all of the variance in the elemental composition of the statolith among the three geographic regions (Figure 27). The jackknife reclassification success was 75.86%, p=0.0001, which rejects the null hypothesis that the reclassification success was no better than would occur by chance.

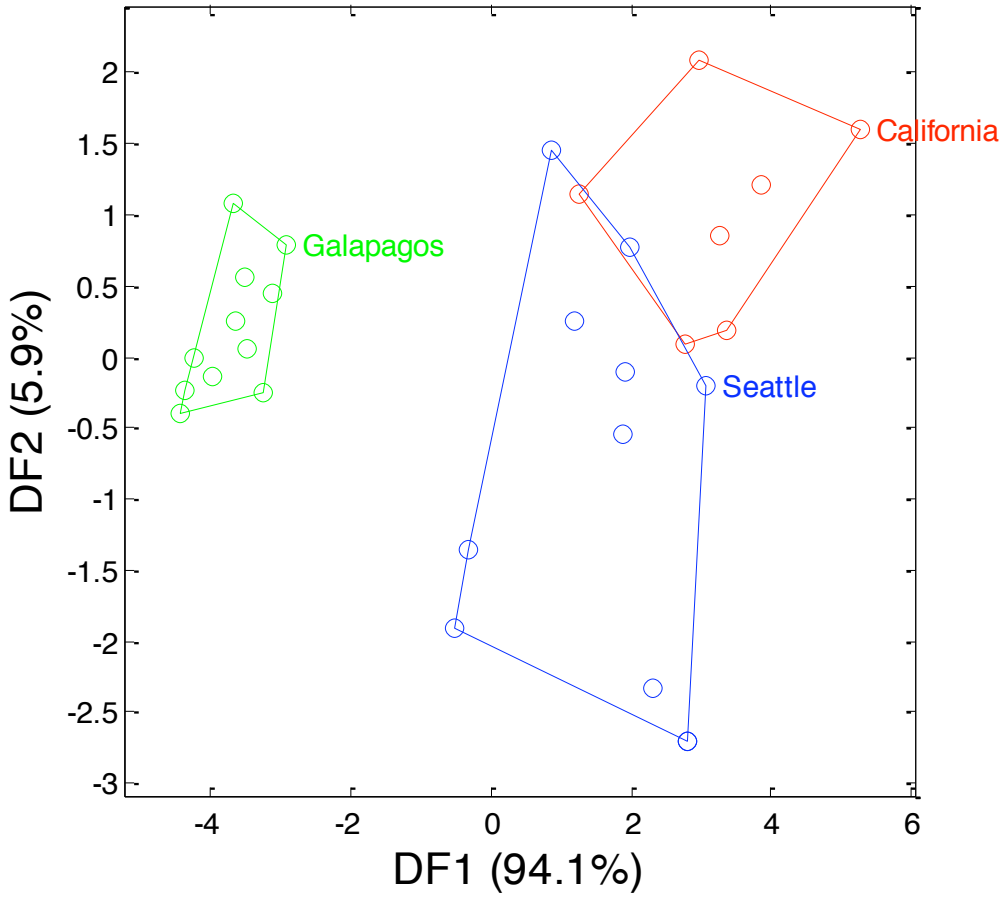

Figure 27. Scatterplot of the first two dimensions of the discriminant function analysis of the normalized data.

4. DISCUSSION

4.1 LA-ICP-MS

The overall performance of the LA-ICP-MS was satisfactory with low relative standard deviations (average < 3%) comparable or much better than previous studies (Zumholz et al., 2007c, Warner et al., 2009) and minimal instrument drift throughout the day. NIST standards performed well for these methods with very good agreement between expected and measured concentrations. However, there was significant variability of statolith measurements taken under the same method in different months (July vs. August) and signs of greater variance in the sample set than found in other studies (Zumholz et al., 2007c). This can most likely be attributed to other ICP-MS users and adjustments made to equipment while incorporating the new laser ablation unit into the laboratory. Overall LA-ICP-MS proved to be an excellent method for ease, time and cost.

4.2 Assumptions

All data sets met necessary the assumptions for statistical testing.

4.3 Descriptive Statistics

When compared with previous studies of similar methods, the elemental ranges and means found for *Dosidicus gigas* in this study were in reasonable agreement with previously published results (Table 15). The most noticeable deviation from congruency is the values for Sr:Ca found by Liu, et al. (2011), which are an order of magnitude higher than most other studies including this one. However, the estimated concentration

ranges found in the lower half of Table 15 match more closely the values found in previous studies. The differences between the values found for this study and others may be attributed to differences in methodology. Liu, et al., (2011) used a method of preserving the statoliths in alcohol after dissection, rather than storing them dry after dissection (Zumholz et al., 2007c, Warner et al., 2009). Some studies used a single point calibration instead of measuring three NIST standard glass materials which may explain how calculated concentrations agree better than Me:Ca values (Zumholz et al., 2007c, Warner et al., 2009). Liu, et al., (2011) also reported a lower overall range for barium concentration (ppm) than the current study, which might be due to the higher barium levels found in the samples taken from regions outside the tropical equatorial Pacific (Seattle and California). The higher Pb:Ca values found by Warner, et al. (2009) may be a sign of coastal influence, as *D. gigas*, *G. fabricii*, and *L. gahi* are larger, more pelagic species than *D. opalescens (Roper et al., 1984)*. Me:Ca ranges for Y and Zr were large with higher maximums when compared to Zumholz, et al., (2007c), which may be due to that study having a larger sample size and all specimens coming from the same month and location. Other Me:Ca values and concentrations are within the same order of magnitude with similar ranges of previous studies. Copper values were not measured in any of the most relevant cephalopod LA-ICP-MS studies, so it is not included in Table 15.

Table 15. Comparison of elemental concentration results with comparable literature sources.

Element	Me/Ca ratio range (µmol mol^{-1})					
	Dosidicus gigas **(Arbuckle)**	***Dosidicus gigas*** **(Arbuckle)(MEAN)**	***Dosidicus gigas*** **(Liu, et al. 2011)**	***Gonatus fabricii*** **(Zumholz, et al. 2007)**	***Doryteuthis opalescens*** **(Warner, et al., 2009)**	***Loligo gahi*** **(Arkhipkin, et al., 2004)**
Mg	105-524	198	79-233	110-590	590-2810	70-350
Sr	1031-1426	1208	14800-16400	6300-8100	9370-10800	8000-8500
Ba	5-32.5	12.8	11.2-23.8	5.7-8.2	6.18-10.71	3-8
Mn	0.3-9.7	2.41	-	3.2-6.8	1.56-24.49	1-3
Pb	0.014-0.27	0.0573	-	0.006-0.037	0.42-2.33	0.002-0.030
Zn	0.12-3.4	0.363	-	0.9-4.5	-	-
Y	0.024-0.11	0.0469	-	0.056-0.081	-	-
Zr	0.0034-0.103	0.0163	-	0.012-0.029	-	-
U	0.0052-0.15	0.0317	-	0.002-0.009	-	-
Element	**Concentration range (ppm)**					
Mg	86.6-568.2	158	30.9-93.9	25-140	-	-
Sr	5632-7743	6643	5871-6570	5500-7100	-	-
Ba	3.4-27.2	9.081	4.5-9.5	7.8-11.3	-	-
Mn	0.195-5.092	1.186	-	1.8-3.7	-	-
Pb	0.026-5.589	0.177	-	0.013-0.076	-	-
Zn	0.154-4.545	0.487	-	0.6-2.9	-	-
Y	0.02-0.132	0.0431	-	0.02-0.14	-	-
Zr	0.006-0.473	0.0345	-	0.01-0.026	-	-
U	0.00002-1.098	0.0225	-	0.005-0.022	-	-

4.4 Analysis of Variance

Analysis of Variance using all ablation locations showed statistically significant variation patterns across the statolith for all geographic regions sampled for all elements except Yttrium and Zirconium (Table 7). Variation was also not significant for Zinc and Lead in the Galapagos samples, though it was significant for the other two geographic regions. This is strong evidence that variations occur in the elemental composition of the statolith as specimens grow, providing a potential record of their environmental surroundings, diet and behavioral shifts. This information might prove a useful tool in explaining ontogeny of neritic to pelagic species and augments previous findings (Liu et al., 2011). These patterns will now be reviewed using post-hoc Tukey HSD multiple comparisons results.

4.4.1 Magnesium

All three geographic regions exhibited the same general pattern of variation across the statolith for magnesium, with the core being enriched compared to post hatching values. According to the multiple comparisons results, the Mg:Ca continued to decline in the Seattle population with significant differences between the second ablation location and the 5^{th},6^{th}, and 7^{th} ablation as well as between the third ablation and the 4^{th},5^{th}, 6^{th} and 7^{th} location. This pattern of magnesium enrichment while embryos feed from the yolk has been well documented in other studies and was expected (Arkhipkin et al., 2004, Zumholz et al., 2007c, Warner et al., 2009). Liu, et al., (2011), did not find significance in Mg:Ca variation across statoliths of *D. gigas*, so this is the first report of this pattern for this species.

4.4.2 Manganese

Manganese demonstrated a similar pattern in all three geographic regions and resembled the core enriched magnesium. Significant differences occurred in the multiple comparisons between the core and all other ablation locations for all three sampling regions. There were also significant differences between the second ablation and the 4th, 5th, 6th and 7th ablation for the California group and the second ablation and the 5th, 6th and 7th ablation for the Seattle group. A 2009 publication found a Pacific species (the market squid) showed a similar decrease in manganese from the core to one ablation point outside of the core (Warner et al., 2009). However, despite the concentration and Mn:Ca values similar to previous studies on a neritic Atlantic squid species, the pattern displayed is nearly the opposite (Zumholz et al., 2007c). This is the first report of the Mn:Ca pattern for *D. gigas*.

4.4.3 Copper

Copper exhibited a more complex pattern than magnesium or manganese. Although the cores were slightly enriched, they were not as dramatic as seen in the previous two elements. In the Galapagos sample, there was a gradual decline in Cu/Ca values and no ablation locations were significantly different. In both Seattle and California, there was an initial decline with a mixed increase after the third or fourth ablation. Significant differences were found in the multiple comparisons for California between the core and the 2nd, 3rd, and 4th ablations, as well as between the sixth ablation and the 2nd, 3rd, and 4th ablations. For Seattle, only the core was significantly different from the 2nd, 3rd, 5th and 6th ablations. Copper was not measured in many previous

studies, but the pattern found here most closely resembles Yttrium as measured by Zumholz, et al. (2007c). Copper was measured in Humboldt squid by Ikeda, et al., (2002b) and significant differences were found between ENSO years, with concentrations being higher in El Niño years. The copper concentrations reported by Ikeda, et al., (2002b) were much higher with larger variances than the current study (10-89 ppm; $s > \bar{x}$). Using back calculated age estimations, the squid sampled in this studied were alive only during the 2007 La Niña conditions, which provides some explanation of the lower copper values found in the current investigation (Wolter, 2012). If surface concentrations of copper are reduced, the pattern found in the current study, especially in the California specimen, might be demonstrating hatchling and young squid living near the surface. This is the first report of statolith copper patterns in *D. gigas*.

4.4.4 Zinc

Zinc showed less variation across the statolith with a very weak U-shape. No individual points were significantly different in the multiple comparisons for either the Galapagos or Seattle. California only showed significant differences between the core and the 4th and 5th ablations, making it the only group which truly exhibited the U-shaped pattern. This pattern is the same as was found in previous studies using other cephalopod species (Zumholz et al., 2007c, Zumholz et al., 2006). Like copper, concentrations ranges for zinc found here were also much lower than found in a previous study involving *D. gigas* in the eastern equatorial pacific, again possibly due to difference in ENSO index or measurement method (Ikeda et al., 2002b). Again, California specimens exhibit a pattern that matches environmental conditions if young

squid remain near the surface and migrate to deeper waters as they increase in size. This is the first report of zinc patterns in *D. gigas* statoliths.

4.4.5 Strontium

Strontium demonstrated a distinctly varied pattern when comparing the three geographic regions, despite being a conservative element (Bruland, 1983). Although all cores are considered enriched with significantly lowered values in the second ablation location, the three populations each demonstrated a different curve for the subsequent ablations. The Galapagos group values remained the lowest, the Seattle group showed a moderate increase and the California group demonstrated a full rebound. Using the multiple comparisons, the Galapagos group only significantly differed between the core and all other ablations, the Seattle group core was significantly different than the 2^{nd}, 3^{rd}, 4^{th} and 6^{th} ablations, and the California group showed significant differences between the core and the 2^{nd} and 3^{rd} ablations as well as the 2^{nd} ablation and the 4^{th}, 5^{th} and 6^{th} ablations. The California curve most closely matched the results found in previous LA-ICP-MS squid studies (Liu et al., 2011, Zumholz et al., 2007c). Strontium has been linked to water temperature in corals and squid (e.g. Arkhipkin et al., 2004, Ikeda et al., 1996, Liu et al., 2011, Smith et al., 1979, Zumholz et al., 2007c), often demonstrating a negative correlation. Although no direct relationship between temperature and strontium incorporation into the statolith has been calculated for Humboldt squid, it may be possible to use the general inverse relationship as a trend to understand the differences found among the ablation locations for the three regions. It is reasonable to assume that paralarval Humboldt squid will remain in surface waters which would generally be

warmer than deeper water where adults are known to spend daylight hours. This would agree with the curves found here except for the Galapagos, which would suggest adults inhabit water no cooler than paralarvae. This is explained by the moderate La Niña event that the Galapagos specimen experienced which reduced the surface to depth temperature gradients in that region (Wolter, 2012). Dietary effects may prevent a simple relationship between temperature and strontium incorporation into the statolith, which might explain why the Sr:Ca curve for Seattle doesn't rebound as drastically than the California group (Zumholz et al., 2006). Additionally, strontium presence in incubation water was determined to be necessary for proper statolith formation in multiple cephalopod species, so it is unlikely that strontium is enriched strictly from yolk concentrations (Hanlon et al., 1989). Although it is not possible to confirm, this suggests that the enriched strontium found in the cores may indicate that the eggs are incubated in waters colder than the surface waters that juveniles inhabit. This is not supported by the only *D. gigas* egg mass being found in warm water at only 16m depth (Staaf et al., 2008). However, if eggs need to be incubated at 18^{o}C as suggested by other Ommastrephid hatching studies, the depth of incubation for the area the *D. gigas* egg mass was found would have been at least 40m (Staaf et al., 2008, Yatsu et al., 1999).

The ranges found in the current study are smaller than those found by studies using particle induced x-ray emissions (PIXE), which noted *D. gigas* as having a strontium range of 8500-9500 ppm. Values reported here for strontium concentration agree with the PIXE study in that specimens caught off South America (Peru or Ecuador) have a lower strontium concentrations than those found farther north (Costa

Rica or the United States) (Ikeda et al., 2002b). However, the more recent study using *D. gigas* and LA-ICP-MS found the opposite for the southern hemisphere with Sr:Ca increasing with decreasing latitude (Liu et al., 2011). As explained earlier, while a direct relationship between statolith strontium levels and ambient water temperature cannot be determined, the variations across the statolith and among populations are significant. Therefore statolith strontium variations are still valuable for population studies, especially distinguishing among specimen from different geographic regions.

4.4.6 Yttrium

Unlike previous studies on Atlantic squid species and cuttlefish, yttrium exhibited no clear pattern across the statoliths of Humboldt squid (Zumholz et al., 2006, Zumholz et al., 2007c). In the previous studies, cores were Yttrium enriched, which might have been a maternal effect or not apparent in pacific squid species. One previous study demonstrated that cuttlefish feeding on a fish only diet would have greater values of Y:Ca (Zumholz et al., 2006). The opportunistic feeding capabilities of the Humboldt squid might explain why little variation is seen in Yttrium for this species. Multiple comparisons and ANOVAs were all not significant for all ablations for all geographic regions.

4.4.7 Zirconium

Zirconium also demonstrated very little variation across the statolith, but the ANOVA for the California group was significant at $\alpha = 0.10$ level. The multiple comparisons revealed that this is due to the core being significantly different than the 2nd ablation ($p < 0.05$). However, the other groups had no significant variations. This is not

consistent with previous studies on Atlantic squid species, which may indicate a species specific systematic control for this element (Zumholz et al., 2007c). Zirconium has a nutrient-scavenged distribution which might explain why the pattern in a pelagic species does not show the same pattern or concentration ranges as previous studies involving more coastal influenced species (Zumholz et al., 2007c).

4.4.8 Barium

Barium demonstrated the highest variation in pattern among the three geographic locations, with the Galapagos being significantly lower and less variable than the other two groups. California and Seattle cores were very similar, but subsequent points exhibit an out of sync, highly variable structure. For the Galapagos group, multiple comparisons show a U-shaped pattern with significant differences between the core and the 2^{nd}, 3^{rd} and 4^{th} ablations; the 2^{nd} ablation and the 5^{th} and 6^{th} ablations; the 3^{rd} ablation and the 4^{th} and 5^{th} ablations; and the 4^{th} ablation and 5^{th} ablation. For the California group multiple comparisons were significant between the 4^{th} ablation and all others except the 5^{th} ablation. For the Seattle group, multiple comparisons revealed significant differences between the core and the 5^{th} ablation; the 2^{nd} ablation and the 3^{rd}, 5^{th}, 6^{th} and 7^{th} ablations; and the 4^{th} ablation and 5^{th} ablation. Zumholz, et al. (2007c) found a u-shaped pattern for barium values in an Atlantic species of squid, but Liu, et al. (2011) found only a significant increase in barium after juvenile stages in Humboldt squid in the southern hemisphere. Barium is well known as a signature of riverine inputs in carbonates due to a nutrient like distribution and this is consistent with the differences in pattern found in this study (Chan et al., 1977). If the Galapagos group is considered

permanently offshore, there would be considerably less barium than would groups near shore, such as the California, Seattle and groups studied in Liu, et al. (2011). Additionally, a 2007 laboratory rearing study supported field evidence that there can be a negative correlation between temperature and barium to calcium ratios in some cephalopod statoliths (Arkhipkin et al., 2004, Zumholz et al., 2007b). This may affect the ability for the colder upwelled barium enriched water to influence the composition of the Galapagos statoliths.

4.4.9 Lead

Lead exhibited a complex pattern across the statoliths, with an initial slight decrease between the core and the 2nd ablation in the California and Seattle groups and an overall increase in subsequent ablations. For the California group, significant differences occurred between the core and the 6th and 7th ablations; the 2nd and the 4th, 5th, 6th, and 7th ablations; and the 3rd ablation and the 6th and 7th ablations. For the Seattle group, significant differences only occurred between the 2nd ablation and the 7th ablation. The Galapagos group did not have any significant differences between ablation locations. As was suggested by Zacherl et al. (2003) , Pb:Ca ratios in gastropod statoliths may be influenced by industrial presence. This might explain why there is a lack of significant increase across the statolith for the Galapagos group, or why there was such a large variance for some ablation locations. Few previous studies attempted to measure lead in squid statoliths, and most found that the values were too often below the detection limits to analyze the patterns (Zumholz et al., 2007c, Warner et al., 2009). Low lead values in the core can be explained by embryos feeding off the yolk and

regulation protection of the chorion, or egg case. Significant increases in Pb:Ca over the life of squid inhabiting water near industrialized nations may be indication of bioaccumulation in prey as individual squid grow and consume larger prey items as found in fish studies (Seymore et al., 1995, Sanchez-Jerez et al., 2005). This is the first report of Pb:Ca patterns for *D. gigas*.

4.4.10 Uranium

Uranium presented a complex pattern with high variability within groups. Although the ANOVA was significant for each group, multiple comparisons revealed only one significant difference for the California group between the core and 3rd ablation. The core was significantly different from all subsequent ablations in the Galapagos group and while the Seattle group showed significant difference between the core and all ablations other than the 4th. These patterns indicate uranium enriched cores. Previous studies found a U-shaped pattern in uranium for an Atlantic squid species and suggested it related to both temperature and salinity (Zumholz et al., 2007c). If this is the case and considering barium indicated highly variable freshwater influences to the two coast groups, it could explain why the values for uranium are more variable and do not demonstrate a clear pattern in those cases. This is the first report of U:Ca patterns for *D. gigas*.

4.5 Analysis of Variance - Part 2

Analysis of Variance was also performed on only the core and the last ablation location available for each group. If no significant differences in elements were found between these ablations it would be considered evidence that squid tended to return to

natal waters. Although there were fewer significant ANOVA results than were found for the overall pattern demonstrated, there were still many elements showing significant differences between the core and the final ablation location (Table 8). Seattle had six elements which significantly differed (Mg, Mn, Sr, Ba, Pb, and U), California had five elements with significant differences (Mg, Mn, Sr, Zr, and Pb), and the Galapagos also had five elements displaying significant differences (Mg, Mn, Cu, Sr, and U). This provides evidence that the environmental conditions which adult populations experience are not the same as they experience as embryos. Unfortunately, maternal effects and dietary influences may be inflating these differences.

To remove the maternal or dietary yolk influences, the analysis was repeated using only the 2nd and the last ablation locations. The second ablation values would represent hatchling or pre-juvenile stages, when the paralarvae are independently feeding. This comparison might elucidate whether behaviors or environmental conditions are similar for very young and adult squid. If significant differences are found, it could be evidence that adults are not returning to hatching grounds. As seen in Table 9, Seattle still had six elements with significant differences (Mg, Mn, Zr, Ba, Pb, and U), California had only four elements showing significant differences (Mn, Cu, Sr, and Pb), and the Galapagos showed only two elements with significant differences (Mg and Ba). Again, depth of water and ambient temperature as well as dietary changes may be inflating these differences; however, results do indicate that adults are not returning to hatching environments.

4.6 Two-Way Analysis of Variance

Two-way ANOVA was performed to ensure that significant differences found among ablation locations were not influenced by interactions effects among variations among specimens. There were no interaction effects ($p>0.7$). Two-way ANOVA confirmed the findings that significant variations in elemental concentrations occur among ablation locations ($p <0.0001$, all regions). Additionally, significant variations among specimens indicated that the specimen groups collected from Seattle and the Galapagos contained a mix of cohorts ($p<0.05$). This might explain the large variances found in some elements and strengthens the use of LA-ICP-MS statolith microchemistry methods for successfully distinguishing elemental patterns even with mixed cohort sampling.

4.7 Multivariate Analysis of Variance

Multivariate methods were employed to investigate differences in overall elemental signatures among geographic regions. The elemental signatures of the three geographic regions were compared using Multivariate Analysis of Variance (MANOVA) at three individual ablation locations using nine of the ten measured element to calcium ratios. The core, second and fifth ablation locations were selected to maximize possible ontogenic explanation of similarities or differences. Significant differences and similarities can help to deduce whether or not populations are experiencing similarities in ontogenic behavior or environments.

All three ablation regions resulted in significant differences ($p<0.05$) in elemental signatures when using MANOVA to compare the three populations. To investigate

more closely, the MANOVA was repeated for each pair of populations. The elemental signature measured for the Galapagos specimen was significantly different ($p<0.05$) from the Seattle group for all three ablation locations. The Galapagos group was also significantly different ($p<0.05$) from the California group at the second and the fifth ablation locations, but only marginally significantly different at the core ($p=0.0502$). This is weak evidence that these two populations may be mixing. This may be an indication that the two groups exhibit similar behaviors when laying eggs, that eggs are incubated in similar water masses, or perhaps even some indication of individuals crossing the equator prior to spawning or after hatching. California and Seattle were significantly different for this test at the core ablation ($p<0.05$). This is especially interesting as some previous investigators of *D. gigas* reproduction suggest that individuals of this species must migrate to the tropics for spawning. Although records of quick sustained horizontal movement of individual Humboldt squid indicate the capability of long distance migrations, the assertion that this capability is equivalent to evidence of full coastal migrations and natal homing is not supported by the disparity of the elemental composition in the statolith cores of these two groups reported here (Stewart et al.). However, the lack of a significant difference in the elemental signature found for the second ablation between California and Seattle specimen indicates that, once hatched, individual environments and behaviors are indistinguishable despite a large geographic difference when caught as adults. California and Seattle groups were also marginally significantly different at the 5th ablation location ($p=0.0572$), indicating that as individuals in these separate populations mature, the differences in environments

or behaviors are more apparent. To investigate this prospect, MANOVA was performed between the California and Seattle elemental signatures on the 6^{th} and the 7^{th} ablation locations separately. The elemental signature measured at the 6^{th} ablation location is significantly different between California and Seattle ($p=0.0008$), and the same is true for the 7^{th} ablation location ($p=0.011$, Pillai's Trace method). These findings also act as evidence against the theory that these two groups are breeding and spawning in the same location, such as the Gulf of California.

4.8 Correspondence Analysis

The first CA plot demonstrates that magnesium, manganese, and uranium are farthest negative from the mean of the first dimension while lead and barium are the most positive. It is also clear that barium is the most negative element in the second dimension while copper and zinc are the most positive elements in the second dimension. In Figure 16 it is difficult to discern the individual squid/ablation values, but Figure 17 makes the geographic trends more apparent. California squid are spread across the mean of the first dimension with some being negative and some positive. However, they are more concentrated in the negative direction for the second dimension. Galapagos are also spread across the first dimension, while predominately positive in the second dimension. Seattle squid/ablation values do not demonstrate a cluster for either dimension. The lack of clear separation may be due to the samples consisting of a mix of cohorts as mentioned earlier.

When the results of the geographic mean CA are plotted in Figure 18, magnesium, manganese, and uranium are again farthest negative from the mean of the

first dimension while lead and barium are the most positive. Other elements also retain their positions in the relative dimensions. In Figure 19 it is clearer that the scores representing the geographic means for California are positive in the first dimension other than the core. California values are also predominantly negative in the second dimension. Meanwhile, the Galapagos means are also positive in the first dimension except the core and also all are positive in the second dimension. Seattle means fall positive on the first dimension except for the core, but the second ablation is positive while all others are negative in the second dimension.

These patterns are indicating that the cores of all three regions are distinctly different from the remaining ablations within their own population. This is most likely due to the enriched values found for magnesium, manganese, copper and uranium. Meanwhile, copper, zinc, barium and lead seem to most highly influence the second dimension which most distinctly separates the Galapagos and California means. While Seattle means do spread across the median, they are still predominately separated from the Galapagos means as well. The California and Seattle populations do not separate well in this analysis.

Overall CA indicates that the elements most affecting the geographic differences in elemental signature include magnesium, manganese, uranium, barium, lead, copper and zinc. Strontium and yttrium do not seem to influence differences as highly as the other elements, though they are not directly at the origin and thus, still considered useful.

4.9 Principle Component Analysis

By filtering the data for only the most valuable element/ablation measurements and standardizing the data set, PCA provides a more clear view of the variations in elemental signatures measured among the geographic regions. Although the scree diagram (Figure 22) suggests that the variance explained by the first principle component dominates subsequent components, the percent of the total variance explained for the first three dimensions being only 65.52% (Table 14) suggests that exploring more dimensions would be beneficial. By plotting the scores on the first two principle components (Figure 24), a strong difference in scores is clear between the California and Seattle groups. By adding 95% confidence ellipses, differences are confirmed despite some overlap with the Galapagos ellipse. The Galapagos and California group are less differentiated when using the first and third principle components (Figure 25), but it is clear that they are distinct in a plot of the second and third principle components (Figure 26). By examining a three dimensional rendering of the PCA scores (Figure 23), it is clear that the Galapagos individuals are most negative on the first principle component axis, while Seattle is most distinctly negative in the second principle component axis. The California group does not fall directly between the other groups but more closely to the origin, while positive in both the first and third principle component axis. These differences suggest that the three populations are distinct and separate groups.

4.10 Discriminant Function Analysis

A discriminate classification method was performed to quantify the differences comprehensively described by the above multivariate ordination analyses. The results showed that 100% of the variance is explained in two dimensions and nearly all individuals are correctly classified within the boundaries set for each group with overlap occurring only between the California and Seattle groups (Figure 27). Additionally, a jackknifed randomization test was performed to determine the confidence of the reclassification success. With 75.86% reclassification success, the classification performed significantly better than possible by chance ($p=0.0001$). This solidifies the successful use of laser ablation elemental analysis of *Dosidicus gigas* statoliths for discriminating among populations.

5. CONCLUSIONS

The chemical analyses used in this study provide substantial evidence that microchemical studies are applicable to population dynamics studies of Humboldt squid. Multiple statistical methods revealed patterns, variations and differences in the chemical composition of the statolith both within and among the three geographic regions sampled. The continued and expanded use of this type of study will enable strategic monitoring of the populations of this species. It may be possible to enhance the functionality of existing fisheries models by incorporating statolith elemental concentrations. This may aid in creating sustainable fishing practices involving cephalopods. Future work would benefit from developing a multiyear sampling plan spanning the maximum habitat range and include analyzing statoliths from paralarval specimen as well as adults.

It is clear from the results of multiple studies that taxonomic differences prevent the direct application of findings from even one species to another within the same taxonomic family or genus. Even if this were not a concern, most elements have been statistically linked to variations with more than one influence in laboratory rearing studies involving cephalopods. The most frequently measured elements (Sr, Ba, Mg, Mn) have all shown significant variations with both environmental conditions (temperature or salinity) and dietary effects. While, dietary effects are easily controlled in laboratory conditions, it is highly unlikely that a fast growing and opportunistic predator, such as the Humboldt squid, would have a traceable dietary behavior in the

wild. Therefore, even if laboratory rearing exercises were possible for this species and correlations were determined for elemental statolith composition and diet or temperature, there is little chance they would be applicable for environmental or dietary reconstructions.

Fortunately, this study still demonstrated a strong potential for distinguishing among populations using statolith elemental chemistry. Additionally, some of the essential groundwork was initiated to begin understanding the fundamental life history of this species. This is the first report of the ranges of Me:Ca values and concentrations of lead, yttrium, zirconium and uranium for Humboldt squid statoliths. This is also the first study to report patterns in *D. gigas* statoliths for manganese, copper, zinc, lead, yttrium, zirconium, and uranium.

The significant differences in measured elemental signatures found among the three sample groups may clarify some of the reproductive questions involving this teuthiod species. There is potential for the data reported here to aid in a better understanding of the life history and spawning behaviors of this squid. If assumptions are correct involving water temperature and strontium concentrations, this data indicates that Humboldt egg masses are incubated deeper in the water column and rise to the pycnocline as they near hatching as suggested in previous work (Staaf et al., 2008). The fact that sample groups consisting of mixed cohorts still produced significant population discrimination results indicates that these methods may be very robust in future stock establishment studies.

The null hypothesis that the elemental signatures found for the three geographic regions would not differ was also soundly rejected. This finding aids in stock establishment and better understanding of Humboldt squid population dynamics. Overall the results presented reject the null hypothesis that using LA-ICP-MS measurements of statolith microchemistry is not useful in studying population dynamics of the Humboldt squid, *Dosidicus gigas*

REFERENCES

ANDERSON, F. E. 2000. Phylogenetic relationships among loliginid squids (Cephalopoda : Myopsida) based on analyses of multiple data sets. *Zoological Journal of the Linnean Society,* 130, 603-633.

ARBUCKLE, N. S. M. & WORMUTH, J. H. 2011. Statolith extraction method improvements for use in microchemistry studies with laser ablation inducitvely coupled plasma mass spectrometry. *MTS/IEEE Oceans, '11.* Kona, Hawai'i, USA.

ARKHIPKIN, A. I. 2005. Statoliths as 'black boxes' (life recorders) in squid. *Marine and Freshwater Research,* 56, 573-583.

ARKHIPKIN, A. I., CAMPANA, S. E., FITZGERALD, J. & THORROLD, S. R. 2004. Spatial and temporal variation in elemental signatures of statoliths from the Patagonian longfin squid (*Loligo gahi*). *Canadian Journal of Fisheries and Aquatic Sciences,* 61, 1212-1224.

BETTENCOURT, V. & GUERRA, A. 2000. Growth increments and biomineralization process in cephalopod statoliths. *Journal of Marine Biology and Ecology,* 248, 191-205.

BETTENCOURT, V. & GUERRA, A. 2001. Age studies based on daily growth increments in statoliths and growth lamellae in cuttlebone of cultured *Sepia officinalis*. *Marine Biology,* 139, 327-334.

BRULAND, K. W. 1983. *Chemical Oceanography.* 2nd ed. London, England, UK: Academic.

CADDY, J. F. & RODHOUSE, P. G. 1998. Cephalopod and groundfish landings: Evidence for ecological change in global fisheries? *Reviews in Fish Biology and Fisheries,* 8, 431-444.

CAMPANA, S. E. & NEILSON, J. D. 1985. Microstructure of fish otoliths. *Canadian Journal of Fisheries and Aquatic Sciences,* 42, 1014-1032.

CHAN, L. H., DRUMMOND, D., EDMUND, J. M. & GRANT, B. 1977. On the barium data from the Atlantic GEOSECS expedition. *Deep Sea Research,* 24, 613-649.

CLARKE, M. R. 1978. Cephalopod statolith - Introduction to its form. *Journal of the Marine Biological Association of the United Kingdom,* 58, 701-712.

COWEN, R. K., GAWARKIEWICZ, G., PINEDA, J., THORROLD, S. R. & WERNER, F. E. 2007. Population connectivity in marine systems: An overview. *Oceanography,* 20, 14-21.

DAWE, E. G., O'DOR, R. K., ODENSE, P. H. & HURLEY, G. V. 1985. Validation and application of an ageing technique for short-finned squid (*Illex illecebrosus*). *Journal of Northwest Atlantic Fishery Science,* 6, 107-116.

DONAT, J. R. & BRULAND, K. W. 1994. *Trace Elements in Natural Waters.* Boca Raton, Florida, USA: CRC Press.

EGGINS, S., DECKKER, P. D. & MARSHALL, J. 2003. Mg/Ca variation in planktonic foraminifera tests: Implications for reconstructing paleo-seawater temperature and habitat migration. *Earth and Planetary Science Letters,* 212, 291-306.

EHRHARDT, N. M. 1991. Potential impact of a seasonal migratory jumbo squid (*Dosidicus gigas*) stock on a Gulf of California sardine (*Sardinops sagax caerulea*) population. *Bulletin of Marine Science,* 49, 325-332.

FOOD AND AGRICULTURE ORGANIZATION OF THE UNITED NATIONS 2007. *FISHSTAT Plus (Verson 2.32)*. Rome, Italy: Food and Agriculture Organization.

FOOD AND AGRICULTURE ORGANIZATION OF THE UNITED NATIONS 2008. *The State of the World Fisheries and Aquaculture:2008*. Rome, Italy: Food and Agriculture Organization.

FIELD, J. C. 2008. Jumbo squid (*Dosidicus gigas*) invasions in the eastern Pacific Ocean. *California Cooperative Oceanic Fisheries Investigations Reports,* 49, 79-81.

FIELD, J. C., BALTZ, K., PHILLIPS, A. J. & WALKER, W. A. 2007. Range expansion and trophic interactions of the jumbo squid, *Dosidicus Gigas,* in the California Current. *California Cooperative Oceanic Fisheries Investigations Reports,* 48, 131-146.

GILLY, W. F., MARKAIDA, U., BAXTER, C. H., BLOCK, B. A., BOUSTANY, A., ZEIDBERG, L., REISENBICHLER, K., ROBISON, B., BAZZINO, G. & SALINAS, C. 2006. Vertical and horizontal migrations by the jumbo squid *Dosidicus gigas* revealed by electronic tagging. *Marine Ecology-Progress Series,* 324, 1-17.

GLASS, G. V., PECKHAM, P. D. & SANDERS, J. R. 1972. Consequences of failure to meet assumptions underlying the fixed effects analyses of variance and covariance. *Review of Educational Research,* 42, 237-288.

GOTELLI, N. J. & ELLISON, A. M. 2004. *A Primer of Ecological Statistics.* Sunderland, Massachusetts, USA: Sinauer Associates, Inc.

HANLON, R. T., BIDWELL, J. P. & TAIT, R. 1989. Strontium is required for statolith development and thus normal swimming behavior of hatchling cephalopods. *Journal of Experimental Biology,* 141, 187-195.

HANLON, R. T. & MESSENGER, J. B. 1996. *Cephalopod Behavior*. Cambridge, England, UK: Cambridge University Press.

HARWELL, M. R., RUBINSTEIN, E. N., HAYES, W. S. & C., O. C. 1992. Summarizing monte carlo results in methodological research: The one- and two-factor fixed effects ANOVA cases. *Journal of Educational Statistics,* 17, 315-339.

HASTINGS, A. & HARRISON, S. 1994. Metapopulation dynamics and genetics. *Annual Reviews of Ecological Systems,* 25, 167-188.

IKEDA, Y., ARAI, N., KIDOKORO, H. & SAKAMOTO, W. 2003. Strontium : calcium ratios in statoliths of Japanese common squid *Todarodes pacificus* (Cephalopoda : Ommastrephidae) as indicators of migratory behavior. *Marine Ecology-Progress Series,* 251, 169-179.

IKEDA, Y., ARAI, N., SAKAMOTO, W., KIDOKORO, H., YATSU, A., NATEEWATHANA, A. & YOSHIDA, K. 1997. Comparison on trace elements

in squid statoliths of different species' origin: As available key for taxonomic and pylogenetic study. *International Journal of PIXE,* 7, 141-146.

IKEDA, Y., ARAI, N., SAKAMOTO, W., KIDOKORO, H. & YOSHIDA, K. 1996. Relationships between statoliths and environmental variables in cephalopods. *International Journal of PIXE,* 6, 339-345.

IKEDA, Y., ARAI, N., SAKAMOTO, W., KIDOKORO, H. & YOSHIDA, K. 1998. Microchemistry of the statoliths of the Japanese common squid *Todarodes pacificus* with special reference to its relation to the vertical temperature profiles of squid habitat. *Fisheries Science,* 64, 179-184.

IKEDA, Y., OKAZAKI, J., SAKURAI, Y. & SAKAMOTO, W. 2002a. Periodic variation in Sr/Ca ratios in statoliths of the Japanese common squid *Todarodes pacificus* Steenstrup, 1880 (Cephalopoda : Ommastrephidae) maintained under constant water temperature. *Journal of Experimental Marine Biology and Ecology,* 273, 161-170.

IKEDA, Y., YATSU, A., ARAI, N. & SAKAMOTO, W. 2002b. Concentration of statolith trace elements in the jumbo flying squid during El Nino and non-El Nino years in the eastern Pacific. *Journal of the Marine Biological Association of the United Kingdom,* 82, 863-866.

JACKSON, G. D. 1994. Application and future potential of statolith increment analysis in squids and sepioids. *Canadian Journal of Fisheries and Aquatic Sciences,* 51, 2612-2625.

JOCHUM, K. P., WEIS, U., STOLL, B., KUZMIN, D., YANG, Q., RACZEK, I., JACOB, D. E., STRACKE, A., BIRBAUM, K., FRICK, D. A., GUNTHER, D. & ENZWEILER, J. 2011. Determination of reference values for NIST SRM 610-617 glasses following ISO guidelines. *Geostandards and Geoanalytical Research,* 35, 397-429.

JOHNSON, K. S., COALE, K. H., BERELSON, W. M. & GORDON, R. M. 1996. On the formation of the manganese maximum in the oxygen minimum. *Geochimica Et Cosmochimica Acta,* 60, 1291-1299.

KEYL, F., ARGUELLES, J., MARIATEGUI, L., TAFUR, R., WOLFF, M. & YAMASHIRO, C. 2008. A hypothesis on range expansion and spatio-temporal shifts in size-at-maturity of jumbo squid (*Dosidicus gigas*) in the eastern Pacific Ocean. *California Cooperative Oceanic Fisheries Investigations Reports,* 49, 119-128.

LEAR, C. H., ROSENTHAL, Y. & SLOWEY, N. 2002. Benthic foraminiferal Mg/Ca-paleothermometry: A revised core-top calibration. *Geochimica Et Cosmochimica Acta,* 66, 3375-3387.

LEVIN, L. A. 2006. Recent progress in understanding larval dispersal: New directions and digressions. *Integrative and Comparative Biology,* 46, 282-297.

LINDMAN, H. R. 1974. *Analysis of variance in complex experimental designs.* San Francisco, California, USA: W. H. Freeman & Co.

LIPINSKI, M. R. 1980. *A Preliminary Study on Age of Squids from Their Statoliths*. Gydina, Poland: Northwest Atlantic Fisheries Organization.

LIPINSKI, M. R. 1986. Methods for the validation of squid age from statoliths. *Journal of the Marine Biological Association of the United Kingdom,* 66, 505-526.

LIU, B., CHEN, X., CHEN, Y., LU, H. & QIAN, W. 2011. Trace elements in the statoliths of jumbo flying squid off the Exclusive Economic Zones of Chile and Peru. *Marine Ecology Progress Series,* 429, 93-101.

MACARTHUR, R. H. & WILSON, E. O. 1967. *The Theory of Island Biogeography.* Princeton, New Jersey, USA: Princeton University Press.

MARKAIDA, U. 2006. Food and feeding of jumbo squid *Dosidicus gigas* in the Gulf of California and adjacent waters after the 1997-98 El Niño event. *Fisheries Research,* 79, 16-27.

MARKAIDA, U., QUINONEZ-VELAZQUEZ, C. & SOSA-NISHIZAKI, O. 2004. Age, growth and maturation of jumbo squid *Dosidicus gigas* (Cephalopoda : Ommastrephidae) from the Gulf of California, Mexico. *Fisheries Research,* 66, 31-47.

MARTIN, G. B., THORROLD, S. R. & JONES, C. M. 2004. Temperature and salinity effects on strontium incorporation in otoliths of larval spot (*Leiostomus xanthurus*). *Canadian Journal of Fisheries and Aquatic Sciences,* 61, 34-42.

NAKAMURA, Y. & SAKURAI, Y. 1991. Validation of daily growth increments in statoliths of Japanese common squid *Todarodes pacificus*. *Nippon Suisan Gakkaishi,* 57, 2007-2011.

NESIS, K. N. 1983. *Cephalopod Life Cycles, Vol. I.* London, England, UK: Academic Press.

NIGMATULLIN, C. M., NESIS, K. N. & ARKHIPKIN, A. I. 2001. A review of the biology of the jumbo squid *Dosidicus gigas* (Cephalopoda: Ommastrephidae). *Fisheries Research,* 54, 9-19.

O'DOR, R. K. 1992. Big squid in big currents. *South African Journal of Marine Science,* 12, 225-235.

PALUMBI, S. R. 2003. Population genetics, demographic connectivity, and the design of marine reserves. *Ecological Applications,* 13, 146-158.

PAPADOPOULOU, C., KANIAS, G. D. & KASSIMATIS, E. M. 1978. Zinc content in otoliths of mackerel from the aegean. *Marine Pollution Bulletin,* 9, 106-108.

PAULY, D., ALDER, J., BENNETT, E., CHRISTENSEN, V., TYEDMERS, P. & WATSON, R. 2003. The future for fisheries. *Science,* 302, 1359-1361.

PEARCY, W. G. 2002. Marine nekton off Oregon and the 1997-98 El Nino. *Progress in Oceanography,* 54, 399-403.

RADTKE, R. L. 1983. Chemical and structural characteristics of statoliths from the short-finned squid *Illex illecebrosus*. *Marine Biology,* 76, 47-54.

RODHOUSE, P. G., ROBINSON, K., GAJDATSY, S. B., DALY, H. I. & ASHMORE, M. J. S. 1994. Growth, Age Structure and Environmental History in the Cephalopod *Martialia hyadesi* (Teuthoidea, Ommastrephidae) at the Antarctic Polar Frontal Zone and on the Patagonian Shelf Edge. *Antarctic Science,* 6, 259-267.

ROOKER, J. R., SECOR, D. H., ZDANOWICZ, V. S. & ITOH, T. 2001. Discrimination of northern bluefin tuna from nursery areas in the Pacific Ocean using otolith chemistry. *Marine Ecology-Progress Series,* 218, 275-282.

ROPER, C. F. E., SWEENEY, M. J. & NAUEN, C. E. 1984. Cephalopods of the world: An annotated and illustrated catalogue of species of interest to fisheries. *FAO Fisheries Synopsis,* 3, 277.

ROSENTHAL, Y., BOYLE, E. A. & SLOWEY, N. 1997. Temperature control on the incorporation of magnesium, strontium, fluorine, and cadmium into benthic foraminiferal shells from Little Bahama Bank: Prospects for thermocline paleoceanography. *Geochimica Et Cosmochimica Acta,* 61, 3633-3643.

RUTTENBERG, B. I., HAMILTON, S. L., HICKFORD, M. J. H., PARADIS, G. L., SHEEHY, M. S., STANDISH, J. D., BEN-TZVI, O. & WARNER, R. R. 2005. Elevated levels of trace elements in cores of otoliths and their potential for use as natural tags. *Marine Ecology Progress Series,* 297, 273-281.

SANCHEZ-JEREZ, P., GILLANDERS, B. M. & KINGSFORD, M. J. 2005. Spatial variability of trace elements in fish otoliths: Comparison with dietary items and habitat constituents in seagrass meadows. *Journal of Fish Biology,* 61, 801-821.

SANDOVAL-CASTELLANOS, E., URIBE-ALCOCER, M. & DIAZ-JAIMES, P. 2007. Population genetic structure of jumbo squid (*Dosidicus gigas*) evaluated by RAPD analysis. *Fisheries Research,* 83, 113-118.

SEMMENS, J. M., PECL, G. T., GILLANDERS, B. M., WALUDA, C. M., SHEA, E. K., JOUFFRE, D., ICHII, T., ZUMHOLZ, K., KATUGIN, O. N., LEPORATI, S.

C. & SHAW, P. W. 2007. Approaches to resolving cephalopod movement and migration patterns. *Reviews in Fish Biology and Fisheries,* 17, 401-423.

SEYMORE, T., DU PREEZ, H. H. & VAN VUREN, J. 1995. Manganese, lead, and strontium bioaccumulation in the tissues of the yellowfish, *Barbu marequensis* from the lower Olifants River, Eastern Transvaal. *Water South Africa,* 21.

SIFNER, S. K. 2008. Methods for age and growth determination in cephalopods. *Ribarstvo,* 66, 25-34.

SMITH, S. V., BUDDEMEIER, R. W., REDALJE, R. C. & HOUCK, J. E. 1979. Strontium-calcium thermometry in coral skeletons. *Science,* 204, 404-407.

SONU, S. C. 2004. *NOAA Technical Memorandum: The Japanese Market for Squid and Cuttlefish*. Long Beach, California, USA: National Marine Fisheries Service.

STAAF, D. J., CAMARILLO-COOP, S., HADDOCK, S. H. D., NYACK, A. C., PAYNE, J., SALINAS, C., SEIBEL, B. A., TRUEBLOOD, L., WIDMER, C. & GILLY, W. F. 2008. Natural egg mass deposition by the Humboldt squid (*Dosidicus gigas*) in the Gulf of California and characteristics of hatchlings and paralarvae. *Journal of the Marine Biological Association of the United Kingdom,* 88, 759-770.

STEWART, J. S., HAZEN, E. L., FOLEY, D. G., BOGRAD, S. J. & GILLY, W. F. Modeling marine predator migration during range expansion: Humboldt squid (*Dosidicus gigas)* in the California Current System. *ASLO Ocean Sciences, 2012.* Salt Lake City, Utah, USA.

SWEARER, S. E., CASELLE, J. E., LEA, D. W. & WARNER, R. R. 1999. Larval retention and recruitment in an island population of coral-reef fish. *Nature,* 402, 799-802.

THORROLD, S. R. 1998. Accurate classification of juvenile weakfish *Cynoscion regalis* to estuarine nursery areas based on chemical signatures in otoliths. *Marine Ecology Progress Series,* 173, 253-265.

THORROLD, S. R., JONES, G. P., HELLBERG, M. E., BURTON, R. S., SWEARER, S. E., NEIGEL, J. E., MORGAN, S. G. & WARNER, R. R. 2002. Quantifying larval retention and connectivity in marine populations with artificial and natural markers. *Bulletin of Marine Science,* 70, 291-308.

WARNER, R. R., HAMILTON, S. L., SHEEHY, M. S., ZEIDBERG, L. D., BRADY, B. C. & CASELLE, J. E. 2009. Geographic variation in natal and early larval trace-elemental signatures in the statoliths of the market squid *Doryteuthis* (formerly *Loligo*) *opalescens*. *Marine Ecology-Progress Series,* 379, 109-121.

WATANABE, H., KUBODERA, T., ICHII, T. & KAWAHARA, S. 2004. Feeding habits of neon flying squid *Ommastrephis bartramii* in the transitional region of the central North Pacific. *Marine Ecology Progress Series,* 266, 173-184.

WHITE, J. W. & RUTTENBERG, B. I. 2007. Dicriminant function analysis in marine ecology: Some oversights and their solutions. *Marine Ecology Progress Series,* 329, 301-305.

WING, B. L. 2006. Unusual invertebrates and fish observed in the Gulf of Alaska, 2004-2005. *PISCES Press,* 14, 26-28.

WOLTER, K. 2012. *Multivariate ENSO Index (MEI), Earth System Research Library, National Oceanographic and Atmospheric Administration, United States Department of Commerce* [Online]. Available: http://www.esrl.noaa.gov/psd/enso/mei/ [Accessed June 12, 2012].

WORM, B., BARBIER, E. B., BEAUMONT, N., DUFFY, J. E., FOLKE, C., HALPERN, B. S., JACKSON, J. B. C., LOTZE, H. K., MICHELI, F., PALUMBI, S. R., SALA, E., SELKOE, K. A., STACHOWICZ, J. J. & WATSON, R. 2006. Impacts of biodiversity loss on ocean ecosystem services. *Science,* 314, 787-790.

WORMUTH, J. H. 1976. The biogeography and numerical taxonomy of the oegopsid squid family Ommastrephidae in the Pacific Ocean. *Bulletin of Scripps Institute of Oceanography,* 23, 1-90.

WORMUTH, J. H. 1998. Workshop deliberations on the Ommastrephidae: A brief history of their systematics and a review of the systematics, distribution and biology of the genera *Martialia* Rochebrune and Mabille, 1889, *Todaropsis* Girard, 1890, *Dosidicus* Steenstrup, 1857, *Hyaloteuthis* Gray, 1849 and *Eucleoteuthis* Berry, 1916. *Systematics and Biogeography of Cephalopods, Smithsonian Contributions to Zoology,* 586, 373-383.

WORMUTH, J. H., O'DOR, R. K., BALCH, N., DUNNING, M. C., FORCH, E. C., HARMAN, R. F. & ROWELL, T. W. 1992. "Larval" and Juvenile Cephalopods: A Manual for their Identification. *Smithsonian Contributions to Zoology,* 513, 105-119.

YATSU, A., MOCHIOKA, N., MORISHITA, K. & TOH, H. 1998. Strontium/calcium ratios in statoliths of the neon flying squid, *Ommastrephes bartrami* (Cephalopoda), in the North Pacific Ocean. *Marine Biology,* 131, 275-282.

YATSU, A., TAFUR, R. & MARAVI, C. 1999. Embryos and rhynchoteuthion paralarvae of the jumbo flying squid *Dosidicus gigas* (Cephalopoda) Obtained through artificial fertilization from peruvian waters. *Fisheries Science,* 65, 904-908.

ZACHERL, D. C., PARADIS, G. & LEA, D. W. 2003. Barium and strontium uptake into larval protoconchs and statoliths of the marine neogastropod *Kelletia kelledi*. *Geochimica Et Cosmochimica Acta,* 67, 4091-4099.

ZEIDBERG, L. D. & ROBISON, B. H. 2007. Invasive range expansion by the Humboldt squid, *Dosidicus gigas*, in the eastern North Pacific. *Proceedings of the National Academy of Sciences of the United States of America,* 104, 12946-12948.

ZUMHOLZ, K., HANSTEEN, T., HILLION, F., HORREARD, F. & PIATKOWSKI, U. 2007a. Elemental distribution in cephalopod statoliths: NanoSIMS provides new insights into nano-scale structure. *Reviews in Fish Biology and Fisheries,* 17, 487-491.

ZUMHOLZ, K., HANSTEEN, T. H., KLUGEL, A. & PIATKOWSKI, U. 2006. Food effects on statolith composition of the common cuttlefish (*Sepia officinalis*). *Marine Biology,* 150, 237-244.

ZUMHOLZ, K., HANSTEEN, T. H., PIATKOWSKI, U. & CROOT, P. L. 2007b. Influence of temperature and salinity on the trace element incorporation into statoliths of the common cuttlefish (*Sepia officinalis*). *Marine Biology,* 151, 1321-1330.

ZUMHOLZ, K., KLUGEL, A., HANSTEEN, T. & PIATKOWSKI, U. 2007c. Statolith microchemistry traces the environmental history of the boreoatlantic armhook squid *Gonatus fabricii*. *Marine Ecology-Progress Series,* 333, 195-204.

APPENDIX

Statolith Extraction Method Improvements for Use in Microchemistry Studies with Laser Ablation Inductively Coupled Plasma Mass Spectrometry

N. Scarlett M. Arbuckle
Oceanography Department
TAMU
College Station, USA
sarbuckle@ocean.tamu.edu

John H. Wormuth

Abstract **Major hindrances for most scientific studies involve a lack of funding, sampling, or equipment. Without large, high resolution sample sets spanning significant spatial scales, long temporal scales, or both, it can be difficult to discern accurate results. This can be the case for some population studies and fisheries management efforts. One novel approach to squid population studies involves harvesting statoliths, but the power of the studies is limited by the scales at which samples are collected. Approaches that involve the characterization of trace elemental chemistry in these aragonite structures could provide a better understanding of the life cycles and behaviors of targeted fisheries species than the common practice of length-frequency studies. Often statoliths are not collected and the absence of consistently periodic or geographically distinct samples potentially limits large scale population studies. One possible reason statoliths are not always removed may be the lack of a thorough, clearly illustrated instructional method on dissection of the statoliths from the cranial cartilage. In an effort to encourage sampling of statoliths, previously published methods are improved upon in this work by including a description of the dissection of the statoliths using layman terms accompanied by detailed photographs. The methods were tested successfully with the Ommastrephid squid Dosidicus gigas and the statoliths obtained will be used to examine trace element variations determined by laser ablation inductively coupled plasma mass spectrometry (LA-ICP-MS).**

Keywords- Squid; Statolith; Dissection; Dosidicus gigas; LA-ICP-MS.

I. INTRODUCTION

First described by Clarke in 1966 [1], statoliths are deposits found in squid and other cephalopods that are necessary for equilibrium orientation and are composed of aragonite calcium carbonate similar to that found in foraminifera, corals, gastropod and bivalve shells, and fish otoliths [2-9]. In cephalopods, statoliths begin forming in the statocysts, cavities in the cranial cartilage, before hatching and continue growing after hatching by the daily deposition of an organic rich layer followed by an organic poor layer [7, 10-11]. This deposition process provides a measurable increment which can be used as an acceptable estimate of the age of an individual. This has been confirmed for some members of the Ommastrephid squid family and is generally assumed as a fair estimation for other species [12-15]. During deposition, trace elements are incorporated into the calcium carbonate matrix of statoliths [8, 16]. Many studies have shown that the patterns and levels of trace elements found in carbonates can be correlated to environmental conditions experienced by an individual or to their feeding behaviors [2-3, 6, 16-17]. The relationship between trace elements in biologically secreted calcified structures and environmental conditions enables the reconstruction of an individual s life history or can be used to distinguish between populations that experience different environments [3, 6, 17-22]. Additionally, trace elemental studies can be used to compliment and strengthen DNA or length-frequency type studies [19, 23]. For thorough reviews and examples of the power and scope and background of biological carbonate chemistry studies see Arkhipkin [24], Campana [25], Campana and Thorrold [24], Smith et al. [2], Zacherl et al. [3], and Zumholz et al. [20].

Despite the usefulness of statolith studies in discriminating between populations, life history reconstruction and behaviors [16, 19], statoliths are not necessarily collected as standard practice whenever possible. Since statoliths are approximately a few millimeters or smaller and can be stored dry, storage space for samples is not a likely hindrance to collection. Rather, the ability for an untrained, unassisted dissector to successfully use the available published methods might prevent collection when occasions have arisen. The original dissection description was given by Clarke [7] in 1978 and improved by Lipinski [26] in 1980 by adding three basic anatomic sketches. However, these methods remain unclear without background knowledge of squid anatomy or an experienced statolith dissector present as an instructor. This work improves upon the first published statolith dissection methods by employing advances in color photography use in digital publication.

II. METHODS

Before Statoliths can be dissected from fresh or frozen squid, but not after preservation as the calcium carbonate dissolves under acidic conditions [16]. The images provided depict the dissection of statoliths from a frozen and thawed specimen of Dosidicus gigas, or the Humboldt squid, from the family Ommastrephidae.

Begin by removing the mantle containing digestive, reproductive, circulatory and respiratory organs from the head and arms of the squid by cutting through the tissue immediately posterior to (behind) the funnel. Ideally, this initial bisection does not involve the cranial cartilage. Although it is not necessary, the funnel can be left attached to the head in larger specimens (Figure 1).

Figure 1. Whole head and arms after removal of mantle.

Next, cut horizontally through the cranial cartilage in a line that bisects the esophagus (Figure 2). You will possibly cut through the eyes, releasing ocular fluid. This step will divide the cartilage into an upper (dorsal) half and a lower (ventral) half. The ventral half, with the funnel attached or funnel groove present, will hold both statoliths. Figure 3 provides a generalized map of what will be visible after bisecting the cranial cartilage.

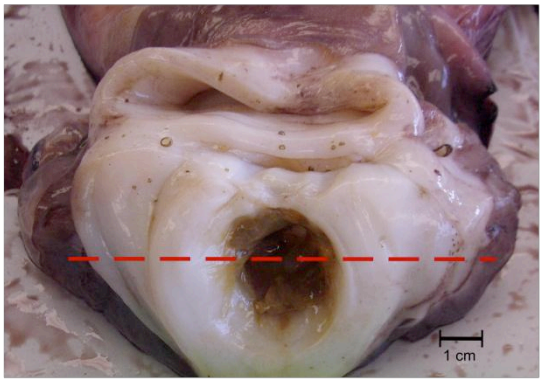

Figure 2. Placement of horizontal incision bisecting the esophagus. Note the head is oriented ventral side up in this image.

Now remove any excess tissue that may be on the cartilage especially in the ventral portion of the esophageal canal, which

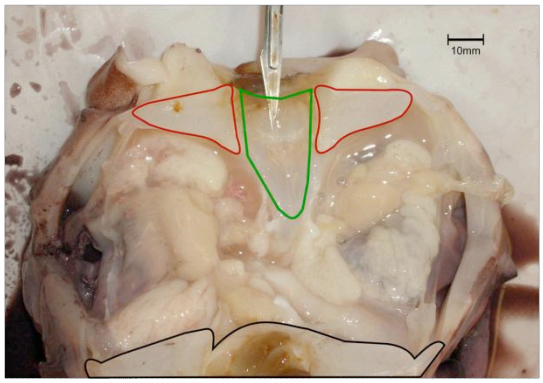

Figure 3. Upper and lower cranial cartilage after horizontal incision. Areas encircled in black are the upper or dorsal section of the cranial cartilage, which has been folded back. Areas encricled in red are unneeded regions of the lower or ventral cranial cartilage. The section of cartilage encircled in green designates the location of the statoliths.

is the passageway for the esophagus through the cranial cartilage. It may be possible to see the statoliths, which appear as faint specks under the cartilage which makes up the lower half of this esophagus canal (Figures 3 and 4). Statoliths are extremely small and therefore challenging to locate through the cartilage, especially if the specimen has been frozen and thawed or if the dissector lacks experience. Figure 4 provides a reference and evidence to this challenge.

After locating the statoliths if possible, cut into the esophageal cartilage vertically toward the arms, or in the sagittial plane, as shown in figure 5. This action should expose the statocyst, or the cavity in which the statolith rests. Use very fine tweezers to retrieve the statolith from the cavity (Figure 6).

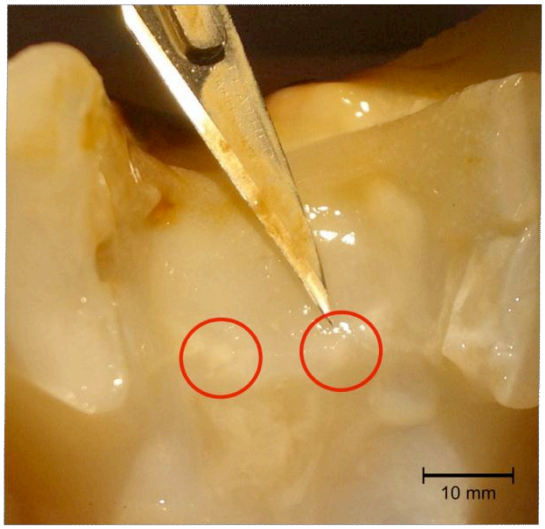

Figure 4. Statoliths viewed through the esophageal cartilage, encircled in red to clarify location.

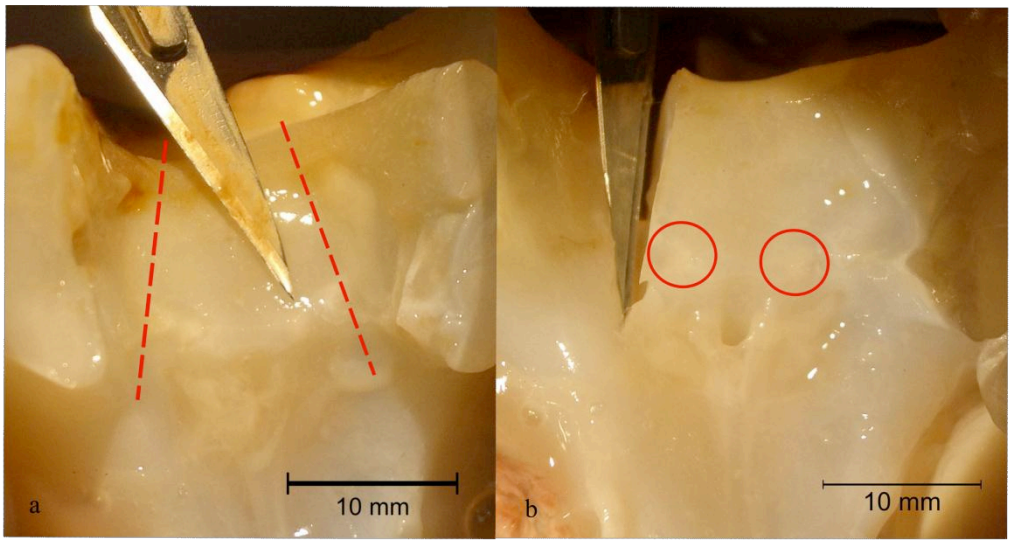

Figure 6. (a) Orientation of incisions to reveal statocysts. (b) After the first of two incisions with statoliths encircled in red.

The second statocyst is often more difficult to find after removing the first statolith due to loss of orientation.

After removal of both statoliths, rinse them thoroughly with deionized or Millipore water if possible. Allow to air dry on a clean surface, and store dry. Figure 7 shows variation in size and development between individuals of Humboldt squid.

III. Remarks and Conclusion

To demonstrate the usefulness of this work in population studies, these methods were field tested by providing them to an individual with no prior statolith dissection experience, who

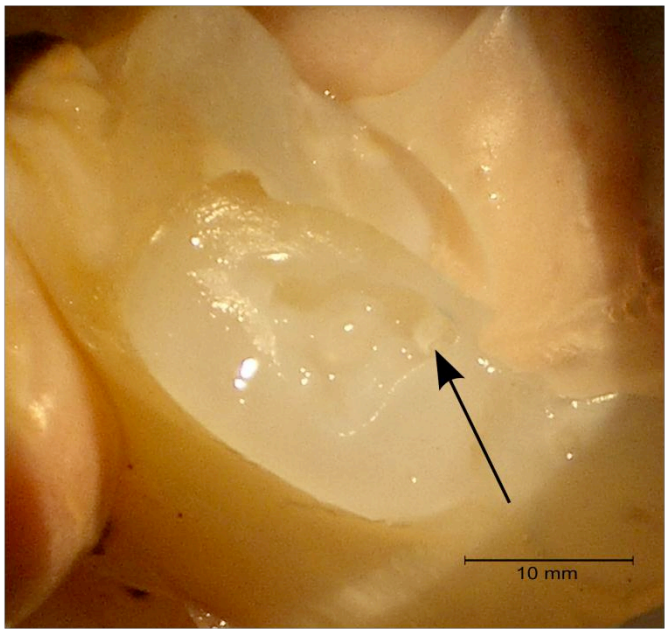

Figure 5. Statolith in statocyst. Arrow indicates location of statolith.

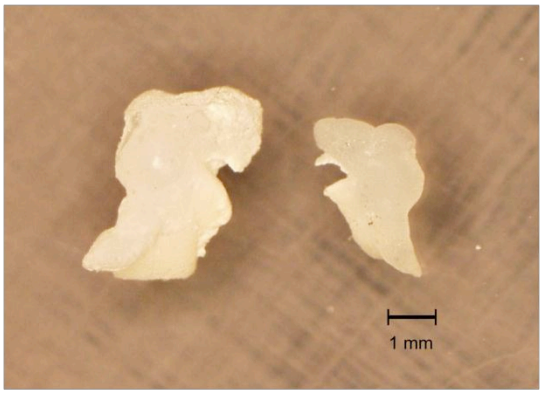

Figure 7. Statoliths from two different specimen of *Dosidicus gigas.*

then successfully removed 14 pairs of statoliths from thawed frozen Humboldt squid specimens with no further assistance or coaching. These statolith samples have been mounted in epoxy resin and prepared for laser ablation inductively couple plasma mass spectrometry. These samples have been utilized in a large scale population study by comparison of the trace elemental chemistry patterns found to those from Humboldt squids captured in various regions of the Pacific Ocean. To date, measurable amounts of trace element have been recorded for magnesium, manganese, copper, zinc, strontium, yttrium, zirconium, barium, lead and uranium. Preliminary data indicate Magnesium enriched cores, which is expected from previous work with other squid species [20, 27]. The availability of these methods and images were critical to accomplish this work. This work is intended to encourage removal of statoliths from squid before they are preserved or otherwise used in scientific study in order to strengthen similar future population studies.

ACKNOWLEDGMENT

This work would not be possible without the collaboration of Kirt Onthank at Washington State University, the unwavering support of Dr. John Wormuth and the efforts of the Department of Oceanography administration at Texas A&M University.

REFERENCES

[1] M. R. Clarke, "Review of the Systematics and Ecology of Oceanic Squid," in Advances in Marine Biology. vol. 4, ed, 1966, pp. 91-300.

[2] S. V. Smith, et al., "STRONTIUM-CALCIUM THERMOMETRY IN CORAL SKELETONS," Science, vol. 204, pp. 404-407, 1979.

[3] D. C. Zacherl, et al., "Barium and strontium uptake into larval protoconchs and statoliths of the marine neogastropod Kelletia kelledi," Geochimica Et Cosmochimica Acta, vol. 67, pp. 4091-4099, Nov 2003.

[4] S. Eggins, et al., "Mg/Ca variation in planktonic foraminifera tests: implications for reconstructing paleo-seawater temperature and habitat migration," Earth and Planetary Science Letters, vol. 212, pp. 291-306, 2003.

[5] L. A. Levin, "Recent progress in understanding larval dispersal: new directions and digressions," Integrative and Comparative Biology, vol. 46, pp. 282-297, 2006.

[6] S. E. Campana and J. D. Neilson, "Microstructure of Fish Otoliths," Canadian Journal of Fisheries and Aquatic Sciences, vol. 42, pp. 1014-1032, 1985.

[7] M. R. Clarke, "Cephalopod Statolith - Introduction to Its Form," Journal of the Marine Biological Association of the United Kingdom, vol. 58, pp. 701-712, 1978.

[8] R. L. Radtke, "Chemical and Structural Characteristics of Statoliths from the Short-Finned Squid Illex-Illecebrosus," Marine Biology, vol. 76, pp. 47-54, 1983.

[9] Y. Rosenthal, et al., "Temperature control on the incorporation of magnesium, strontium, fluorine, and cadmium into benthic foraminiferal shells from Little Bahama Bank: Prospects for thermocline paleoceanography," Geochimica Et Cosmochimica Acta, vol. 61, pp. 3633-3643, 1997.

[10] K. Zumholz, et al., "Elemental distribution in cephalopod statoliths: NanoSIMS provides new insights into nano-scale structure," Reviews in Fish Biology and Fisheries, vol. 17, pp. 487-491, Aug 2007.

[11] V. Bettencourt and A. Guerra, "Age studies based on daily growth increments in statoliths and growth lamellae in cuttlebone of cultured Sepia officinalis," Marine Biology, vol. 139, pp. 327-334, Aug 2001.

[12] P. G. Rodhouse, et al., "Growth, Age Structure and Environmental History in the Cephalopod Martialia-Hyadesi (Teuthoidea, Ommastrephidae) at the Antarctic Polar Frontal Zone and on the Patagonian Shelf Edge," Antarctic Science, vol. 6, pp. 259-267, Jun 1994.

[13] E. G. Dawe, et al., "Validation and Application of an Ageing Technique for Short-finned Squid (Illex illecebrosus)," Journal of Northwest Atlantic Fishery Science, vol. 6, pp. 107-116, 1985.

[14] Y. Nakamura and Y. Sakurai, "VALIDATION OF DAILY GROWTH INCREMENTS IN STATOLITHS OF JAPANESE COMMON SQUID TODARODES-PACIFICUS," Nippon Suisan Gakkaishi, vol. 57, pp. 2007-2011, Nov 1991.

[15] M. R. Lipinski, "Methods for the validation of squid age from statoliths," Journal of the Marine Biological Association of the United Kingdom, vol. 66, pp. 505-526, 1986.

[16] A. I. Arkhipkin, "Statoliths as 'black boxes' (life recorders) in squid," Marine and Freshwater Research, vol. 56, pp. 573-583, 2005.

[17] K. Zumholz, et al., "Food effects on statolith composition of the common cuttlefish (Sepia officinalis)," Marine Biology, vol. 150, pp. 237-244, Nov 2006.

[18] R. R. Warner, et al., "Geographic variation in natal and early larval trace-elemental signatures in the statoliths of the market squid Doryteuthis (formerly Loligo) opalescens," Marine Ecology-Progress Series, vol. 379, pp. 109-121, 2009.

[19] A. I. Arkhipkin, et al., "Spatial and temporal variation in elemental signatures of statoliths from the Patagonian longfin squid (Loligo gahi)," Canadian Journal of Fisheries and Aquatic Sciences, vol. 61, pp. 1212-1224, Jul 2004.

[20] K. Zumholz, et al., "Statolith microchemistry traces the environmental history of the boreoatlantic armhook squid Gonatus fabricii," Marine Ecology-Progress Series, vol. 333, pp. 195-204, 2007.

[21] S. R. Thorrold, et al., "Quantifying larval retention and connectivity in marine populations with artificial and natural markers," Bulletin of Marine Science, vol. 70, pp. 291-308, Jan 2002.

[22] Y. Ikeda, et al., "Concentration of statolith trace elements in the jumbo flying squid during El Nino and non-El Nino years in the eastern Pacific," Journal of the Marine Biological Association of the United Kingdom, vol. 82, pp. 863-866, Oct 2002.

[23] F. Feyrer, "Otolith microchemistry provides information complementary to microsatellite DNA for a migratory fish," Transactions of the American Fisheries Society, vol. 136, p. 469, 2007.

[24] S. E. Campana and S. R. Thorrold, "Otoliths, increments, and elements: keys to a comprehensive understanding of fish populations?," Canadian Journal of Fisheries and Aquatic Sciences, vol. 58, pp. 30-38, 2001.

[25] S. E. Campana, "Otolith science entering the 21st century," Marine & freshwater research, vol. 56, p. 485, 2005.

[26] M. R. Lipinski, "A preliminary study on age of squids from their statoliths. ," NAFO SCR Doc. No. 22, 17pp.1980.

[27] V. Bettencourt and A. Guerra, "Growth increments and biomineralization process in cephalopod statoliths," Journal of Marine Biology and Ecology, vol. 248, pp. 191-205, 2000.